INDIAN OCEAN SKIPJACK TUNA STOCK ASSESSMENT 1950-2016 (STOCK SYNTHESIS)

PREPARED BY: IOTC SECRETARIAT[1], 02 OCTOBER 2017

[1] Dan.Fu@fao.org; Fabio.Fiorellato@fao.org

Contents

SUMMARY

This report presents a stock assessment for Indian Ocean Skipjack (*Katsuwona pelamis*) using *Stock Synthesis 3* (SS3). The assessment uses a spatially aggregated, age structured model that integrates multiple datasets into a unified framework. The assessment includes catch data grouped into four separate fisheries covering the period from 1950 through to 2016, two CPUE series, length composition data, and tag-recapture data. Key elements and core assumptions in the assessment model are summarised below:

- The population model is age based, spatially aggregated, and seasonally structured. The model is iterated on an annual cycle consisting of four seasons.
- The model assumes that there is a shared spawning stock and total recruitment follows a Beverton-Holt relationship, with annual deviates and temporal variability in the proportional distribution of recruits among four seasons.
- There are four fisheries including Maldives Pole and Line (PL) fleet, FAD/log associated Purse Seine (PS) sets from the EU/Seychelles fleets, unassociated PS sets from the EU/Seychelles fleets, and PS from other nations and all other fleets.
- Standardised CPUE series are available from Maldives PL fleet and EU associated PS sets. Length composition data are available from all four fisheries. Tagging data are available from the RTTP-IO and small-scale tagging programmes.
- The model estimated non-parametric (cubic spline) length-based selectivity for each fleet independently (with sufficient flexibility to describe logistic, dome-shaped or polymodal functions).
- Estimated parameters include virgin recruitment, selectivity functions, recruitment deviations, and the seasonal pattern of recruitment, natural mortality (in some models), and the tag recovery reporting rate for the PL fleet (for models using RTTP-IO plus small scale tagging data).
- Fixed parameters include stock recruit steepness and life history parameters describing growth and the maturity schedule.

A range of exploratory models are presented to explore the impact of key data and model assumptions on the stock assessment conclusions. A systematic approach was undertaken to evaluate interactions of model assumptions and to develop management advice. Possible combinations of model options considered in the exploratory phase were included in a final grid of model runs. Stock status was estimated for 144 models running a permutation of the parameters, including combinations of the following options:

- 2 CPUE options: Maldives PL indices + EU PS indices, and Maldives PL only.
- 2 growth options: a Richards curve approximating the 2 stanza curve of Eveson et al. (2012), a von Bertalanffy curve of Eveson (2011) with Linf fixed at 83cm
- 3 values of stock recruit steepness: h=0.7, 0.8, 0.9,
- 2 tagging program release/recovery options: RTTP-IO, RTTP-IO plus small-scale tagging programme
- 2 tag mixing period options: (t = 2, 4 quarters)
- 2 tag recovery negative-binomial overdispersion options (τ = 2, 20)
- 2 M options: estimated (age-specific), a constant value of 0.8.

IOTC Resolution 16/02 adopted a harvest control rule (HCR) for skipjack tuna, which shall recommend a total annual catch limit based on a relationship between stock status (spawning biomass relative to unfished levels) and fishing intensity (exploitation rate relative to target exploitation rate), estimated from a model-based stock assessment. Therefore this assessment reported depletion-based reference

points including $SSB_{40\%}$ (40% of unfished spawning biomass) and $F_{40\%SSB}$ (Fishing mortality corresponding to an equilibrium spawning biomass of 40% unfished level).

Estimates from the majority of models from the assessment grid (Grid-IO) suggested the Indian Ocean skipjack tuna stock as a whole is currently not overfished, and not subject to overfishing. Estimates of key management quantities are summarized below (mean and 90% quantiles from the distribution of the MPD estimates):

- $SSB_{current} / SSB_{\%40} = 1.24$ (0.90–1.52)
- $F_{current} / F_{\%40SSB} = 0.60$ (0.24–1.21)
- $SSB_{current} / SSB0 = 0.49$ (0.36–0.61)
- MSY = 893 250 (430 710–1 622 320)
- Current catch 446 723 t

The results of 10 years projections over a range of constant catch levels (60, 80, 100, 120, and 140% of current) are summarized in a management decision table (Kobe 2 Strategy Matrix), based on the average of the model results. Projections from models of Grid-IO suggest that the risk of the spawning biomass falling below the target ($SSB_{40\%}$) is less than 10% for both the short (3 years) and medium (10 years) term, if the catch remains at the current level.

Additional models based on alternative temporal and/or spatial structures were investigated to assess robustness of assessment conclusions, including a quarterly-based model in which calendar seasons are configured as model years, and a two-area model in which the stock is partitioned into the east and West Indian Ocean.

The alternative temporal configuration allows seasonal recruitment to be generated from the stock-recruitment relationship (rather than apportioned among four seasons from a single recruitment event), and also allows the tag release to be grouped by finer age classes (however, our investigation showed this is not influential). Overall the quarterly-based model had a similar performance to the original year-season model. A grid of 144 models (Grid-Q0, with the fore-mentioned parameter options) was also run using this alternative temporal structure and the estimated stock status is summarized as below:

- $SSB_{current} / SSB_{\%40} = 1.17$ (0.75–1.58)
- $F_{current} / F_{\%40SSB} = 0.83$ (0.30–1.53))
- $SSB_{current} / SSB0 = 0.47$ (0.30–0.63)
- MSY = 184 050 (106 620 – 369 250) (quarterly)
- Current catch 111 680 t (quarterly average)

The two area model allows differential depletion by area, and potentially accounts for spatial heterogeneity in tag mixing rate. However, the two-area models examined so far across a range of model options did not appear to provide credible estimates of relative biomass distribution between the two regions. Further investigation and improvement are required to assess this model's ability to estimate stock status and its applicability to provide management advice.

1. INTRODUCTION

The Indian Ocean skipjack tuna (*Katsuwona pelamis*, SKJ) fishery is one of the largest tuna fisheries in the world, with total catches of 400-600 thousand t over the past decade. Some bioeconomic modelling of the fish population and fishery was undertaken a few years ago (Mohamed 2007). Before 2010, management advice has relied on data-based indicators, and mortality estimates from analyses of the recent RTTP-IO tagging data (Edwards et al. 2010). A full integrated model-based assessment was developed in 2011 (Kolody 2011 et al), and further updated in 2012 (Sharma et al. 2012) and 2014 (Sharma et al. 2014).

The other tropical tuna RFMOs have conducted model-based assessments for SKJ (Maunder and Harley 2003, ICCAT 2009, Hoyle et al. 2011, Rice et al. 2014, McKechnie et al. 2016). However, this is recognized as a difficult species to assess (e.g. because the population dynamics are very rapid, spawning may be continuous, the selectivity is generally uninformative about year-class strength, and relative abundance indices derived from pole and line and purse seine fisheries are generally considered to be less reliable than those derived from longline fisheries). These problems have led the IATTC to move away from model-based assessments to provide advice on the basis of data-based indicators (Maunder 2009).

Since 2013, the Maldives has been working with the IOTC to undertake a Management Strategy Evaluation (MSE) for the IO SKJ fishery, to partially fulfil the conditions of the Marine Stewardship Council (MSC) certification for the domestic SKJ fishery (Nokome & Adam 2015). During 2014 and 2015, the results of this work program, including the operating model, evaluation methods, performance statistics, and approaches for developing harvest control rules (HCRs) were reviewed by meetings of the Working Party on Tropical Tunas (WPTT), Working Party on Methods (WPM), and the Scientific Committee (SC). In 2016, the IOTC commission adopted a pre-agreed Harvest control rule (HCR). The Skipjack tuna HCR shall recommend a total annual catch limit based on a relationship between stock status (spawning biomass relative to unfished levels) and fishing intensity (exploitation rate relative to target exploitation rate) estimated from a model-based stock assessment (Resolution 16/02).

In 2017, The Technique Committee on Management Procedure recommended that the Commission considers establishing a procedure for implementing the HCR contained in Resolution 16/02 as soon as the catch limit is estimated by the SC (IOTC–TCMP01 2017). Following the review by the SC of the stock assessment of skipjack tuna in 2017, such a procedure would lead to an administrative procedure by which the Secretariat notifies CPCs of the catch limit to be enforced from 1st January 2018.

In this context, this report provides an update and further development of the integrated stock assessment for skipjack in the Indian Ocean using fishery data up to 2016. The model incorporates three additional year of data (2013-2015), improved information on nominal catches from IOTC database, and revised CPUE time series for the Maldives Pole and line and European Purse Seine fleets. The assessment provides estimates of population parameters, stock status and reference quantities (required for calculating the catch limit from the HCR). Model uncertainties are characterised under combinations of model assumptions and parameter values using a grid approach. The assessment builds on the work by Sharma et al. (2012, 2014), and Kolody (2011), and uses a size based, age structured population model. The model is spatially aggregated, and seasonally structured, iterated on annual cycles from 1950-2016. Additional models based on alternative temporal and/or spatial structures are investigated to assess robustness of assessment conclusions.

1.1 Fishery overview

The Indian Ocean skipjack catch history is shown in Figure 1. Catches increased steadily from the 1980s to a peak in 2006, but have been decreasing since the mid-2000s. Catches have increased over the last four years and have been at 68-73% of the peak. Figure 2 illustrates the spatial distribution of the catches from the purse seine, pole and line (bait boat) fleets. In 2016, purse seine and pole and line accounted for about 40% and 15% of the total catches respectively.

The Maldives has sustained a pole and line (PL, bait boat) skipjack fishery for many centuries, with catches increasing dramatically with the uptake of mechanization and deployment of larger vessels (more poles, larger bait and storage capacity, longer range) starting in the 1980s. The Maldives has experienced substantial catch declines since the peak in 2006, for reasons that are not entirely clear. Adam (2010) suggests that this may reflect declining skipjack abundance, limitations to bait availability or changing economic incentives (e.g. high fuel prices).

There has been a rapid increase in skipjack catches with the introduction of the purse seine fleets in the 1980s (e.g. Chassot 2010, Delgado de Molina 2010). The European/Seychelles PS catch has fluctuated considerably since around 2000 without a clear trend. Catch declines in the most recent years are probably partly attributable to the effects of piracy in the prime fishing area near Somalia. The EU/Seychelles PS vessels still operate in this area, but the nature of the fishery has changed, and the effects of the piracy are not clear. There has been a steep decline in the nominal purse seine FAD-set catch rates since 2002, however, this decline is not seen in the free school sets from the same fleet, and the inter-annual catch rate variability is very high (see Figure 15, Dorizo *et al.* 2008). From 2003-06 the decline was due to very good fishing of large YFT on free-schools. After 2007 piracy or other 'unknown' reasons may be the cause of the decline. Fishing for free-schools does not normally happen in waters off Somalia. (Sharma et al. 2014)

A substantial portion of the total catch is taken by a mix of artisanal and semi-industrial gears, with minor catches dating back before the pre-industrial period. For the assessment, these fleets have been pooled together, in the heterogeneous *Other* fleet. The bulk of the recent catch in this fishery is from the gillnet fisheries of Sri Lanka, Indonesia, Iran and Pakistan. These fleets were mostly operating in coastal waters historically, but long distance trips to international waters have been noted in recent years (spatial data is largely unavailable for these fleets). The aggregate catches of these fleets has been increasing steadily.

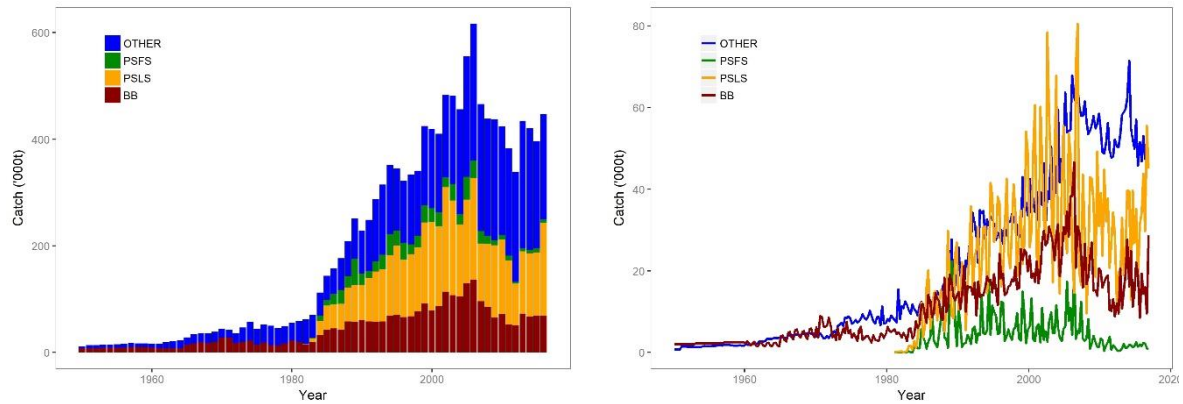

Figure 1: Total Skipjack catch in tonnes by fishery fleet over time in the Indian Ocean: Left panel - stacked annual catches; right panel – quarterly time series.

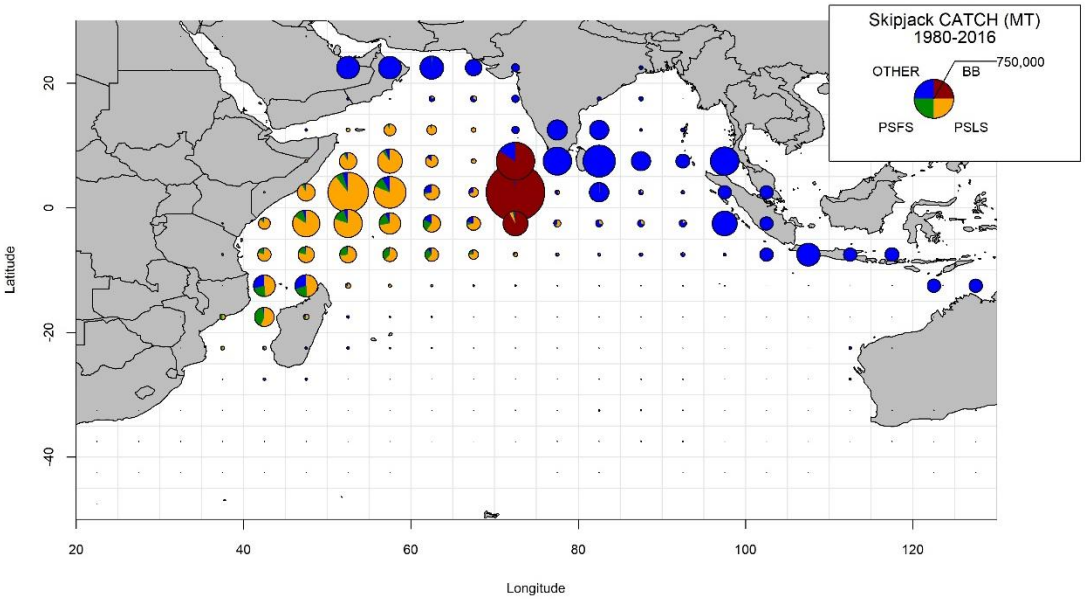

Figure 2: Indian Ocean skipjack catch distribution 1980-2016 by fisheries.

1.2 Biology and stock structure

Skipjack are the smallest of the major commercial tuna species and are found mainly in the tropical areas with geographic limits between 55-60° N and 45-50° S.

Skipjack are highly fecund and can spawn year round over a wide area of the tropical and subtropical waters. Environmental conditions are believed to significantly influence recruitment and can produce widely varying recruitment levels between years (Mackenzie et al. 2016). The historical Japanese surveys of skipjack larvae have identified large quantities of skipjack larvae in the Equatorial Eastern IO (Nishikawa et al 1985), but these surveys have been quite rare in the Western IO. The location of skipjack nurseries remain widely unknown, as well as the biology of skipjack early juveniles, because very small sizes of skipjack have never been exploited significantly in the IO (Fonteneau 2014)

A substantial amount of information on skipjack movement is available from tagging programs, which have documented some large-scale movement within the Indian Ocean. The average range of movement during the skipjack lifetime can be estimated at about 1000 miles, with maximum distance of about 2000 miles (Fonteneau 2014). Skipjack movement is highly variable and is thought to be influenced by large-scale oceanographic variability (Mackenzie et al. 2016).

Genetic analyses by Dammannagado *et al.* (2011) have suggested that there might be two (or more) skipjack populations in the Indian Ocean. If this is correct, an aggregated assessment may not be appropriate. But we currently do not have enough information to know what the appropriate structure should be. A very recent stock structure study based on analysis of the shape of otolith from four areas south of Java showed that they are not statistically different among regions, suggesting that these skipjack belongs to a single stock (Wujdi et al. 2017). However, Due to the limited spatial range of the samples, this conclusion cannot be applied to the whole Indian Ocean.

2. OBSERVATIONS AND MODEL INPUTS

Data used in the stock assessment of skipjack tuna using SS3 consist of catch, length frequency data for the fisheries defined in the analysis, and tag-recapture data. SS3 requires the definition of fisheries that consist of fishing units with similar selectivity and catchability characteristics. Four fleets were defined on the basis of gear, fleet and area of operation:

1. PL – Maldivian Pole and Line fleet.
2. PSLS - FAD/log associated Purse Seine (PS) sets from the EU/Seychelles fleets.
3. PSFS - unassociated PS sets from the EU/Seychelles fleets.
4. Other - includes all other fleets, primarily gillnet fleets from Sri Lanka, Iran, Indonesia and Pakistan, but also non-EU/Seychelles PS fleets, and small coastal fleets (including non-PL fisheries from the Maldives), and a trivial catch from longliners.

The *Other* fleet is a heterogeneous mix of fisheries. However, further partitioning this fleet is not expected to make much difference to the analysis because the size composition data are not very good for most of these fleets and none of these fleets are considered to provide informative data with respect to catch rates or tag recoveries.

2.1 Catch history

The total catches were calculated by the Secretariat (Geehan et al. 2017). The nominal catches are not always reported by species and/or gear by the responsible institutions in each country. The catches reported under species and/or gear aggregates are decomposed by the IOTC secretariat using alternative sources of information (if available), or a pre-defined criteria so that all catches are separated into individual gears and species (IOTC 2004). The catch time series for the 4 fleets is shown in Figure 1. Catch in mass was used in the model for all fleets, and was assumed to be known without error.

Pakistan has reconciled the official catch estimates for tropical tuna species based on the observer program implemented by WWF-Pakistan (Khan 2017). The revised estimates for skipjack are somewhere between 2000–4000 t less annually between 1999 and 2016 than those previously reported to the Secretariat. The revised estimates from Pakistan have not been incorporated into this assessment as further verification needs to be undertaken by the Secretariat.

2.2 Relative abundance estimates

Maldives PL CPUE series

Medley and Adam (2017) described the standardised Maldives PL CPUE series adopted as the relative abundance index for the period 2004–2015. The standardisation was based on a combined dataset including historical trip reports and more recent log-book (2014–2015). The standardisation was undertaken using a Bayesian generalised linear model, incorporating year, quarter, atoll, vessel, and a source variable to distinguish the two datasets. Quarterly indices were derived based on the mean of posterior samples, which has a similar trend (but smoother) to the indices produced using the maximum likelihood approach.

Indices have been produced for skipjack by number as well as by weight, and both indices exhibited very similar trends. The majority of data in the historical records appear to be reported in numbers, whereas the majority of logbook data are reported in weight. The difference between the two data sets represents the bias in conversion. The number-based models are probably better for the older data, whereas the weight based model will be better for newer data. (The difference for the older data is that the weight estimate uses different assumed weights for large and small skipjack which may increase the variance). The indices by numbers are used in this assessment considering that the logbook has been available for only two years. However, the weight-based indices are considered to be more appropriate for future assessments (Paul Medley, pers. comm.)

There are a number of concerns about using this CPUE series in this assessment, stemming from the fact the time series is very short, the spatial area may not represent the Indian Ocean, and the indices

may not be representative of the overall abundance due to the effort being concentrated on FADs in recent years.

EUROPEAN PSLS CPUE series

The European and associated flags purse seine fishing activities in the Indian Ocean during 1981–2016 have been monitored through the collection of logbook and observer sampling. Standardised indices of the biomass of skipjack caught by the European purse seiners (Spain and France) under floating objects (including primarily sets on drifting fishing aggregating devices) was developed through a dedicated working group held in Spain, July 17 to 21, 2017 (Gaertner et al. 2017). The standardisation was based on the application of a generalized linear mixed model which considered a comprehensive list of candidate covariates, including non-conventional covariates. Standardised indices based on catch per set were developed for the whole time series (1986–2016) using only part of the covariates, as well for the reduced time series (2004–2016) accounting for all the covariates. Indices based on catch per hour were also derived.

Both units of efforts exhibited similar trends (Figure 4) and there are the two major drops (1997 and 2007) in both series which corresponded to two positive dipoles events in the Indian Ocean (Marsac et al 2017). It is considered that CPUE per set is more appropriate as fishing hour is not really a good metric for describing the time devoted to locate a FAD (Daniel Gaertner per. comm.).

CPUE OPTIONS EXPLORED

Overall the PSLS series (both the long and short time series) are very comparable to the PL series for the overlapping years. But the PSLS series doesn't show the same increase in 2005 and 2006 as observed in the PL series. The short PS indices show a somewhat larger drop in 2007. In general the PL series show a rather steady but a slightly larger decline than the two PSLS series.

The following options were examined in exploratory runs:

- Ua = preferred PL CPUE series only
- U1 = preferred PSLS CPUE series 1986–2016
- U3 = preferred PSLS CPUE series 2004–2016
- UUa1 = preferred PL CPUE series and PSLS CPUE series 1986–2016

The reference model is based on the UUa1 option (PL CPUE and PSLS CPUE series 1986–2016).
The final assessment grid included the Ua option as well (PL CPUE only).

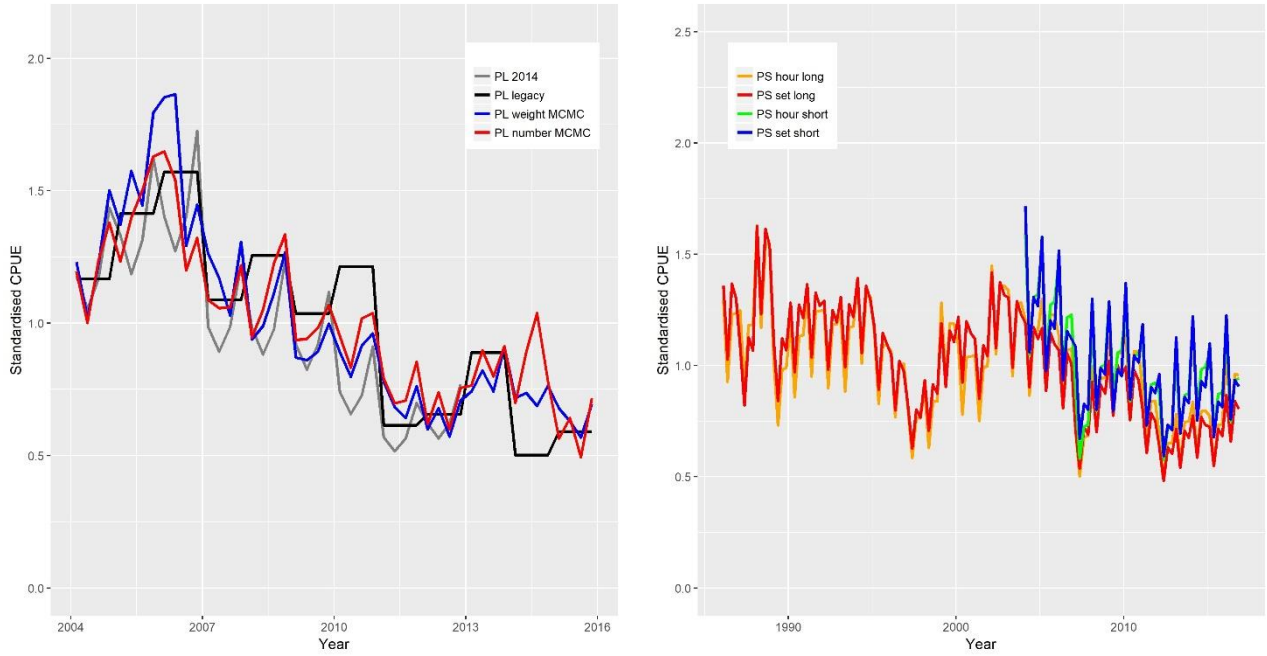

Figure 3: Standardised CPUE by weight and by number derived from the Bayesian GLM model for the Maldives PL fisheries (left, the CPUE used in 2014 assessment, and an update of the 2014 GLM model is also shown), and the standardised CPUE series from the European Purse seine fleet (right) for the whole time series (1986–2016) and reduced time series (2004–2016), by set and by fishing hour.

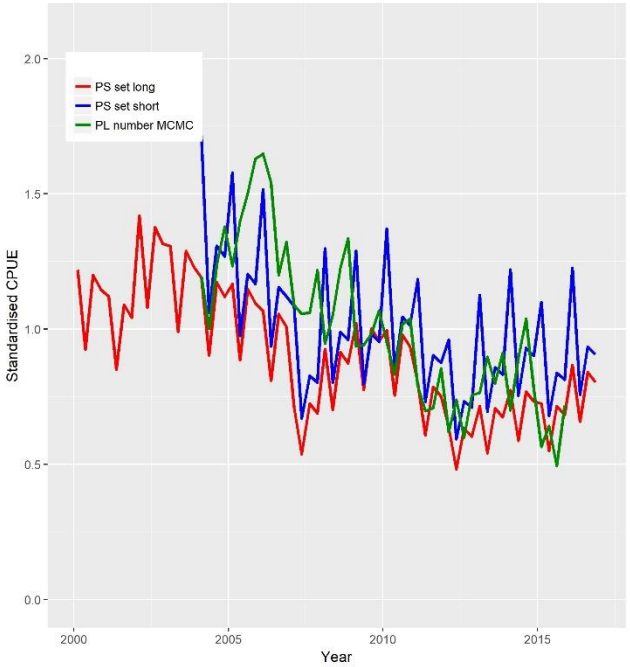

Figure 4: A comparison of the standardised CPUE series used in the assessment: Maldives PL CPUE and EU PSLS CPUE (1986–2016 and 2004–2016, based on catch by set).

2.3 Length frequency data

The catch-at-length data were compiled by the IOTC Secretariat (xxx 2017). This process involves a number of approximations, substitutions and unit conversions because some fleets have very poor data, some fleets do not report data at the appropriate resolution, and different measurement procedures are often used (*e.g*. mass vs: length). The sampling proportion was very low for the PL and the *Other* fisheries. The sampling proportion is high for PSFS and PSLS fisheries but very variable. The assessment used the reported length frequency (unraised) for the PL and the *Other* fisheries. However, Purse Seine size frequency has been raised at the source by the EU prior to the submission to the Secretariat therefore the raised length frequency for the PSFS and PSLS fisheries are used in the assessment noting that strata where length frequency exists but the reported number of fish sampled is zero are excluded. A sensitivity analysis using the raw, unraised EU,Spain PS size data is also undertaken (Appendix B).

Time series of mean length for each fisheries are shown in Figure 6. Catch-at-length distributions over time are shown in Figure 6. The bimodal distribution in the PL fishery suggests a heterogeneous mix of two life history stages. Brief exploration did not reveal any obvious spatial/seasonal explanation for the two modes. Size data for Maldivian PL from 1987 to 2000 have been removed from the database as they are considered extremely unreliable. Similarly the data for 2015/2016 was removed as only extremely small fish (less than 1kg on average) were reported.

The recent decline in mean size in the *Other* fleet probably reflects the erratic sampling from this fleet. It has been noted previously that the length frequency data from Thailand small purse seiners in 2007 and following years were of extremely poor quality. For the ‘Other’ category, size data between 2007 and 2010 were not used.

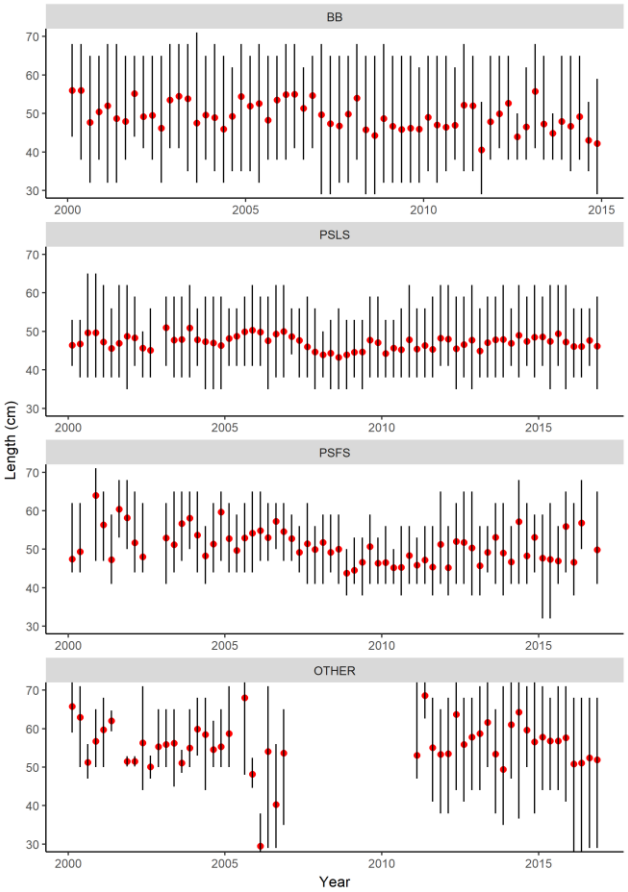

Figure 5: Quarterly time series of mean length by fleet

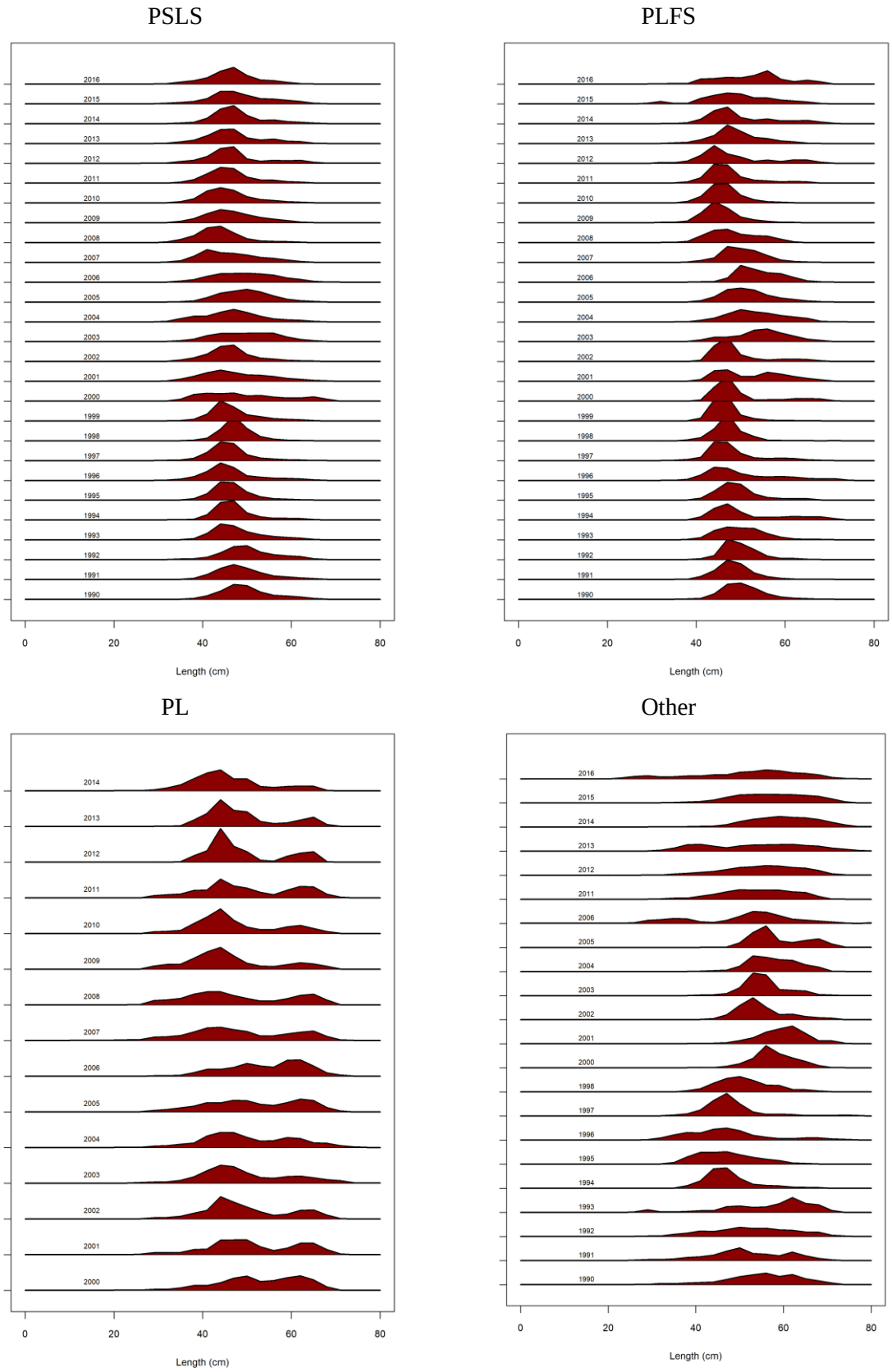

Figure 6: Length composition of samples for all years by fleet. Note that quarterly length frequencies are fitted in the assessment model.

2.4 Tagging data

Tag Release and Recovery Data

Hallier and Million (2009) provide an overview of the RTTP-IO tagging project. Between 2005 and 2007, about 77000 tagged skipjack were released from Tanzania, Seychelles and Mozambique Channel, with returns coming primarily from the purse seine fishery in the western Indian Ocean within four years after release (Figure 7). Additional tagging (~22000 releases) also occurred in the eastern Indian Ocean as part of small-scale tagging operations in 2004 and 2007-2009 (Figure 8). The most substantial small-scale project was based in the Maldives (Jauharee and Adam 2009), but tags were also released near Lakshadweep, Mayotte, western Sumatra and the Andaman Islands. The percent of tag returns is approximately 14% for skipjack. The low number of returns from other fisheries is partly due to lower catch numbers, particularly of the smaller size classes that were tagged, but probably due in most part to non-reporting (Eveson 2012 et al.). Table 1 describes key features of the two tagging datasets explored in the assessment. Figure 9 provides graphical summaries of RTTP-IO tag releases, recoveries, time at liberty and net movement.

We have more confidence in the RTTP-IO data than the small-scale tagging programs, because the RTTP-IO has a much larger number of tags, released by more experienced taggers, and a database that has been gradually developed over time by the IOTC secretariat. In contrast, we have no tag shedding estimates for the fleets conducting the small-scale tagging programs, and it is possible that the fish tagged in the eastern regions may be more closely affiliated with Pacific skipjack populations. However, the possible benefits of the small-scale tagging program include i) a longer time series of releases, ii) inclusion of a broader range of fish sizes/ages, and iii) potentially additional insight into spatial dynamics

The two different approaches for using the tag data were compared, with model grid definitions:

- rttp – RTTP-IO releases, PSLS and PSFS recoveries
- rtss – RTTP-IO and small-scale releases, PL, PSLS and PSFS recoveries

We have the most confidence in the tag recovery data from the PSLS and PSFS fleets, because of the reporting rate estimates derived from the tag seeding experiments (e.g. Hillary *et al*. 2008). Quarterly point estimates of the reporting rates were included from the analysis shown in Table 2. The tag recovery from the PSLS and PSFS fleets were adjusted for the estimated reporting rates before inclusion in the assessment model.

We do not have reporting rate estimates from the PL fleet. However, as appreciable numbers were returned, it is thought that recoveries from this fleet might still be informative (at least putting a minimum bound on the return rate). In model runs that included the PL recoveries, a stationary reporting rate for the PL fleet was estimated (with a very diffuse prior). But the result may be misleading if the reporting rates have a temporal trend).

In general we have a poorer understanding of the operations of the *Other* fleets, and there are no reporting rate estimates. These recoveries were excluded from the analyses, and reporting rates set to 0 (the PL fleet received a similar treatment, in the runs from which this fleet was excluded).
Several irregularities in the tagging data were addressed in the following ad hoc ways:

- A small number of tags were omitted from the analysis because of:
    - no recorded release length,
    - no recovery fleet,
    - no release or recovery date (or recovery precedes release)
- A small number of releases recaptured by the tagging vessels were ignored.

- The EU PS tag recoveries of unknown set-type were assigned a set-type according to the total proportion of known FS and LS set types in the PSFS and PSLS fisheries (by quarter).
- The coastal fleets on the east coast of Africa, *i.e.* in Kenya and Zanzibar, have presumably intercepted some tags near the primary release location, before they were fully mixed with the broader population. This is an unknown, but probably small number of tags.

Tag Recovery pre-processing for Stock Synthesis

The model tracks multiple homogenous tag groups over time, where a tag group consists of all individuals of a particular age class released in a particular year/quarter. For the 2-3 fleets which were considered informative, each tag recovery observation for a particular tag group and recovery period was calculated:

$$R_{LS}^{Total} = \frac{(1-\hat{P}_{outside}^{SEZ})}{r^{sea}} \quad (R_{LS}^{sea} + \hat{P}_{LS}^{sea} R_{unk}^{sea}) + \frac{1}{\hat{P}_{outside}^{SEZ}} \left(\frac{1}{r^{SEZ}} \quad (R_{LS}^{SEZ} + \hat{P}_{LS}^{SEZ} R_{unk}^{SEZ}) \right)$$

$$R_{FS}^{Total} = \frac{(1-\hat{P}_{outside}^{SEZ})}{r^{sea}} (R_{FS}^{sea} + (1-\hat{P}_{LS}^{sea}) R_{unk}^{sea}) + \frac{1}{\hat{P}_{outside}^{SEZ}} \left(\frac{1}{r^{SEZ}} \quad (R_{FS}^{SEZ} + (1-\hat{P}_{LS}^{SEZ}) R_{unk}^{SEZ}) \right)$$

$$R_{PL}^{Total} = R_{PL}^{MLD}$$

where:

subscripts indicate fishery/landing types (LS = EU/Seychelles PS log set, FS = EU/Seychelles PS free school set, unk=unknown set-type, PL = Maldivian Pole and Line, outside = EU/Seychelles catch landed outside of the Seychelles),

superscripts indicate recovery locations (sea = aboard fishing vessel, SEZ = port of Seychelles, MLD = Maldives).

For readability, scripts denoting tag release group and recovery time period are omitted:

R^{Total} = number of observed (from the perspective of the model) recaptures for a particular fishery (and tag group and time period), as input to the model.

r = the reporting rate. Note that for PS tags removed at sea, r was assumed to be 1.0. Reporting rates from the Seychelles are listed in Table 2. Within the model, PS reporting rates were set to 1.0, while PL reporting rates were estimated as a free parameter (and ignored in the pre-processing).

$\hat{P}_{LS}$ is the proportion of PS tags recovered from unknown set-type which are actually of set-type LS, estimated as the proportion of tags of known set-type LS recoveries at sea of all known set-type recoveries at sea (by quarter).

$\hat{P}_{outside}$ is the scaling factor to account for the EU PS recaptures not landed in the Seychelles, estimated by the mean of the quarterly proportions of EU PS catch landed in the Seychelles relative to the total EU PS catch (by quarter).

These calculations estimate the full number of tag recoveries that should have been made in the PS fisheries, such that the reporting rates can be set to 100% in the model. In part, this represents a work-around solution because *Stock Synthesis* cannot represent temporal variability in reporting rates. This ignores potential variance implications, but given that the reporting rates were generally very high for the PSFS and PSLS fleets, this is probably not a big problem. The alternative work-around solution of defining a different fleet for each recovery time period could be employed, but this extra complication does not seem justified in this case.

Tag Mixing

In the population model, tagged fish are assumed to have identical dynamics to the general population. We expect that a reasonable period of mixing is required before this assumption would be valid. Figure 9 suggests that tag displacement within the core PS area reaches a plateau within a few weeks of release.

If this displacement was entirely due to random movement, it might suggest that 1 full quarter would be sufficient to achieve full mixing. However, the figure does not account for the distribution of fishing effort (i.e. if all the gear is deployed a long way from the release site, all recoveries will suggest rapid movement, but they might not represent the movement of the general population). Also, directed seasonal migration can cause large displacements, without necessarily resulting in uniform mixing. Sensitivity to the mixing assumption was examined with mixing periods of 2 and 4 quarters (as shown figure 5, there are so few tag recoveries with a time of liberty exceeding 5 quarters that longer mixing periods probably do not contain much useful information):

- t2 = 2 quarter mixing period
- t4 = 4 quarter mixing period

Tag-induced Mortality and Shedding

Following Gaertner and Hallier (2009), we assumed that there was no tag-induced mortality, and the tag shedding was very low (0.015 y^{-1}).

Tag Age Assignment

The length of release of each tag is recorded in the database (Figure 10), but the model dynamics are based on ages. The age of each individual tag was estimated from the mean of the growth curve, assuming a 1 January birthdate, and an independent tag group was defined for each age/year/quarter release strata. The age estimation occurs external to the model (in a process similar to 'cohort-slicing' that is sometimes used to infer catch-at-age from catch-at-length data). Figure 11 illustrates the age assignment based on two growth curves used in the assessment (see Section 3.4 for growth options).

Note that this annual resolution of tag age assignments might introduce aggregation errors for this species (i.e. tags of age 1.0 and 1.75 are assigned externally identical biological characteristics), as *Stock Synthesis* automatically truncates fractional tag age assignments to the nearest annual age class. This could be circumvented by reconfiguring the model with quarters defined as years, and assign tags to quarterly age classes. This alternative configuration (Calendar Season as Model Year, or CSMY, as opposed to the current SS internal Year-Season structure, or SSYS) is described in detail in Section 3.2. However, given the variability in size-at-age distribution, the assignment of tags to finer quarterly age is unlikely to be accurate in reality (particularly for large/old fish). For CSMY models, we considered three options when assigning quarterly age from the length:

CSaMS - Q0 – 1 to 1 conversion (e.g. annual age 1 is simply converted to a quarterly age 4)
CSaMS - Q2 – 1 to 2 conversion (annual age 1 is converted to quarterly age 2 or 4 depending on size)
CSaMS - Q4 – 1 to 4 conversion (annual age 1 is converted to quarterly age 1–4 depending on size)

Tag releases were stratified by release region, time period of release (quarter) and the age classes. The returns from each tag release group were classified by recapture fishery and recapture time period (quarter). The model will predict expected recaptures by fishery for each release group. The number of tag release events and subsequent recovery groups will depend on the options of the tag age assignment (obviously there are more release events with finer quarterly age assignment), growth function (for cohort slicing), tag program, and spatial structure of the model. The number of tag release/recovery groups for different modelling options are summarized in Table 3. Note that not all options have been explored in the assessment (e.g. Q2 and Q4 have only been applied with the slow growth option).

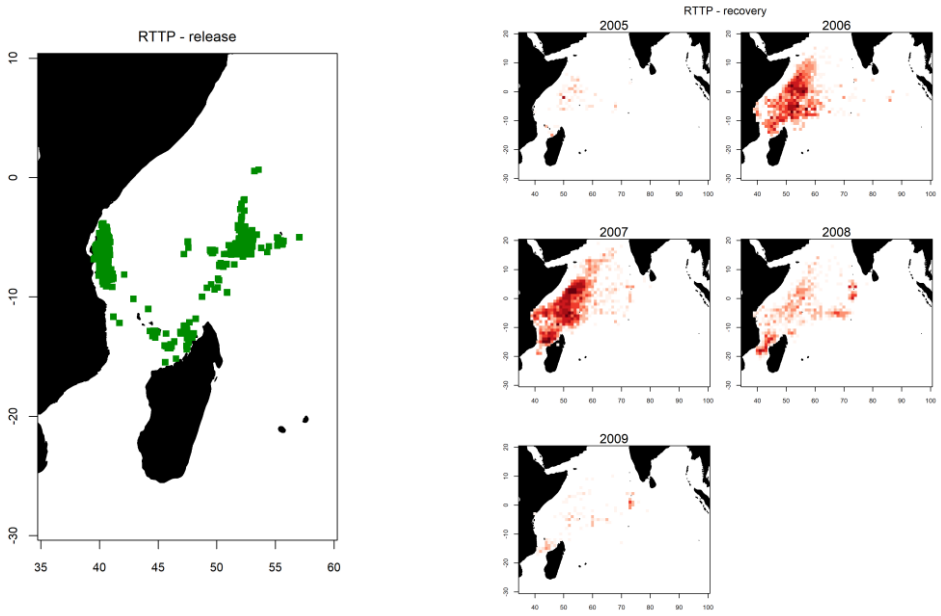

Figure 7: The total number of skipjack tuna tag releases (left) from the RTTP-IO tagging program and subsequent recovery by one degree of latitude and longitude.

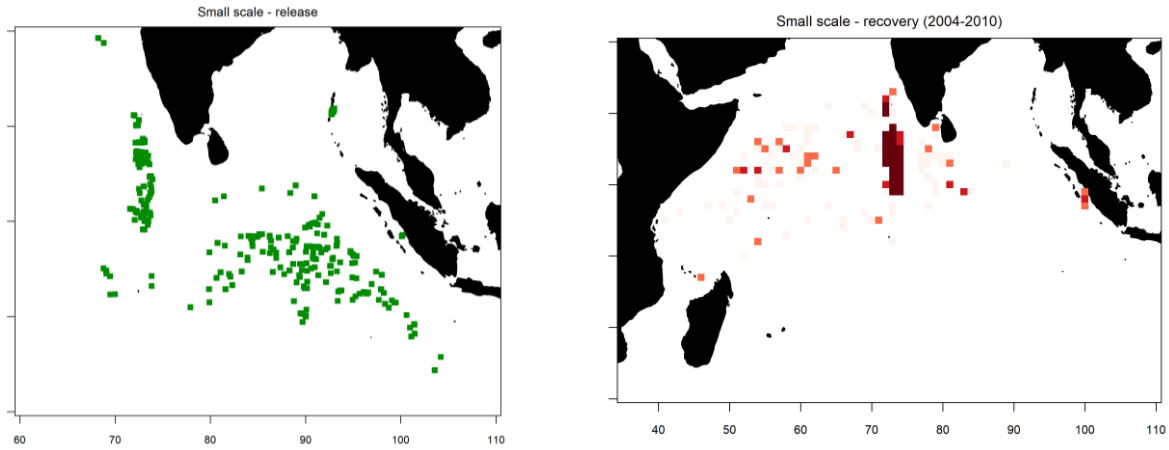

Figure 8: The total number of skipjack tuna tag releases (left) from the small scale tagging program and subsequent recovery by one degree of latitude and longitude.

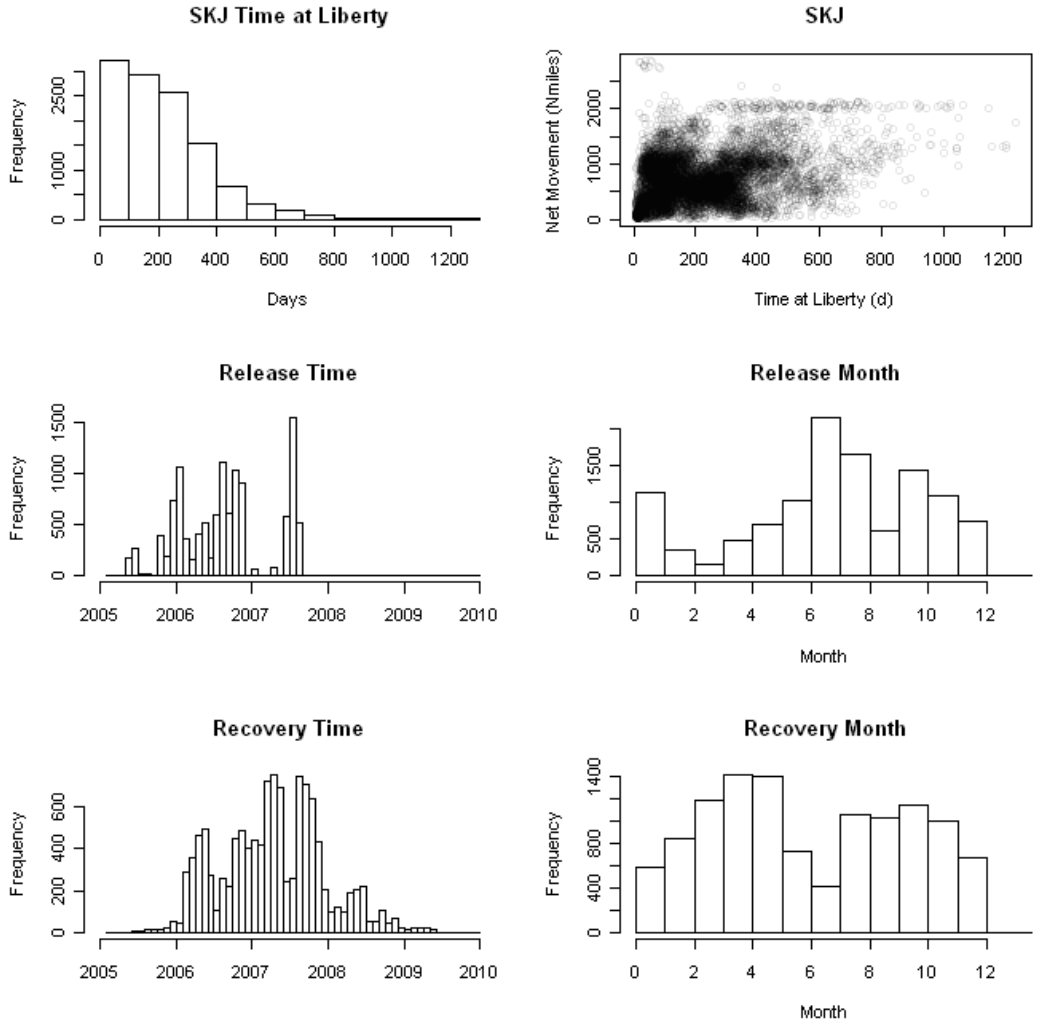

Figure 9. Summary of RTTP-IO SKJ tag release and recovery information 2005-2009.

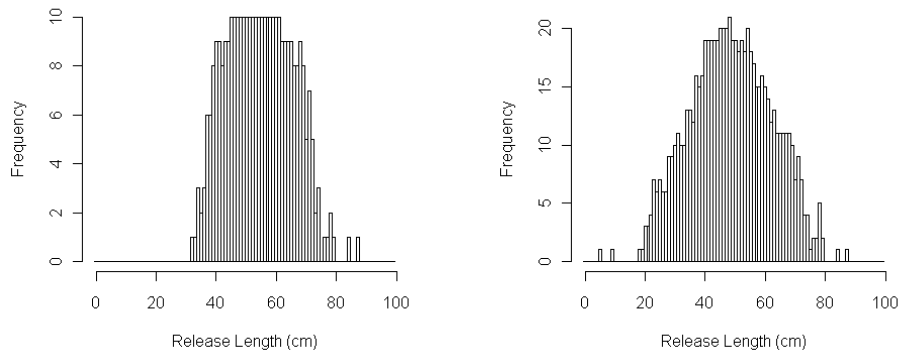

Figure 10: Distribution of tag release length-classes from the RTTP-IO (left) and combined RTTP-IO and small-scale tagging programmes (right). (Note that this is not the number of actual tags released)

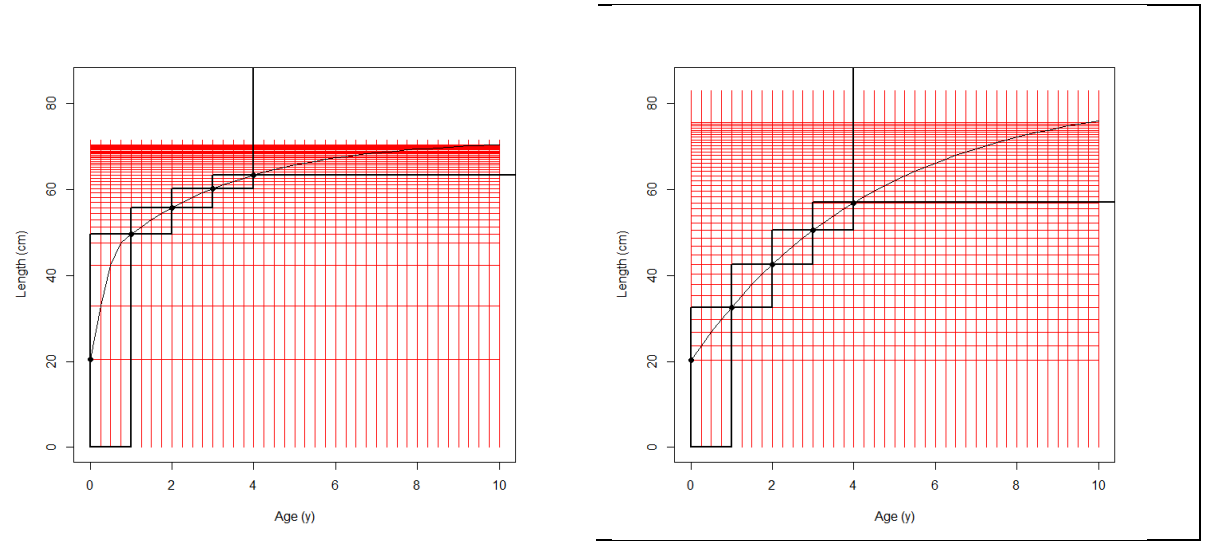

Figure 11. Relationships used for the assignment of tag lengths to ages for the annual 4 season configuration for the two growth curves: LR, left, and L83 right (see section for growth options). The tag release age is defined by the black circle preceding the black box that encompasses the tag release length.

.

Table 1: Summary of the two sets of tagging data compared within different assessment models.

model Grid option	rttp	Comments	rtss	Comments
Release Programme	RTTP-IO		RTTP-IO + small-scale	Includes Maldives, Sumatra, Lakshadweep, Mayotte and Seychelles
Release Period	2005-7		2002-9	
Recovery Fleets	EU/Sey PS	Reporting rates from tag seeding	EU/Sey PS Maldives PL	PS reporting rates from tag seeding; PL estimated
Recovery Period	2005-9		2004-9	
Total number of releases	78333		100620	
Number of releases in analysis	77893	Removed observations with no release size	100088	Removed observations with no release size
Total number of recoveries	10458		15270	
Total number of recoveries include in the analysis	10248	Removed observations with no release size, recovered on tagging vessel	12765	Removed observations with no release size, recovery on tagging vessel, recovery date earlier than release date, recovery fleet not EU/Seychelles PS or Maldivian PL

Table 2: Raw tag seeding data for the for EU/Seychelles PS vessels unloading in the Seychelles, and the reporting rate (point estimates) adopted in the assessment.

Year	Quarter	Tags Seeded	Seeds Recovered	Replace with updated estimates Reporting Rate in the assessment
2004	1	1	-	*45%
2004	2	1	-	*45%
2004	3	11	5	45%
2004	4	2	1	50%
2005	1	36	23	64%
2005	2	21	19	90%
2005	3	72	37	51%
2005	4	47	25	53%
2006	1	-	-	*76.5%
2006	2	36	36	100%
2006	3	69	60	87%
2006	4	204	191	94%
2007	1	99	91	92%
2007	2	77	73	95%
2007	3	188	173	92%
2007	4	151	139	92%
2008	1	30	30	100%
2008	2	22	16	73%
2008	3	78	74	95%
2008	4	52	45	87%
2009	1	29	25	86%
2009	2	-	-	*86%
2009	3	-	-	*86%
2009	4	-	-	*86%

*extrapolation or linear interpolation

Table 3: Number of release and recover groups (year/season/age strata) defined in SS3 for the different options on tagging program, growth, spatial structure, and temporal structure (see section 3) models options.

Program	Growth	Spatial structure	Temporal structure	Release group	Recovery group
RTTP	LR	IO	SSYS	49	489
		IO	CSMY - Q0	49	489
		IO	CSMY - Q2	87	712
		IO	CSMY - Q4	147	1107
	L70	IO	SSYS	45	487
		IO	CSMY - Q0	45	487
		IO	CSMY - Q2	74	732
		IO	CSMY - Q4	131	1096
	L83	IO	SSYS	40	470
		IO	CSMY - Q0	40	470
		IO	CSMY - Q2	66	687
		IO	CSMY - Q4	118	1052
RTSS	LR	IO	SSYS	78	653
		IO	CSMY - Q0	78	653
		IO	CSMY - Q2		
		IO	CSMY - Q4		
	L70	IO	SSYS	83	685
		IO	CSMY - Q0	83	685
		IO	CSMY - Q2		
		IO	CSMY - Q4		
	L83	IO	SSYS	79	676
		IO	CSMY - Q0	79	676
		IO	CSMY - Q2	139	956
		IO	CSMY - Q4	252	1397
	LR	IO2	SSYS	98	662
	L70	IO2	SSYS	104	694
	L83	IO2	SSYS	100	681

3. ASSESSMENT MODEL DESCRIPTION

The most important model assumptions are described in the following sections. The analysis was undertaken with Stock synthesis SS V3.24, 64 bit version (Methot and Wetzel 2013, Methot 2013). Standard population dynamics are described below, and equations can be found in Methot & Wetzel (2013). The template SS3 specification files for all of the models are archived with the IOTC Secretariat (The template control file is given in Appendix B).

3.1 Spatial structure

Similarly to the 2012 assessment, two spatial structured option are examined

IO model

The population dynamics are spatially aggregated. This model examined the entire Indian Ocean area as one unit, with the different fisheries operating in this one area. There remains an open question of the appropriate spatial structure to use for this tuna population (and most others). Qualitatively, the tagging data suggest that SKJ migrate quickly. Unfortunately, the limited distribution of tag releases, and small number of returns (and absence of tag reporting rate estimates) outside of the European/Seychelles purse seine fleets (mainly operating in the western equatorial Indian Ocean) makes it difficult to quantify large-scale movements at this time. It is notable that basin-scale movements into the eastern Indian Ocean were observed from the EU/Seychelles fleet, even though very little fishing occurred in this area. But we currently do not have enough information to know what the appropriate structure should be.

IO2 model

Recent genetic analyses (Dammannagado *et al.* 2011) have suggested that there might be two (or more) SKJ populations in the Indian Ocean. If this is correct, an aggregated assessment may not be appropriate. The 2nd model assumed that there are discrete populations west and east of 80° with the exception of the East Indian Ocean including the Maldives (Figure 12). Fonteneau (2014) suggested that this partition appears to be valid (but probably not ideal) as the major fisheries are located in the Western Indian ocean, and well fitted with the geographical scale of the observed skipjack movements.

With the two-area model. The PSLS and PSFS fisheries are assumed to be operating in the western IO, and the Maldives PL in the eastern IO. *Other* fisheries are partitioned between the eastern and western IO based on the finer scale (5x5) catch-effort datasets compiled by the Secretariat. Movement rates between the eastern and western IO are estimated only if the small scale tag data are included (assigning RTTP tag releases to the western IO, and small scale tags to the eastern IO), otherwise movement is not allowed. The Maldives PL and EU PS CPUE are assumed to index the abundance in the eastern and western IO respectively.

We note that the two-area model is only an approximation: the small amount of EU/SEZ operations in the eastern IO (including tag recoveries) were assumed to be part of the western population, and ii) not all of the catches from the *Other* fishery can be accurately allocated (e.g. it is known that Sri Lankan vessels operate in the west as well, but the Secretariat has no information describing the spatial distribution), (iii) and some of the releases from the small scale tagging programmes also occurred in the western IO.

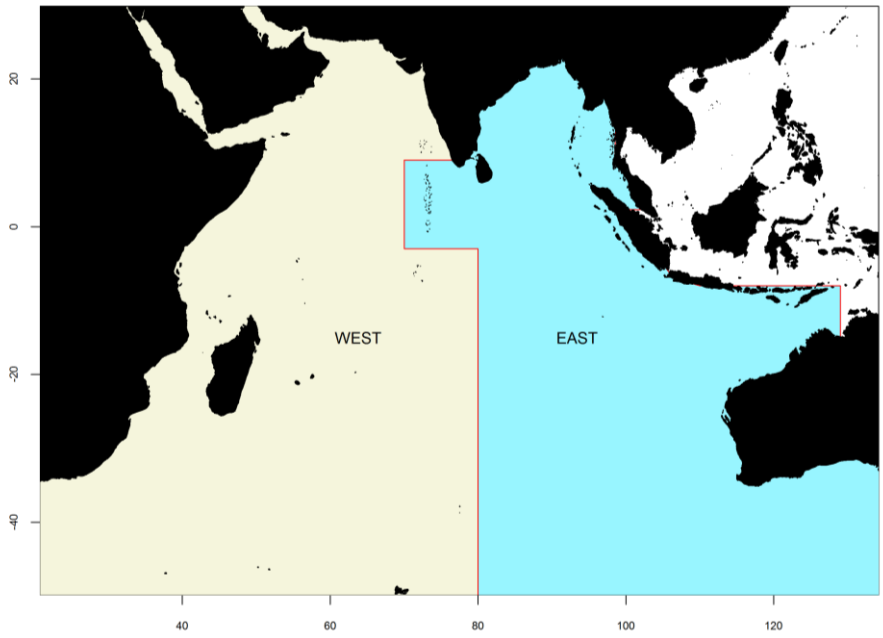

Figure 12: Areas used in two-area spatial structure model (rather than the 80 degree line, Maldives Atoll is included in the East so tag data can incorporate some movement)

3.2 Temporal units

Two alternative temporal structures are considered for the assessment.

SS3 internal year-season structure (SSYS)

This is the same as all previous assessments. The SKJ population dynamics were represented with an annual/four season configuration, referred as the SS3 internal year-season (SSYS). The model was iterated on quarterly time-steps, to represent potentially important seasonal dynamics, over the period 1952-2016 (plus 10 years of projections). However, the tag ages are assigned to annual increments, (see the tag section above). Also the spawning biomass is calculated once a year.

Calendar season as model year structure (CSMY).

The alternative option is to define quarterly time periods as years. The SS3 is set-up so that each quarter appears as a year, but the season duration is set to 3 (rather than the normal 12). (This means that the rate parameters such as M and K can stay in their normal per year scaling and this shorter season duration makes the necessary adjustments internally. Some other adjustments include re-indexing all "year season" inputs to be in terms of quarter-year (data has already been disaggregated by quarter as in the other option). This is referred to as the Calendar season as model year (CSMY). This is the configuration used for the Indian Ocean Yellowfin and Bigeye assessments (Langley 2016a, b).

With this option each age class is 3 months and each model “year” is a three month period. This allows for short term dynamics in SS and approximate continuous recruitment for tropical species (4 separate recruitments in one 12 month period). The quarterly time step allows for fine resolution in the growth and age specific selectivity (selectivity is modelled using length based functions, but is operated on an age-basis internally). Note that the SSYS structure already does resolve many population features on a seasonal basis including growth, and selectivity. In addition, the continuous recruitment can be approximated in a 12 month year model by estimating the seasonal recruitment distribution and then estimating temporal deviates on that distribution recruitment. However, perhaps the main advantage of

the CSMY structure is to allow tag release to be assigned to finer age classes (the annual age structure is considered be too coarse for fast growing tropical tuna). But it is not immediately clear whether there is any advantage of dong this and we considered the three options (Q0, Q2, and Q4) for assigning quarterly age with the CSMY model, as described in the earlier tag section.

With the Q0 option, the resolution of the tag age is the same as the annual model (annual age is simply multiplied by 4 to obtain a quarterly age), this was implemented to compare other aspects of model (i.e. growth, selectivity, and recruitment). The Q2 and Q4 options are to evaluate the effect of assigning finer quarterly ages to tagging data.

3.3 Population Dynamics

The dynamics described below pertains to the aggregated spatial model with the year-season structure (the IO model).

The model was sex-aggregated (and reported spawning biomass is the summed mass of all mature fish). The stock assessment model partitioned the Indian Ocean skipjack age groups 0–8 years with the last age a plus group (in unfished equilibrium, <0.25% of the population survives to reach the plus-group with the constant M value considered).

The population was assumed to be in unfished equilibrium in 1950, the start of the catch data series. The model was iterated from 1950-2015 using a quarterly time-step. The nominal unit of time in the model is one year during which population processes (e.g., recruitment, spawning, and ageing) were applied in sequence according to the dynamics implemented within the Stock Synthesis model (Methot 2013). Recruitment occurs once a year, and the SS3 will allocate recruitment to each season (the population will have a collection of seasonal cohorts with different birthdays), with the proportion being estimated as time-varying parameters. The Observations were fitted to model predictions on the seasonal basis within the year.

3.4 Growth

Skipjack growth is rapid compared to yellowfin and bigeye tuna. The 2011 assessment adopted two mean length-at-age relationships derived from tagging data. The two curves followed the standard von Bertalanffy growth function, with length at age zero fixed at 20cm. The two growth curve options were:

- L70 – L_{inf} = 70cm (Alejandro Anganuzzi and Julien Million, pers. comm.)
- L83 – L_{inf} = 83cm (Eveson 2011)

The shorter curve was estimated with unconstrained L_{inf}. It is notable that substantially higher L_{inf} values were estimated for the Atlantic (95-97 cm, ICCAT 2009) and Pacific (80cm, Hoyle *et al.* 2011). Accordingly, the L83 curve was fit with L_{inf} = 83 cm fixed, in recognition of the mode of large SKJ observed in the (poorly sampled) longline fishery.

The WPTT raised concern that the growth curves might not be capturing the rapid initial growth rate for this species (e.g. Kayama et al. 2009). The 2014 assessment (Sharma et al. 2014) considered the two stanza VB-logK curve of Eveson (2012), also derived from the tag-recapture data (Laslett et al. 2002). The VB-logK curve was approximated using a Richards curve in SS3:

- LR (Richards curve) – L_{inf} = 70cm, k=0.34, length at age zero fixed at 5 cm, and Richards parameter, 2.96, the age at which inflexion occurs on the skipjack.

All three options were considered in exploratory runs (Figure 13), only the Richard growth (LR) and the von Bertalanffy curve with L_{inf} of 83 cm (L83) are used in the final assessment grid.

Figure 14 visually compares the growth curves (LR and L83) to the tag length increment data (only a subset of data with known set type from the EU PS sets are shown), with the initial age at release assigned using a length-age key (assuming an equilibrium age-length structure based on an M of 0.8, the length-at-age from the respective growth curve with a CV 0.15). This illustrates that both growth curves appears to be visually consistent with the tag increment, depending on the assumed age at release (Note that these growth parameters were originally estimated with constraint on the initial size or age, or assumptions concerning other parameters).

The weight-length relationship has been updated using Chassot et al. (2016), where $W = 4.97\text{e-}006\ L^{3.39292}$.

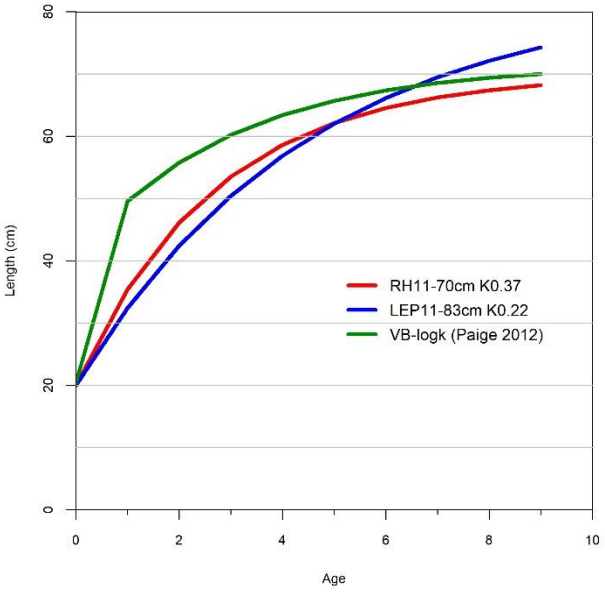

Figure 13: SKJ length-at-age relationships considered in 2017 assessment. L70 = RH11-70cm K0.37, L83 = LEP11-83cm K0.22, and LR = VB-logK. Note L83 and LR are used in the final assessment grid.

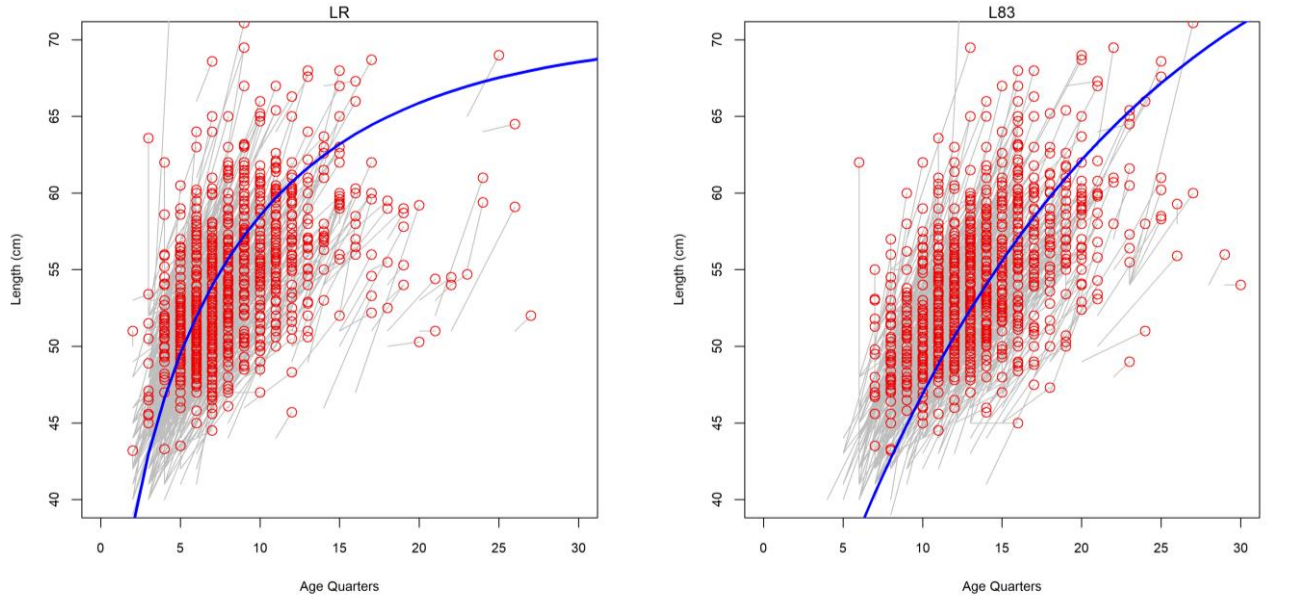

Figure 14: A visual comparison of the two growth curves (left, LR; right, L83) with tag-increments recovered from EU PS fleets (using recoveries with known set types). Start of segment is the release age-length, release age is assigned using the age-length-key derived from the growth curve and recovery age is the release age plus period at liberty.

3.5 Natural Mortality

Following previous assessments, two options were considered for natural mortality

- MAt – M equal to the ICCAT value (0.8), constant across all ages
- MeAs – M estimated ages 0-4

With the 2nd option, M at age was described by a series of annual nodes (with linear interpolation for ages between nodes). Parameters consisted of a normal prior (sd=1) with mode 0.8 for the first age, and deviations from the preceding age for subsequent ages, prior log(dev) = 0, sd=1). .

Kolody et al. (2011) showed that M estimates for ages 0-1 are very low and unrealistic for the RTTP tag option, and concluded that the low estimates are supported by the RTTP tagging data. We investigated this a bit further (as the fast growth option was not available in 2011, which created different age-at-release distributions) but reached the same conclusion. Therefore M was only estimated within the model when the small-scale data were included (*rtss* option). The independent Brownie estimates (Everson 2011) from tagging data explored in early assessment are not used this time (they are derived using a population model with a very different temporal structure, see Kolody et al. 2011, and they also appear to be very low compared to the assumed or estimated M in the other oceans).

3.6 Maturity

Maturity estimates from Grande *et al.* (2010) were adopted: invariant over time with 50% maturity at length 38 cm (Figure 15). This is very similar to the 40 cm value reported in the WCPFC assessment (Hoyle *et al.* 2011). But note that this estimate corresponds to age-at-maturity of 0.4 y with the Richard growth assumption, much younger than the knife-edge age 2.0 y assumption adopted for the Atlantic (ICCAT 2009).

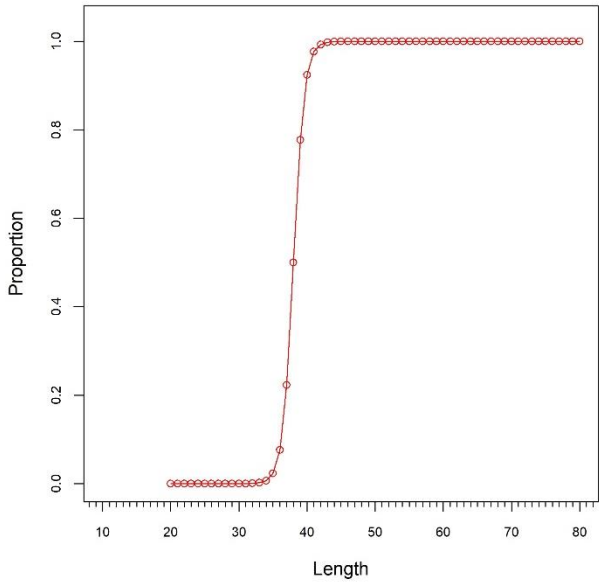

Figure 15: **SKJ maturity-at-length estimates from Grande *et al.* (2010).**

3.7 Selectivities

A non-parametric, length-based function was estimated independently for the selectivity of the 4 fleets. Selectivity parameters are estimated for a series of uniformly distributed length-class nodes, with cubic spline interpolation between nodes. Within the model, the length-based concept is used to calculate the

predicted catch-at-length distribution. Selectivity is converted to an age-based selectivity for purposes of removing the appropriate portion of the population in the catch. The function is flexible enough to represent dome-shaped, monotonically increasing (e.g. logistic), and polymodal functions (and was motivated by the clear bimodal distribution of the PL fleet). Seven nodes were estimated for the PL fleet, and 5 nodes for the PSLS, PSFS and Other fleets.

Given the high resolution information on selectivity (for some age classes) that may be available through the tagging studies, alternative models were also explored in which annual selectivity deviates were estimated for the PSLS and PSFS fleets 2004-9. It may also be worth considering seasonally-varying selectivity, but there was not time to pursue this. Only the stationary selectivity is considered in the assessment grid.

3.8 Recruitment

For some of the tuna species there is an indication of a strong seasonal pattern in recruitment (Adam Langley per. comm.). However, Itano (2000) suggested tropical tuna spawning does not always follow a clear seasonal pattern but occurs sporadically when food supplies are plentiful. SKJ has been assumed to have a more or less continuous spawning season

Recruitment was assumed to occur annually at the start of the year. New recruits enter into the population as age-class 0 fish (averaging approximately 20 cm). Annual recruitment deviates from the recruitment relationship were estimated in the model.

A Beverton-Holt stock recruitment relationship was assumed with steepness fixed at a range of options. ISSF (2011) summarises steepness estimates from tuna fisheries, the high values reported seem to be consistent with SKJ life history. The three steepness options below are defined in the model grids:

- H70: steepness (h=0.70)
- H80: steepness (h=0.80)
- H90: steepness (h=0.90)

Annual deviations from the stock-recruitment relationship were estimated for 1983–2015, assuming a lognormal distribution. The recruitment variability parameter σ_R is estimated assuming a prior mean of 0.6.

Spawning biomass (biomass of mature population) is calculated annually, and produces one annual total recruitment. This annual recruitment is distributed among seasons. These distribution parameters are time-varying, estimated for the period 1983-2015.

For models adopting the CSMY structure, spawning biomass is calculated at beginning of each quarter (modelled as year) and recruitment is generated from the stock-recruitment relationship. Recruitment deviations are estimated for each quarter from 1983–2015.

For the two-area model, annual recruitment is distributed among seasons as well as regions. These distribution parameters are assumed to be constant by area and season. When migration rates are estimated, they are also assumed to be time-invariant.

3.9 Assumptions about the Catch-at-Size data

Catch-at-length sample sizes are often very large, however, in these sorts of models, it is generally a bad idea to allow the size composition data to be weighted too highly. The size composition data influence these models in two main ways: i) ensuring that the correct age distribution is removed from

the population by the fishery, and ii) providing information about relative year class strength through the stationary selectivity assumption. The second point in particular can often lead to dangerous inferences for a number of reasons, including: selectivity (gear selectivity combined with spatial distributions and environmental variability) is often not stationary, samples are often not really representative of the catch, and growth/mortality assumptions may not be appropriate.

In this assessment, all length composition strata from all fleets were down-weighted to a considerable degree, and a range of options were explored to test if the model was sensitive to these assumptions. The *Other* fleet was further downweighted, because it represents a heterogeneous mix of fisheries, many of which are poorly sampled. Different input sample size assumption options were examined in the exploratory runs:

- CL5: $N_{PL,PS\ input} = \min(N_{obs}/50, 200)$; $N_{Other,input} = \min(N_{obs}/50, 20)$
- CL05: $N_{PL,PS\ input} = \min(N_{obs}/200, 50)$; $N_{Other,input} = \min(N_{obs}/200, 5)$
- CL01: $N_{PL,PS\ input} = \min(N_{obs}/1000, 10)$; $N_{Other,input} = \min(N_{obs}/1000, 1)$

Only option CL05 were considered in the assessment grid. The size distributions are represented in 22 bins of length 3 cm (≤20 to >80 cm). The multinomial likelihood was used in the model, with an additional 1% added to each length bin (predicted and observed) to make the term more robust to outliers.

3.10 Modelling methods, parameters, and likelihood

The model is conditioned on catch (weight), such that it is assumed to be known without error, and extracted perfectly. The SS3 "hybrid" fishing mortality parameterisation was used, where SS3 starts with Pope's approximation and then conducts a fixed number (4) of iterations to approximate instantaneous F from the Baranov catch equation.

The parameters of the model were estimated by maximising the log-likelihood of all data components plus the log of the probability density functions of the priors and penalties terms

- Likelihoods
    - Relative abundance indices – lognormal observation errors.
    - Length frequencies – multinomial sampling assumptions
    - Tag-recaptures – multinomial likelihood for the distribution of recaptures among fleets and the negative binomial distribution for expected and observed total recaptures following an initial mixing period.

- Prior distributions and Penalties:
    - Annual recruitment deviates – lognormal distribution
    - Other estimated parameters – generally diffuse priors

Assumed CV of 10% (lognormal observation errors) was applied to both standardised CPUE indices. We do not actually believe that the CV of 10% is realistic for these fisheries, however, in general, we would not have much confidence in any stock status inferences from models that fail to fit the core features of the relative abundance series.

The negative binomial distribution allows for overdispersion relative to the ideal, independent movement, fully-mixed, tag recovery distribution (*e.g.* which might be expected to conform to the Poisson distribution). Three options were explored for the overdispersion parameter τ (applied equally across all tag groups):

- t02 : $\tau = 2$ (close to ideal Poisson tag recovery assumptions)

- t20 : τ = 20
- t70 : τ = 70 (overdispersion is high, but note that this is not the same as down-weighting the tagging data in the likelihood)

We also attempted to estimate τ but the estimate is strongly driven by prior (i.e. the overage of τ is about 9 if the (beta) prior has a mean of 10, or 19 if the prior has a mean of 20).

The parameters estimated by the model included:
- Catchability for the CPUE series
- Selectivity parameters
- Virgin recruitment
- Annual recruitment deviations from the stock recruitment relationship
- Annual seasonal-specific recruitment deviations (SSYS models only)
- Recruitment distribution by area (IO2 models)

3.11 Reference points

The Skipjack tuna HCR adopted by IOTC has an output of a total annual catch limit based on a relationship between stock status (spawning biomass relative to unfished levels) and fishing intensity (exploitation rate relative to target exploitation rate). Therefore here we report depletion-based reference points including $SSB_{40\%}$, which is 40% of unfished spawning biomass, and $F_{40\%SSB,}$ which is fishing mortality corresponding to an equilibrium spawning biomass of 40% unfished level.

MSY, BMSY, FMSY and equilibrium yield estimates are calculated on the basis of the selectivity and F distribution among fleets observed in 2016. Kolody (2011) found that the FMSY calculation for SKJ usually failed, either due to a blatant numerical problem, or a more subtle inability to find the correct value. Furthermore, some models suggested a situation in which catch increases as fishing mortality increases toward an asymptote. This means that FMSY can be extremely high (Previous assessments reported the proxy C/MSY, which was considered to be more informative than F/FMSY).

4. ASSESSMENT MODEL RUNS

The approach we have taken here is to explore a range of model assumptions and parameter configurations, and to identify areas of uncertainty that would impact assessment results. The exploratory runs are used for examining model fits and diagnostics. Uncertainties are quantified using a grid of models running over permutations of plausible parameters and/or assumption options (an approach commonly used by t-RFMOs in the context of stock assessment, and in the development of operating models for Management Strategy Evaluation). Table 4 lists the assumption options that were explored in exploratory runs, as well as combined in a balanced “grid” design (i.e. possible combinations of a specified set of listed assumption options).

Table 4: Summary of SS3 specification options for the Indian Ocean assessment models. Other assumptions were constant for all models or specified separately for a particular model. The options below were applied in exploratory and grid runs (see Table for the details of grid run configurations). A few options that are not included in the grid runs are shown in grey. Options for the reference case are shown in red.

Assumption	Option Abbreviation
Spatial Option	io – whole Indian Ocean one area model (default unless stated otherwise) io2 – East and western Indian Ocean two area model
Temporal Option	SSYS – SS internal Year-season structure (default unless stated otherwise) CSMY – Calendar seasons as model years
Tag age assignment	Annual age (SSYS Option only) Q0 – 1 annual age to 1 quarter age conversion (CSMY Option only) Q2 – 1 annual age to 2 quarter age conversion (CSMY Option only) Q4 – 1 annual age to 4 quarter age conversion (CSMY Option only)
Tag Data	rttp – only RTTP releases, only EU/PS recoveries rtss – RTTP and small-scale releases, EU/PS and Maldives recoveries
Tag Mixing Periods	t2 – 2 quarters t4 – 4 quarters
Tag Recovery Overdispersion	od02 – negative binomial over-dispersion parameter 2 od20 – negative binomial over-dispersion parameter 20
Growth	L70 – update of Hillary et al 2008, Linf = 70cm L83 – Eveson et al 2011, Linf = 83cm LR – Eveson 2012 two-stanza growth (approximated by the Richard curve)
Stock-Recruit Steepness	h70 – steepness = 0.70, etc. h80 h90
Natural Mortality	MeAs – M estimated: ages 0-4 for (rtss option only) MAt – M fixed from the ICCAT values (0.8)
CPUE Series	Ua –PL CPUE series only U1 –PSLS CPUE series 1986–2016 U3 –PSLS CPUE series 2004–2016 UUa1–PL CPUE series and PSLS CPUE series 1986–2016
Catch-at-Length	CL01 – $N_{PL,PS\ input}$ = min(N/1000, 10), or min(N/1000, 1) for *Other* fishery CL05 – $N_{PL,PS\ input}$ = min(N/200,50), or min (N/200, 5) for *Other* fishery CL5 – $N_{PL,PS\ input}$ = min(N/50,200), or min(N/50,20) for *Other* fishery

4.1 Exploratory and reference models

Exploratory runs were undertaken under four alternative spatial and temporal model configurations as explained below (The description of all the models are given in Table 4):

One-area, SS interval year-season structure (IO)

These exploratory runs were undertaken to examine the options on:

- Choice of CPUE series as relative abundance indices (Models 1–4),
- Size-frequency sample size (Models 5–6)
- Growth (Models 7–8)
- Natural mortality (Models 9–11)
- Tag mixing period (Models 12)
- Tag recovery overdispersion parameter (Models 13–14),
- Tagging program options (Models 15–16)
- Stock-recruitment relationship steepness (Models 17–18).

Model 4 (referred to as model IO) is considered as a reference case where other models generally represent a single change to this model (each model is labelled according to the differences to model IO). A number of sensitivities were also undertaken: alternative PS CPUE series (catch per hour), and time-varying selectivity for PSLS and PSFS, the results are inconsequential and are not reported here.

One-area, Calendar season as model year (Q0, Q2, and Q4)

Four runs were carried out to explore option Q0, with a combination of growth and natural mortality options (Models 19–22). Other parameters are the same as the reference case. They are used to assess the change of the temporal structure of the model (without changing the tagging release age resolution).

Models 23–26 explored option Q2 and Q4 to assess of the effect of using finer tag release ages. We note that these runs are based on the slow growth option (L83) only.

Two-area, SS interval year-area structure (IO2)

Two runs were considered: model 27 included RTTP-IO plus small scale tag data (estimating migration between the two areas), and model 28 included only the RTTP-IO data (model 28, assuming no migration).

Two-area, Calendar season as model year (IO2Q0)

Here we simply converted the tag-release age to a quarterly notion (Q0). Similarly to IO2 models, two runs were carried out: model 29 included RTTP-IO plus small scale tag data (estimating migration), and model 30 included only the RTTP-IO tag data (model 28, assuming no migration).

Table 5: Names and descriptions of the exploratory runs (classified into four groups according to the spatial and temporal structure of the model). The reference case is highlighted in grey (model 4). Other runs are sensitivities with one off changes highlighted in red.

Run	Label	Spatial structure	Temporal structure	CPUE	LF Sample	M	Growth	h	Tag mix	Tag OD	Tag program
M1	Ua	IO	SSYS	Ua	CL05	Mat	LR	h80	t2	od20	rtss
M2	U1	IO	SSYS	U1	CL05	Mat	LR	h80	t2	od20	rtss
M3	U3	IO	SSYS	U3	CL05	Mat	LR	h80	t2	od20	rtss
M4	IO	IO	SSYS	UUa1	CL05	Mat	LR	h80	t2	od20	rtss
M5	CL01	IO	SSYS	UUa1	CL01	Mat	LR	h80	t2	od20	rtss
M6	CL5	IO	SSYS	UUa1	CL5	Mat	LR	h80	t2	od20	rtss
M7	L70	IO	SSYS	UUa1	CL05	Mat	L70	h80	t2	od20	rtss
M8	L83	IO	SSYS	UUa1	CL05	Mat	L83	h80	t2	od20	rtss
M9	MeAs	IO	SSYS	UUa1	CL05	MeAs	LR	h80	t2	od20	rtss
M10	MeAs-L70	IO	SSYS	UUa1	CL05	MeAs	L70	h80	t2	od20	rtss
M11	MeAs-L83	IO	SSYS	UUa1	CL05	MeAs	L83	h80	t2	od20	rtss
M12	t4	IO	SSYS	UUa1	CL05	Mat	LR	h80	t4	od20	rtss
M13	od02	IO	SSYS	UUa1	CL05	Mat	LR	h80	t2	od02	rtss
M14	od70	IO	SSYS	UUa1	CL05	Mat	LR	h80	t2	od70	rtss
M15	rttp	IO	SSYS	UUa1	CL05	Mat	LR	h80	t2	od20	rttp
M16	rttp-MeAs	IO	SSYS	UUa1	CL05	MeAs	LR	h80	t2	od20	rttp
M17	h70	IO	SSYS	UUa1	CL05	Mat	LR	h70	t2	od20	rtss
M18	h90	IO	SSYS	UUa1	CL05	Mat	LR	h90	t2	od20	rtss
M19	Q0-LR-Mat	IO	Q0	UUa1	CL05	Mat	LR	h80	t2	od20	rtss
M20	Q0-LR-MeAs	IO	Q0	UUa1	CL05	MeAs	LR	h80	t2	od20	rtss
M21	Q0-L83-MAt	IO	Q0	UUa1	CL05	MAt	L83	h80	t2	od20	rtss
M22	Q0-L83-MeAs	IO	Q0	UUa1	CL05	MeAs	L83	h80	t2	od20	rtss
M23	Q2-L83-MAt	IO	Q2	UUa1	CL05	Mat	L83	h80	t2	od20	rtss
M24	Q2-L83-MeAs	IO	Q2	UUa1	CL05	MeAs	L83	h80	t2	od20	rtss
M25	Q4-L83-MAt	IO	Q4	UUa1	CL05	MAt	L83	h80	t2	od20	rtss
M26	Q4-L83-MeAs	IO	Q4	UUa1	CL05	MeAs	L83	h80	t2	od20	rtss
M27	IO2	IO2	SSYS	UUa1	CL05	Mat	L83	h80	t2	od20	rtss
M28	IO2-rttp	IO2	SSYS	UUa1	CL05	Mat	L83	h80	t2	od20	rttp
M29	IO2Q0	IO2	Q0	UUa1	CL05	Mat	L83	h80	t2	od20	rtss
M30	IO2Q0-rttp	IO2	Q0	UUa1	CL05	Mat	L83	h80	t2	od20	rttp

4.2 Quantification of uncertainty

A common approach utilized by t-RFMOs to assess the structural uncertainty in the assessment is to run a grid of models that explore the interactions among model assumptions. The grid contains combinations of plausible parameter and assumption options to assess the sensitivity of stock status and management quantities to this uncertainty, with the aim of providing an approximate understanding of variability in model estimates due to assumptions in model structure not accounted for by statistical uncertainty estimated in a single run (McKechnie et al. 2016). The approach used here focuses on the model selection uncertainty, which is usually much greater than the statistical uncertainty conditional on any individual model (Kolody et al. 2011).

For each of the four spatial/temporal model structures explored, an examination of uncertainty in the model structure was integrated into a single assessment grid. In an assessment grid, a separate model was run for each combination of parameter and assumption options. This is useful to determine if there are particular interactions between model assumptions. Model option combinations for these assessment grids are summarised in Table 6. Grid-IO and Grid-Q0 have 144 models each, and Grid-IO2 and Grid-IO2Q0 have 72 models each. The models in each assessment grid were assumed to have equal plausibility (weight).

Table 6: Model configuration combinations used in assessment grids (where a grid represents the list of models with a balanced design of all possible permutations of the indicated options. Number of models included in each grid is shown in the bracket. Note that only *Mat* option is used for tag program *rttp*

Configuration	Grid-IO (144)	Grid-Q0 (144)	Grid-IO2 (72)	Grid-IO2Q0 (72)
Spatial structure	IO	IO	IO2	IO2
Temporal structure	SSYS	CSMY - Q0	SSYS	CSMY - Q0
CPUE	Ua,UUa1	Ua,UUa1	UUa1	UUa1
LS sample	CL05	CL05	CL05	CL05
Growth	LR, L83	LR, L83	LR, L83	LR, L83
steepness	h70, h80, h90	h70, h80, h90	h70, h80, h90	h70, h80, h90
M	Mat, MeAs	Mat, MeAs	Mat, MeAs	Mat, MeAs
tag mix period	t2, t4	t2, t4	t2, t4	t2, t4
tag OD parameter	od02, od20	od02, od20	od02, od20	od02, od20
tag program	rtss, rttp	rtss, rttp	rtss, rttp	rtss, rttp

4.3 Projections and Kobe 2 Strategy Matrix

Projections were conducted from the MPD estimates of all grid models at catch levels of 60%, 80%, 100%, 120% and 140% of 2015 levels (assuming 2015 selectivity and catch allocations among fisheries). The projections used deterministic recruitment from the stock recruitment relationship (starting in 2013). This approach ignores two important sources of uncertainty: statistical uncertainty in the parameter estimates, and recruitment variability. However, the approach does incorporate the model selection uncertainty, which is usually greater than both of these other sources of uncertainty in most cases. However, if the model selection process results in a very small subset of heavily weighted models, or important decision are required in relation to the tails of the distribution, the additional sources of uncertainty should be considered. Three and ten year projection results are summarised in a management decision table (Kobe 2 Strategy Matrix), i.e. The projections are summarised in terms of a weighted average of results that describe the proportion of scenarios in which $SSB_{2019} < SSB_{40\%}$, $SSB_{2026} < SSB_{40\%}$, $F_{2019} > F_{40\%SSB}$, $F_{2026} > F_{40\%SSB}$

5. RESULTS

We discuss the main results of exploratory model runs below. Given the large number and complexity of the models, it is not possible to show all the details, we mainly address the key aspects or emphasise the main points of interest. Diagnostics plots including model comparisons are given in Appendix A, and those related to key conclusions are given in the section below. Estimates of management quantities for all the exploratory models are shown in Table 7.

5.1 Reference case

The profile likelihood on R0 for the reference case (model IO) confirmed that the global minimum was obtained by the maximum likelihood estimate (Figure 16). It suggested that there is no major conflict among various sources of likelihood components, in particular between the abundance indices, size frequency, and tag recoveries data. However, the size data appears to support a higher R0 (i.e. higher B0) – this is not too surprising as the size structure of the catch was generally stable over-time for the main fisheries. There is also reasonable contrast in the profile, indicating sufficient information existed in the data for estimating absolute abundance. But we caution that the profile likelihood is conditioned on the configurations of this particular model including fixed parameters and data-weighting, therefore the general conclusion may not be drawn for other models runs.

The model fitted Maldives PL and EU (long) CPUE indices reasonably well, and it captured the inter-annual variability of both time series (Figure 17). There appears to be no coherent seasonal trend in either time series and the pattern in the predicted indices is due to one or two dominant seasonal cohorts estimated by the model. Standardised residuals from the fits show no obvious unexplained variations in the fits (Figure 18).

The models provided a good fit to the aggregate size composition data (Figure A4). However, the fit to individual years is much less impressive for PLFS and the Other (Figure 19), where the size distribution varied greatly between years. There appears to be some seasonality to the selectivity (particularly for the PSFS fleet), which is not captured in the current model (Figure A4).

The selectivity estimates show that larger fish are caught in the PL and Other fisheries, and that the youngest ages (including the 38cm maturity threshold) are only weakly vulnerable to the fisheries (Figure 20).The dome shape could be an artefact of the fixed M assumption for all ages over 4 years, combined with the small number of observations of large fish, and uncertain growth curves.

Estimated annual recruitment suggested moderate variability (sigmaR was estimated to be 0.30) is required to match the size composition and CPUE data. Recent recruitment has been below the historical average (Figure 21-left). Continuous spawning might be expected to cause important seasonal variability in recruitment for this species. The model estimated one dominant recruitment season, with trivial recruitment in the other seasons (Figure 21-right). This appears to be a feature of the fast growth option (LR), and therefore we do not have have much confidence in that pattern.

Overall there is a reasonable fit to the tag recoveries (Figure 22). However the fit to the mode of the recoveries from the PL fishery is poor. The recoveries by the PL fleet are mostly releases from the small scale program in the eastern IO, which may have different mixing dynamics to RTTP-IO releases in the western IO (the spatially aggregated model assumes all the tag releases came from a homogenous population). There is further complication of the low reporting rate of the PL fleet (which may not be constant over time). The spatial heterogeneity in mixing rate can be partially accounted for by assuming a longer mixing period or introducing spatial structure into the model (see the next section).

Estimated biomass showed two steep declines, one in the late-1990s and the other in the mid-2000s (Figure 23), possibly explained by catch removals and recruitment variability. The biomass has increased over the last four years. The spawning biomass in 2016 is estimated to be about 49% B0.

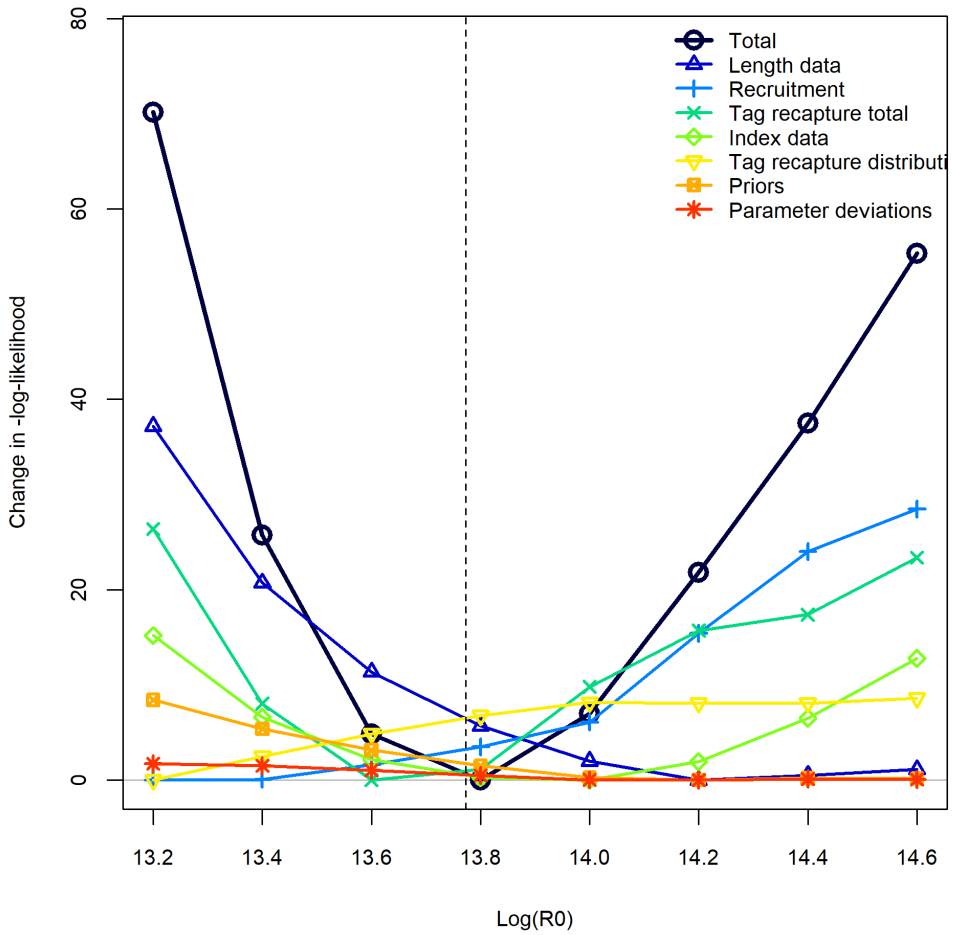

Figure 16: Likelihood profile on R0 from reference model IO.

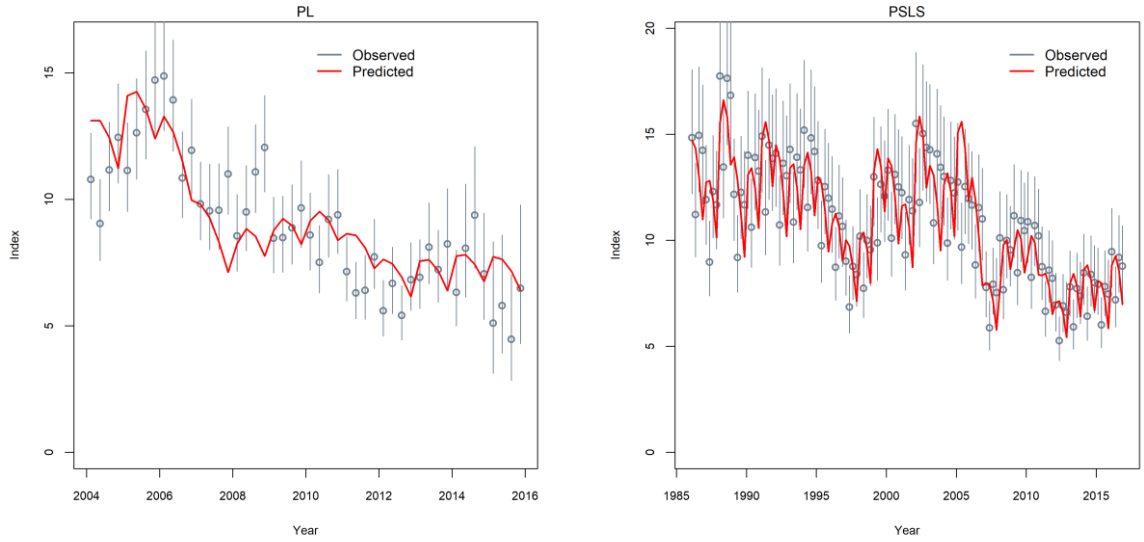

Figure 17: Fits to Maldives PL CPUE and the EU PS CPUE (long) for the reference model IO.

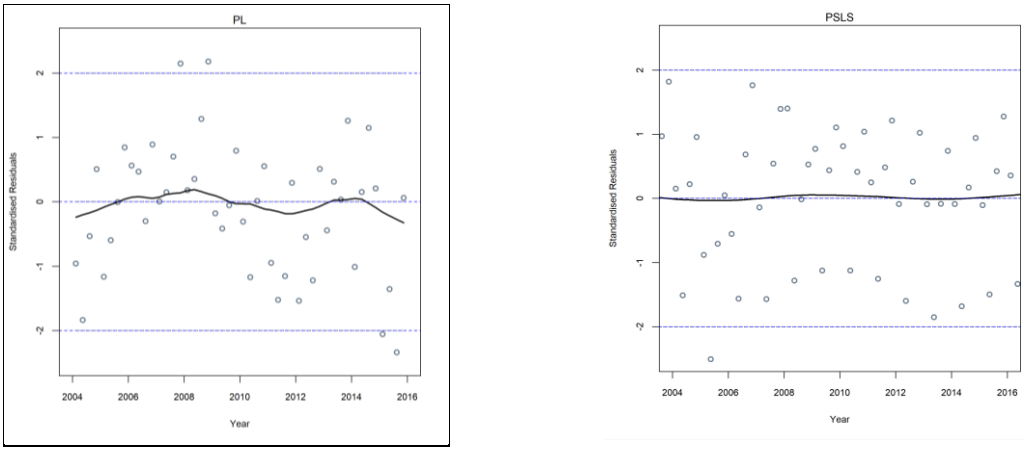

Figure 18: standardised residuals from the fits to Maldives PL CPUE (left) and the EU PS CPUE (long) for the reference model IO (right).

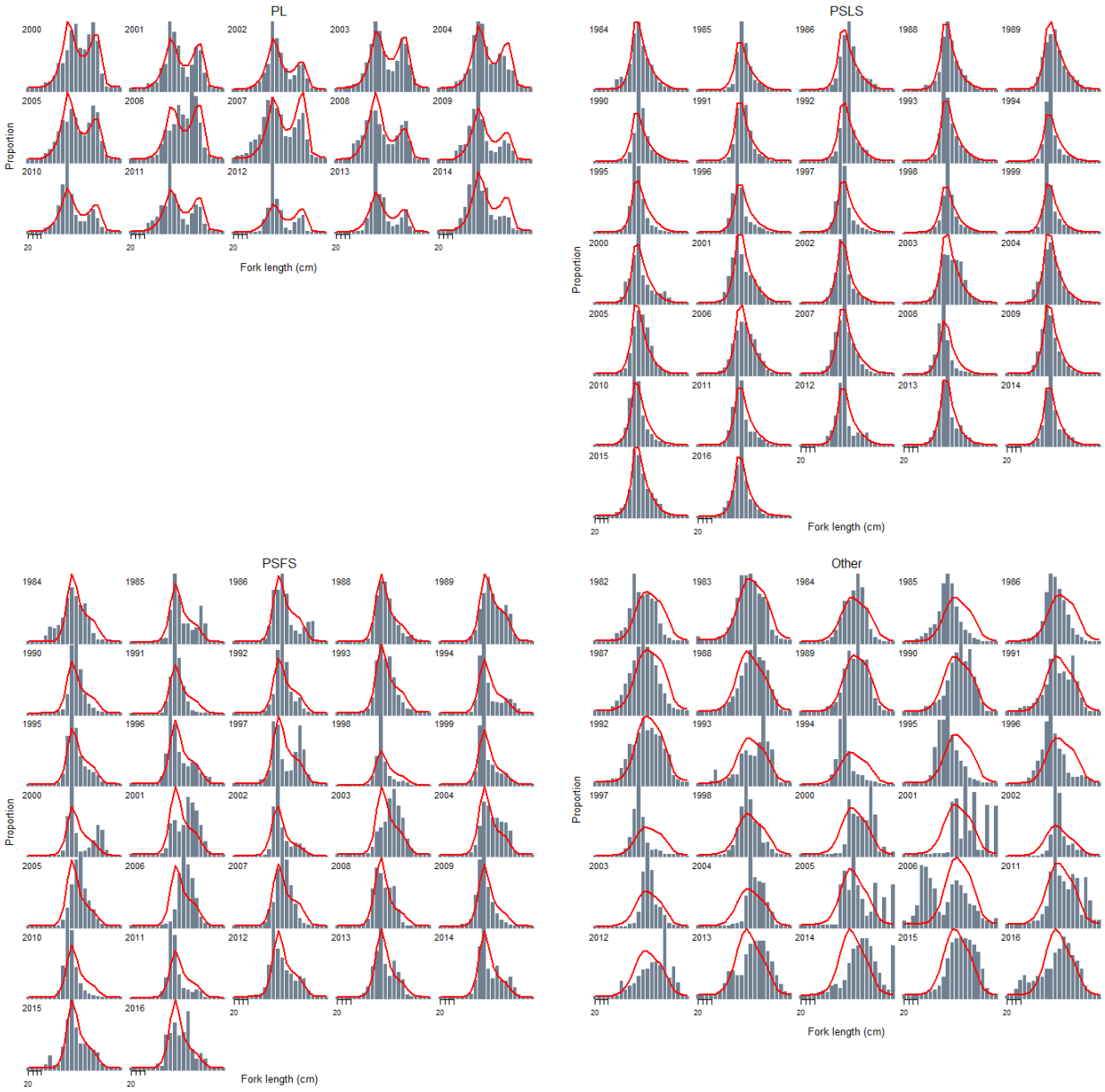

Figure 19: Annual aggregated fits to length frequencies from the PL, PSLS, PLFS, and Other fisheries for reference model IO.

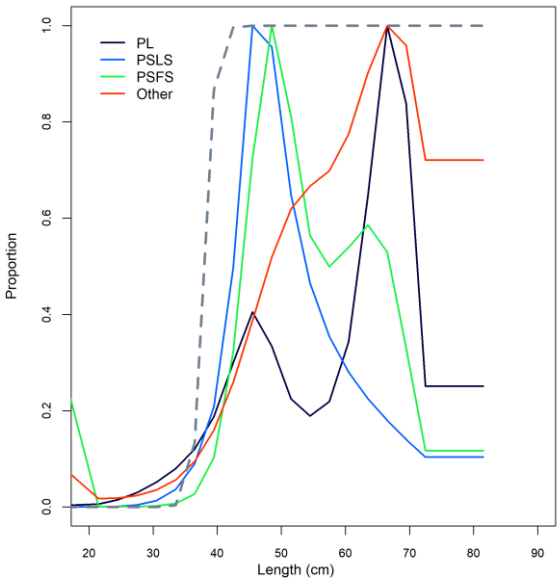

Figure 20: Estimated spline selectivity for the PL, PSLS, PSFS, and Other fisheries, overlaid with the maturity-at-length for SKJ for the reference model IO.

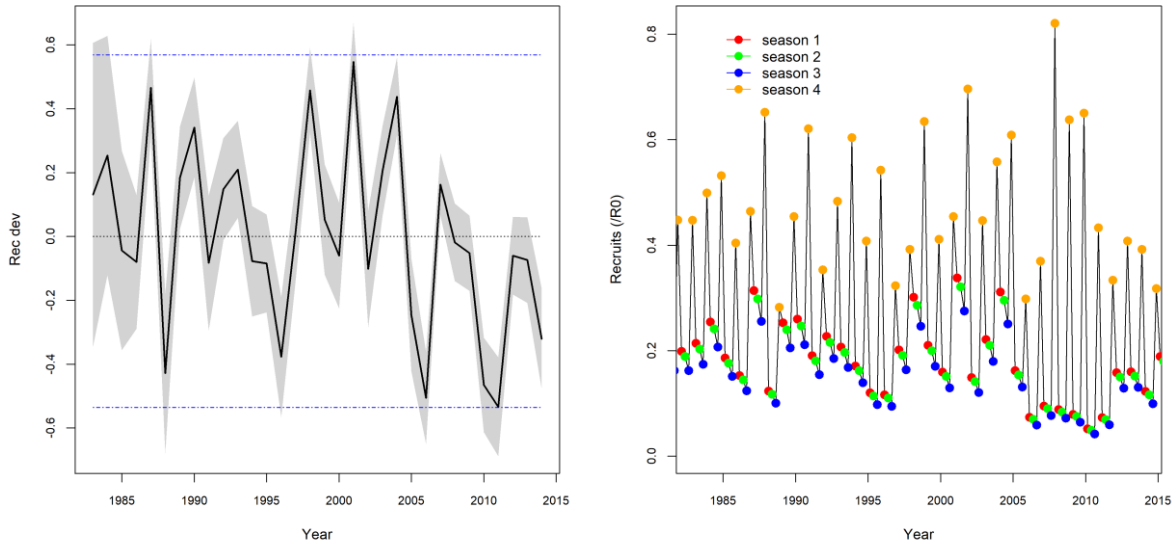

Figure 21: Estimated annual recruitment deviations (left) and recruits by season (right) for the reference model IO. The shaded area represents uncertainty estimates from the MPD fits.

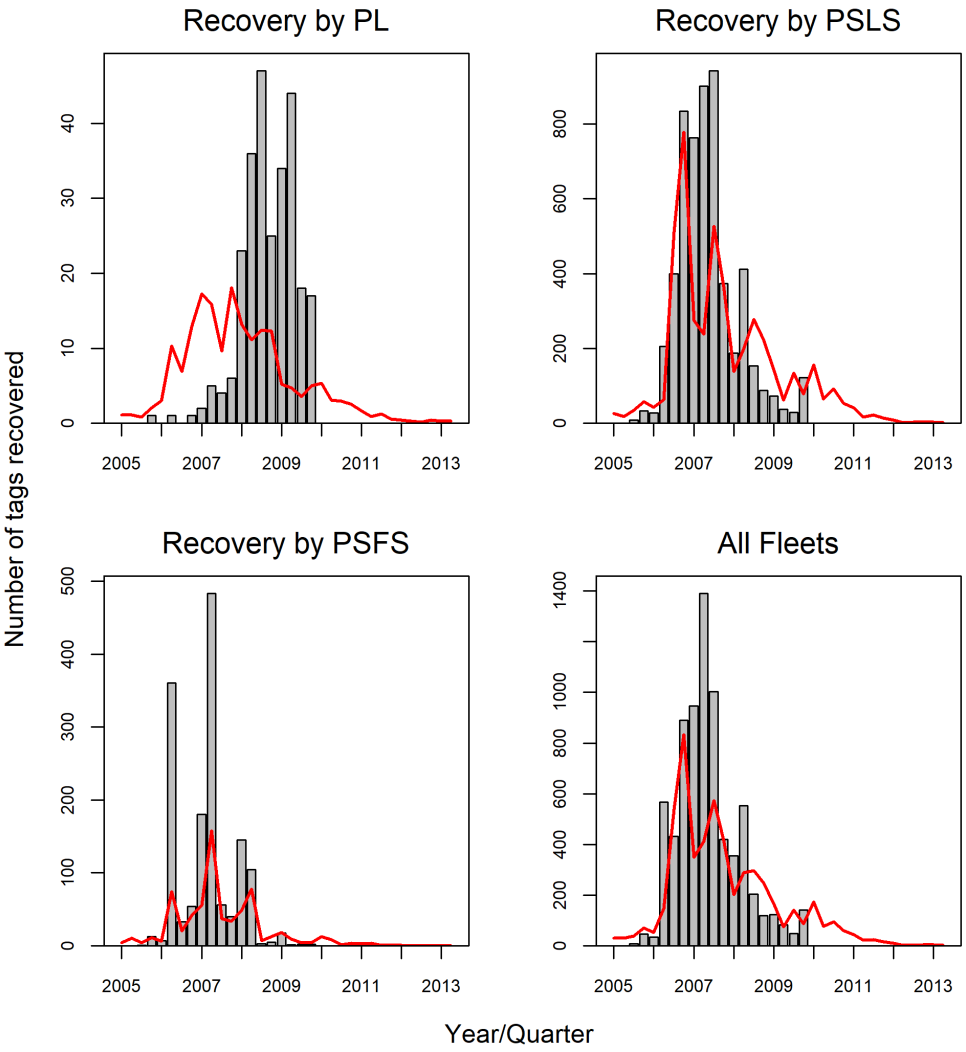

Figure 22：Predicted and observed tag recaptures by recapture year/quarter and fleets aggregated across tag groups for the reference model (IO). Note that only observed recaptures after the mixing period are included

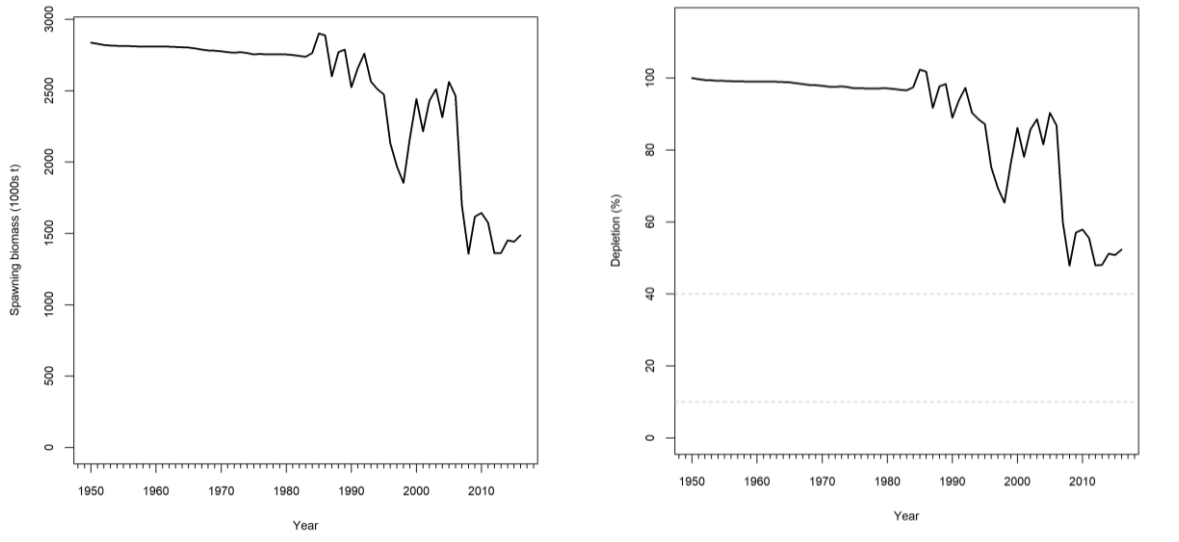

Figure 23: Estimated Spawning biomass (left), and depletion for the reference model (IO).

5.2 Exploratory runs

One-area, SS interval year-season structure

CPUE options

Separate models were fitted to the three sets of CPUE (Ua, U1, and U3). The CPUE series are generally fitted well (Figure A1). The predicted abundance in the 1980–2003 period are different between these models (Figure A2). Models Ua (PL CPUE) and U3 (short PS CPUE) both estimated a steep population decline in 1980–1990, followed by a large increase 1994 – 2000 (model U3 showed a four-fold change in biomass). As no CPUE was fitted during that period for both models, the signal is driven by the recruitment pattern (Figure A3).

LF weighing

The model with large LF sample sizes (CL5, capped at 200) showed poor fits to recent CPUE (Figure A4), indicating that the model may have over-fitted to the noise in the LF data. This model did not fit the size data appreciably better than the CL05 option (Figure A4). The model with smaller sample sizes (CL01, capped at 10) appeared to have some bias in the fits to the mean length for the PL fishery (Figure A4).

Growth

The slow growth options (L83 and L70) resulted in smoother predicted CPUE (and mean sizes), with an overall similar trend to the fast growth option (Figure A5). This is because the models have apportioned recruitment among the four seasons equally (Figure A6). This indicates that the dominant seasonal recruitment estimated by model IO may be an artefact of the fast growth option used in that model.

Natural mortality estimation

Models with combined RTTP and small-scale tagging data often provided natural mortality estimates that suggests M at age 2 was high, and M at age 33) was low (Figure A7). The overall pattern appears to be similar to those estimated in the WCPO SKJ assessment (see Figure 12 of McKechnie et al. 2016). The estimates are also similar in magnitude to the assumed M in the ICCAT assessment. The estimated M at ages 0 and 1 is undoubtedly low for the rttp option (not shown).

The estimates of M represent a compromise between the catch-at-size and tagging data: the catch-at-size data supported a smaller M, whereas tag recovery data are in favour of a higher M (Figure A8). This is not too surprising as catch-at-size data suggest a maximum age of at least 8 y (if the growth is correct), whereas the tag-capture data implied that SKJ will not survive longer than four years after release. The difference in M estimates among various growth options is possibly to do with the assumed age at the tag-release.

Tag options

The two quarter mixing period is probably not long enough to insure full mixing throughout the Indian Ocean, but may be reasonable for the core PS area. The 4 quarter mixing period improved the fits to PL tag recovery (Figure A9), but may erode the information content in this key data, given the small number of releases at liberty for greater than a year. Assuming tag recovery is close to an ideal, independent, and fully-mixed process (option od02) only marginally improved the fits (Figure 10).

The longer mixing period, lower overdispersion parameter value, and the inclusion of the small-scale tagging programmes would suggest a more productive stock (Figure A11).

The rtss option included the recoveries from PL fishery, which is not expected to contribute much to the model as the reporting rate is estimated in the model. But the inclusion of the small amount of recoveries by the PS fleet of the tags released by the small-scale tagging program in the east (~0.9% recovery rate compared to the ~15% recovery rate for the tags released from the RTTP program) is expected to increase the biomass estimates.

Steepness

It is well known that a key parameter determining the value of the ratio SSBMSY/SSB0 is the shape of the stock-recruitment relationship. SSBMSY/SSB0 was estimated to be 0.22 for h=0.8, and much lower for h=0.9 (Figure A12-left). The combination of high M, young maturity and weak selectivity of young fish suggest that it could be very difficult to seriously overfish this population (Kolody et al. 2011). Figure A12 shows that there is a protected part of the spawning population that will not be touched even with large increases in effort. It appears that Fmsy cannot be estimated reliably when steepness is very high. The reference point $F_{\%40SSB}$ appears to be less sensitive to the range of steepness examined (Figure A12-right).

One-area, Calendar season as model year (Q0, Q2, and Q4)

We first compare model IO and Q0 to evaluate the change of the temporal structure. Then we assess the effect of assigning finer tag release age classes.

For the SSYS model (IO), the recruitment occurring in each season is assigned the same growth pattern, but each seasonal cohort's growth is shifted along the age/time axis (Methot 2014). Therefore the size-at-age, when tracked for fish of different birthdays, is identical to that of the CSMY model (Q0), except for a negligible difference in variability as a result of the interpolation between age classes (Figure A13).

Similarly the selectivity at age (which dictates how catch are removed from the population) in the SSYS model, when joined for all seasonal cohorts, are almost identical to the selectivity-at-quarterly-age-class of the CSMY structure (Figure A14). The minor difference is due to differences in the estimated length-based selectivity parameters.

The main difference between the two models is the recruitment. The annual recruitment deviation estimates are similar (not shown), but the CSMY model had much less seasonal variation compared to the SSYS model, which is dominated by one seasonal class (Figure A15-left). The difference is smaller with the slow growth option (Figure A15-right). In general the CSMY model estimated a smoother pattern in seasonal recruitment, and as the result, there is less variability in predicted CPUE or mean length (Figure A16), but the overall fits to these data are similar to the SSYS model.

There appears to be some marginal improvement in the fits to the tagging data in the model Q0. This can only be attributed to the change of the temporal structure as the tag release age are not affected (Figure A17).

Assigning finer age classes to tag releases (model Q2 and Q4) had very minimum effects on the fits to the tagging data (either by recovery age or year, Figure A17).

When M was estimated in the CSMY models, the estimates appeared to be less variable across ages (Figure A18), but the overall pattern is similar to the SSYS models. Assigning finer age classes to tag releases had only minor effects on the estimates.

Overall, the CSMY models suggested a somewhat less productive stock, with lower biomass estimates compared to the SSYS models. But this appears to be dependent on the growth options, and the difference is smaller between the two model structures with the slow growth option (Figure 24-left). Assigning finer age classes to tag releases had little effect on biomass estimates (Figure 24-right).

Two-area models (IO2 and IO2Q0)

The two-area model was implemented for both SSYS (IO2) and CSMY (IO2Q0) configurations, and adopted rtss or rttp options.

The IO2 model that included the rtss data estimated zero movement rate from the eastern to the western Indian Ocean; the IO2Q0 model estimated about 15% movement rate at age between 0 and 1 from the east to west (Figure A19-left). Both models estimated about 60% movement rate from west to east Indian Ocean from age 4 (Figure A19-right). Neither of these estimates appear sensible. We do not have much confidence in the model's ability to estimate migration as there are very few tags that had crossed the border. Nevertheless, the two-area model improved the fits to the tag-recovery data (Figure A20) by partitioning the tag-release groups between the eastern and the western areas.

The four models estimated very different biomass distribution between the eastern and western Indian Ocean (Figure 25). In this type of multi-area models, additional constraint is sometimes required to allow the model to estimate the relative biomass among areas (e.g. the use of common catchability parameter between CPUE in the absence of tagging data). For skipjack, the catchability of PS CPUE is not comparable to that of PL, and the tagging data is mostly from the western Indian Ocean. We examined the biomass distribution (east relative to west) for all the two-area models defined in the assessment grid (Figure 26). The biomass ratio of the east to the west varied greatly among parameter options, tag program, and model structure (the ratios ranged from 0.5 to 80 for IO2 models using rtss data). The estimates appear to be more sensible for models using rttp data, but there are marked differences between models of different temporal structure. We believe the two-area model requires further investigation or development. And at this stage, management quantities are not derived using the two-area spatial structure.

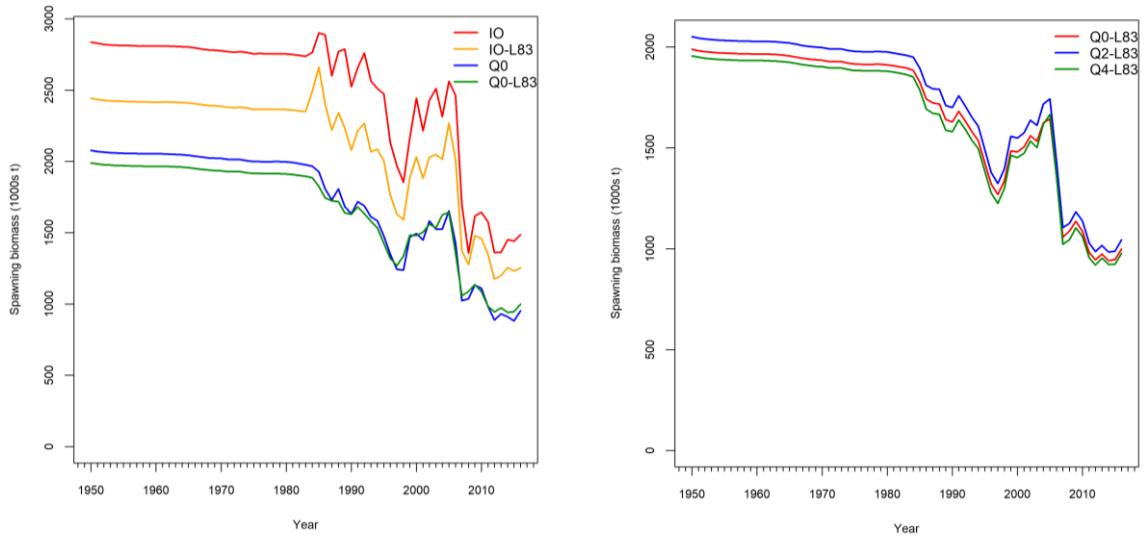

Figure 24: Estimated spawning biomass for models IO, IO-L83, Q0, Q0-L83 (left), and for models (Q0-L83, Q2-L83, Q4-L83).

IO2-rtss IO2-rttp

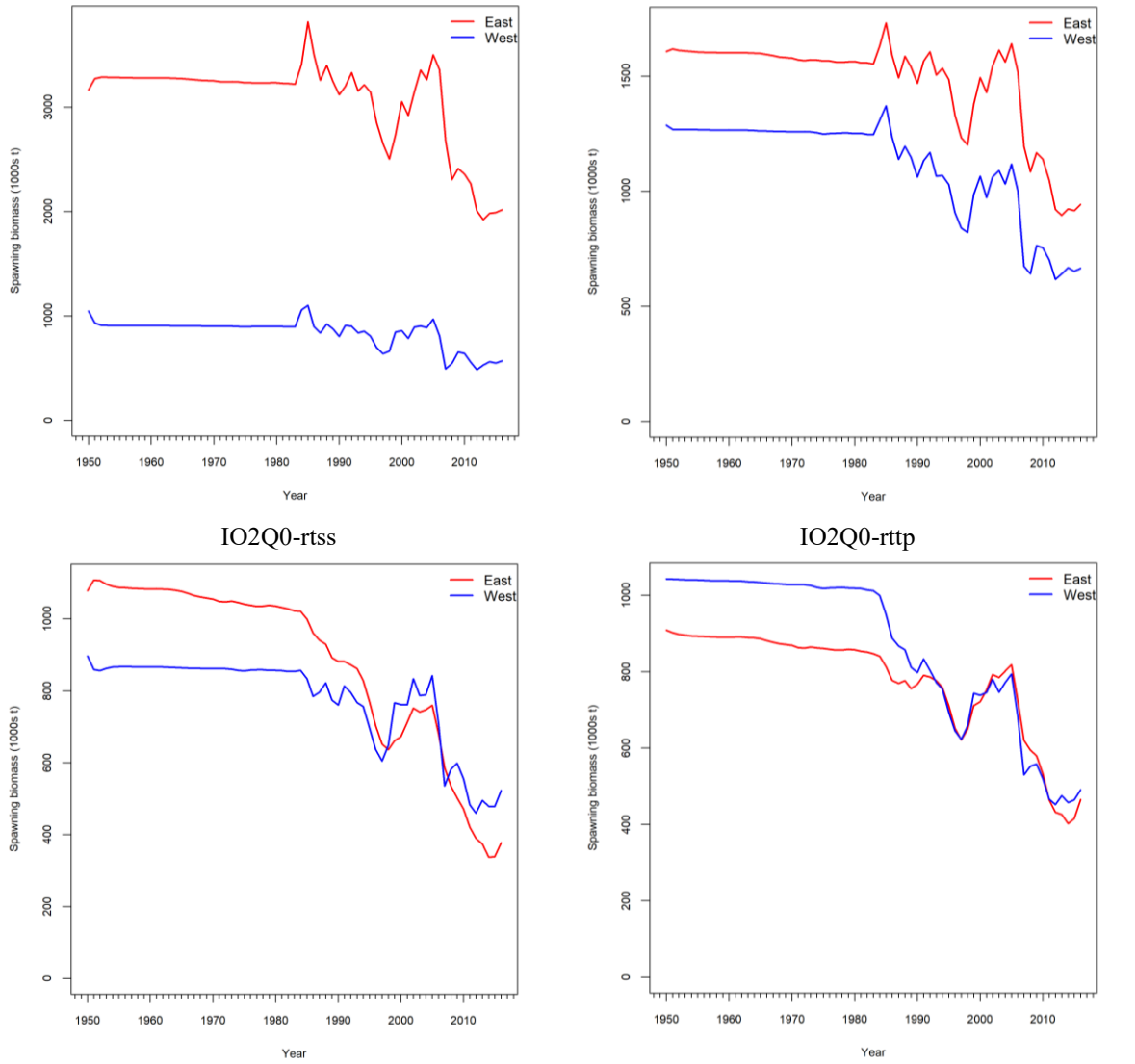

Figure 25: Estimated spawning biomass by area for models IO2-rtss, IO2-rttp, IO2Q0-rtss, IO2Q0-rttp.

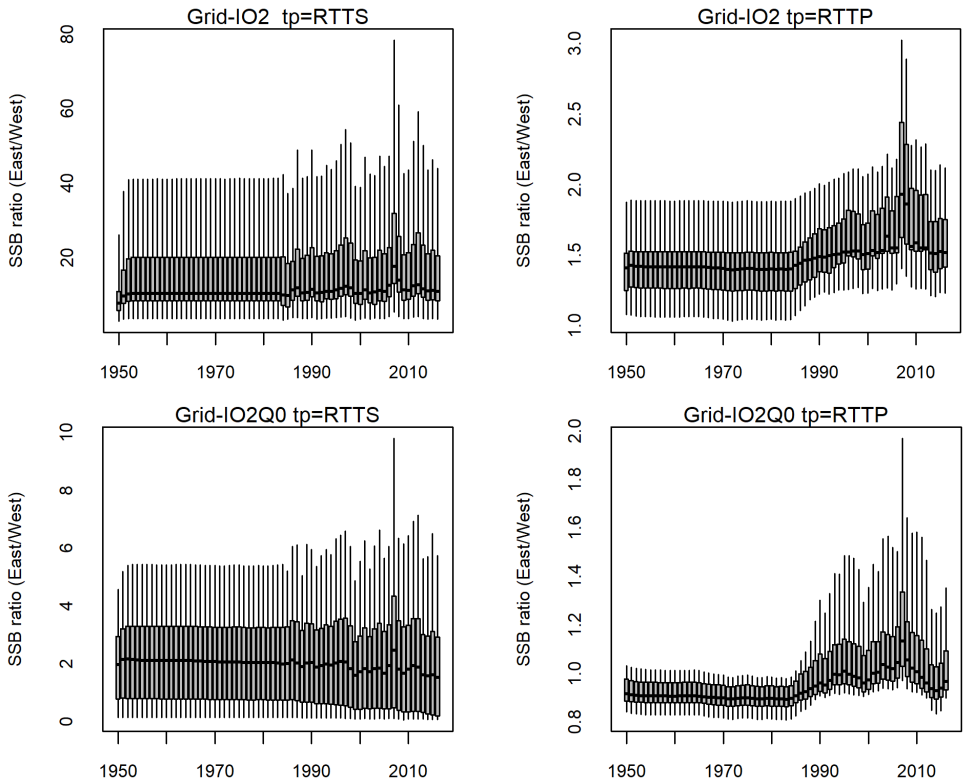

Figure 26: Ratio of spawning biomass in the east to the west IO estimated from the grid of model runs Grid-IO2 and Grid-IO2Q0 (defined in Table 6). The results are shown for models using rtts and rttp options separately.

Table 7: Estimates of management quantities for the reference case and key model runs. Shaded rows are reference models.

Run	Label	MSY (000)	F2016	Fmsy	$F_{\%40SSB}$	F_{2016} /Fmsy	F_{2016} /$F_{\%40SSB}$	SSB_{2016} (000)	SSBmsy (000)	$SSB_{\%40}$ (000)	SSB0 (000)	SSB_{2016} /SSBmsy	SSB_{2016} /$SSB_{\%40}$	SSB_{2016} /SSB0
M1	Ua	655	0.36	1.01	0.56	0.35	0.64	1085	502	888	2221	2.16	1.22	0.49
M2	U1	870	0.25	1.00	0.56	0.25	0.44	1571	668	1172	2931	2.35	1.34	0.54
M3	U3	848	0.24	1.01	0.56	0.24	0.43	1662	653	1162	2906	2.54	1.43	0.57
M4	IO	838	0.26	0.86	0.56	0.30	10.17	1484	765	1134	2834	1.94	1.31	0.52
M5	CL01	1324	0.15	1.03	0.55	0.15	0.27	2695	1016	1853	4634	2.65	1.45	0.58
M6	CL5	844	0.26	1.00	0.58	0.26	0.45	1464	641	1099	2747	2.28	1.33	0.53
M7	L70	864	0.26	1.06	0.57	0.25	0.46	1358	540	1019	2548	2.52	1.33	0.53
M8	L83	870	0.26	0.99	0.52	0.26	0.50	1254	489	977	2443	2.57	1.28	0.51
M9	MeAs	917	0.23	0.85	0.59	0.26	0.38	1763	881	1269	3173	2.00	1.39	0.56
M10	MeAs-L70	765	0.26	0.83	0.50	0.31	0.51	1428	665	1108	2769	2.15	1.29	0.52
M11	MeAs-L83	843	0.25	0.93	0.46	0.27	0.55	1276	517	1039	2596	2.47	1.23	0.49
M12	t4	1142	0.18	0.99	0.55	0.18	0.32	2218	876	1554	3885	2.53	1.43	0.57
M13	od02	897	0.24	1.00	0.55	0.25	0.44	1576	683	1211	3027	2.31	1.30	0.52
M14	od70	670	0.36	1.00	0.57	0.36	0.63	1065	512	887	2217	2.08	1.20	0.48
M15	rttp	605	0.42	1.00	0.57	0.42	0.73	905	460	795	1988	1.97	1.14	0.46
M16	rttp-MeAs	811	0.31	0.96	0.73	0.32	0.43	1311	725	953	2383	1.81	1.38	0.55
M17	h70	744	0.26	0.76	0.51	0.34	0.51	1486	788	1156	2891	1.88	1.28	0.51
M18	h90	961	0.26	1.25	0.60	0.21	0.43	1487	552	1119	2798	2.69	1.33	0.53
M19	Q0-LR-Mat	148	0.11	0.23	0.14	0.48	0.78	979	522	832	2081	1.88	1.18	0.47
M20	Q0-LR-MeAs	136	0.14	0.28	0.15	0.50	0.93	723	348	661	1652	2.08	1.09	0.44
M21	Q0-L83-MAt	175	0.08	0.21	0.12	0.38	0.68	1019	410	797	1992	2.48	1.28	0.51
M22	Q0-L83-MeAs	190	0.07	0.18	0.10	0.39	0.69	993	433	776	1940	2.29	1.28	0.51
M23	Q2-L83-MAt	181	0.08	0.21	0.12	0.36	0.65	1067	422	822	2055	2.53	1.30	0.52
M24	Q2-L83-MeAs	179	0.07	0.15	0.09	0.43	0.77	1056	490	875	2186	2.15	1.21	0.48
M25	Q4-L83-MAt	172	0.08	0.21	0.12	0.38	0.69	996	403	784	1959	2.47	1.27	0.51
M26	Q4-L83-MeAs	155	0.07	0.13	0.07	0.53	0.94	984	504	911	2279	1.95	1.08	0.43

M27	IO2	1522	0.13	0.98	0.53	0.13	0.25	2586	871	1685	4213	2.97	1.53	0.61
M28	IO2-rttp	1046	0.20	0.99	0.52	0.21	0.39	1608	592	1158	2895	2.71	1.39	0.56
M29	IO2Q0	173	0.09	0.21	0.12	0.40	0.73	930	402	791	1978	2.32	1.18	0.47
M30	IO2Q0-rttp	174	0.08	0.21	0.12	0.39	0.69	980	407	782	1955	2.41	1.25	0.50

5.3 Stock status from exploratory runs

Combined Kobe plot showing the estimates of current spawning stock and fishing mortality (F) in relation to target spawning stock size ($SSB_{40\%}$) and fishing mortality ($F_{\%40SSB}$) for all exploratory models are shown in Figure 27. All the exploratory runs suggested the current stock size is above target and fishing mortality is less the than F of the target stock size. The results do not include all the uncertainties arising from interactions of the assumption and parameter options.

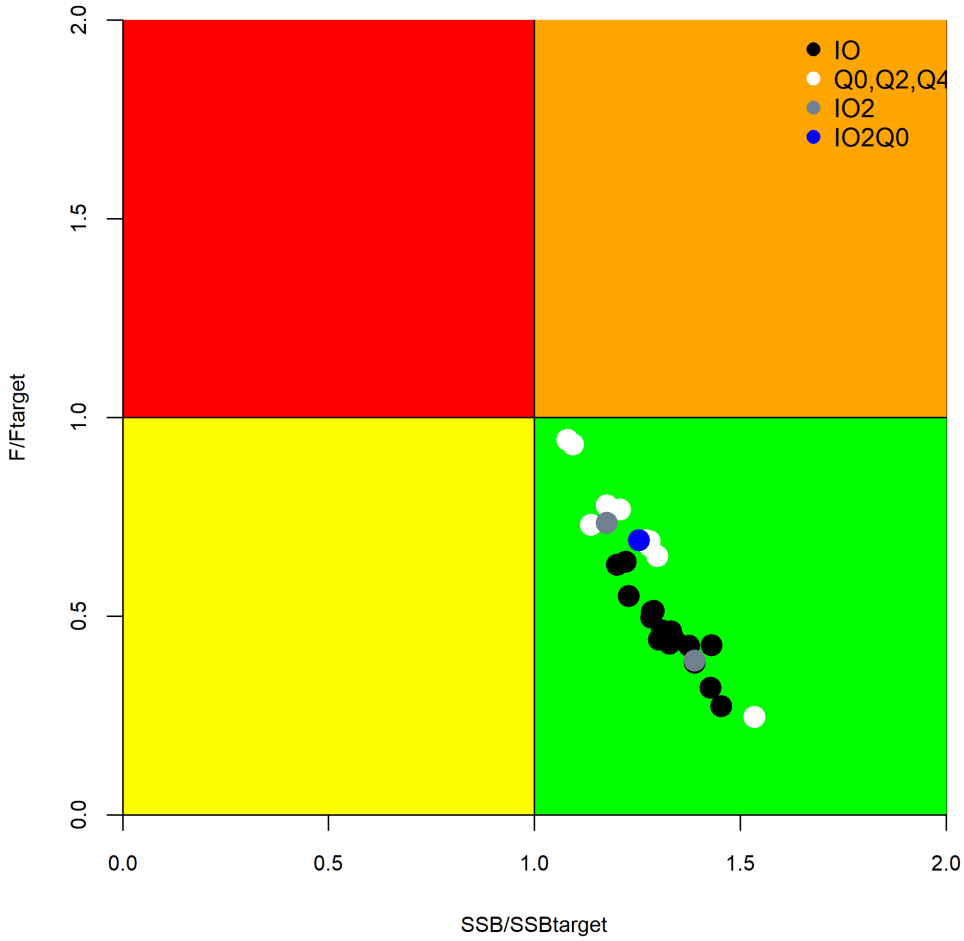

Figure 27: Combined Kobe plot for SKJ showing the estimates of current spawning stock and current fishing mortality (F) in relation to target spawning stock size ($SSB_{40\%}$) and fishing mortality ($F_{\%40SSB}$) for all exploratory models defined Table 5. Model with different spatial and temporal structure are shows in different colours.

5.4 Stock status from assessment grids

Time series of stock status and other management reference values estimated from Grid-IO and Grid-Q0 are shown in Figure 28 & Figure 29. Two models from Grid-IO and six models from Grid-Q0 resulted spurious stock trajectories or crash within a few years in the projection, and are therefore excluded. All models in the grid are equally weighted. It is clear that the MPD estimates from most the runs (over 50%) suggest that $SSB_{current} > SSB_{\%40}$, and $F_{current} < F_{\%40SSB}$.

Biomass trend for the 142 models from Grid-IO and 138 models from Grid-Q0 are shown in Figure 30 & Figure 31. Generally, models based on both Maldives PL and EU PS CPUE have estimated high stock status than models using only Maldives PL CPUE; models including the small scale tag programme estimated more optimistic stock status.

The biomass and fishing mortality time series with respect to the target reference point are shown with the Kobe plots in Figure 32 & Figure 33. Kobe plots from both assessment grids suggest that the stock is not overfished and overfishing has not occurred. For Grid-IO, $SSB_{current}/SSB_{\%40}$ is estimated to be 1.24 with a 90% quantile range 0.90–1.52, and $F_{current}/F_{\%40SSB}$ is estimated to be 0.60 with a 90% quantile range 0.24–1.21 (Table 8). For Grid-Q0, $SSB_{current}/SSB_{\%40}$ is estimated to be 1.17 with a 90% quantile range 0.75 –1.58, and $F_{current}/F_{\%40SSB}$ is estimated to be 0.83 with a 90% quantile range 0.30–1.53. Overall the two assessment grids led to very similar conclusions on stock status. But models based on the SSYS structure generally estimated slightly more optimistic results.

The estimates of stock status and fishing pressure were generally influenced by the same assumptions in the same direction. More pessimistic results were generally associated with lower steepness, slower growth/lower M, short tag mixing period, exclusion of the small scale tag program and/or EU PS CPUE (Figures A21-A26). MSY estimates are sensitive to the steepness, tag mixing period, tagging program options, with higher values associated with higher steepness, long tag mixing period, and the use of the small-scale tagging data.

The projection results are summarised in the Kobe 2 Strategy Matrix Table 9. For both assessment grids, there is very little risk of breaching the target reference points if future catch remained at the 2015 level, both for the short (3 years) and medium term (10 Years).

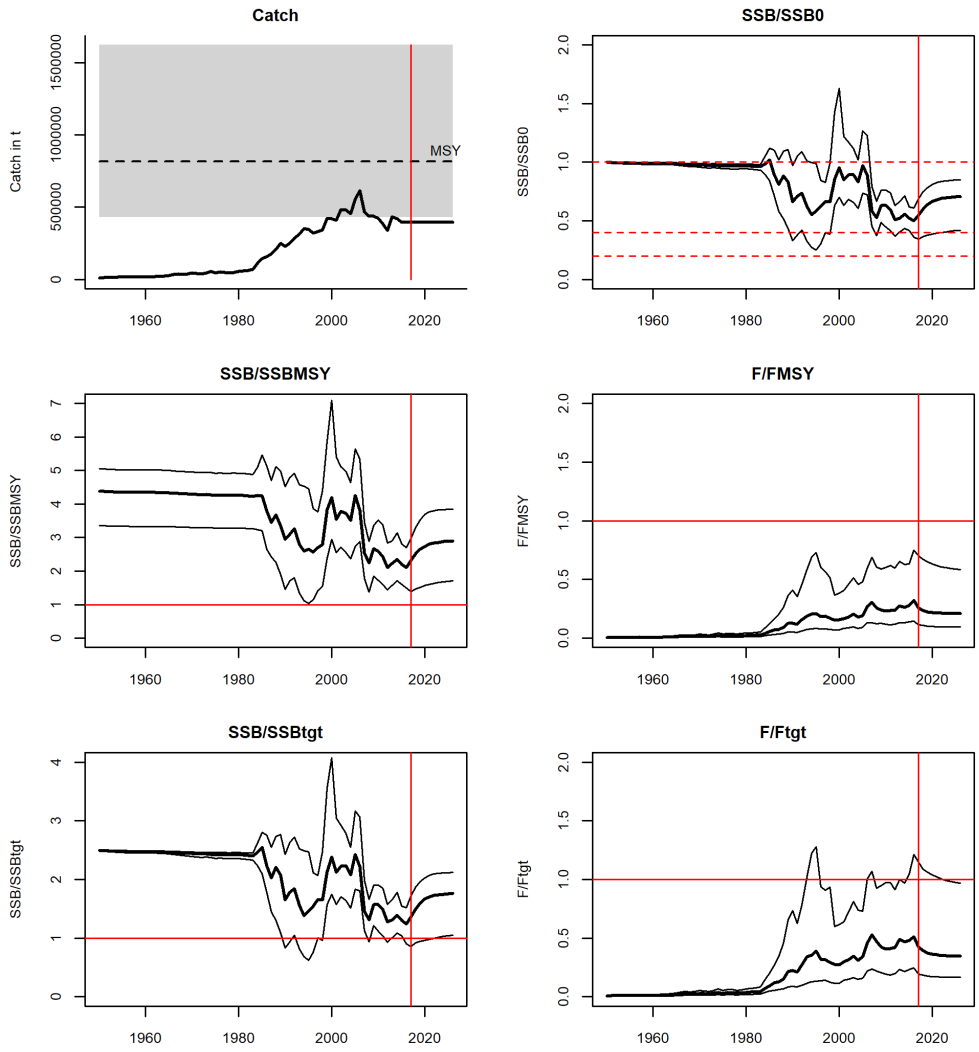

Figure 28: Stock status summary for the Indian Ocean Skipjack for assessment grid-IO. Thick black lines represent the median of the aggregate results, thin lines represent 5th and 95th percentiles. In the catch plot, dotted lines represent mean MSY, the shaded area represents 5th and 95th percentiles. The red vertical line indicate the start of projection years (10 year projection at current catches).

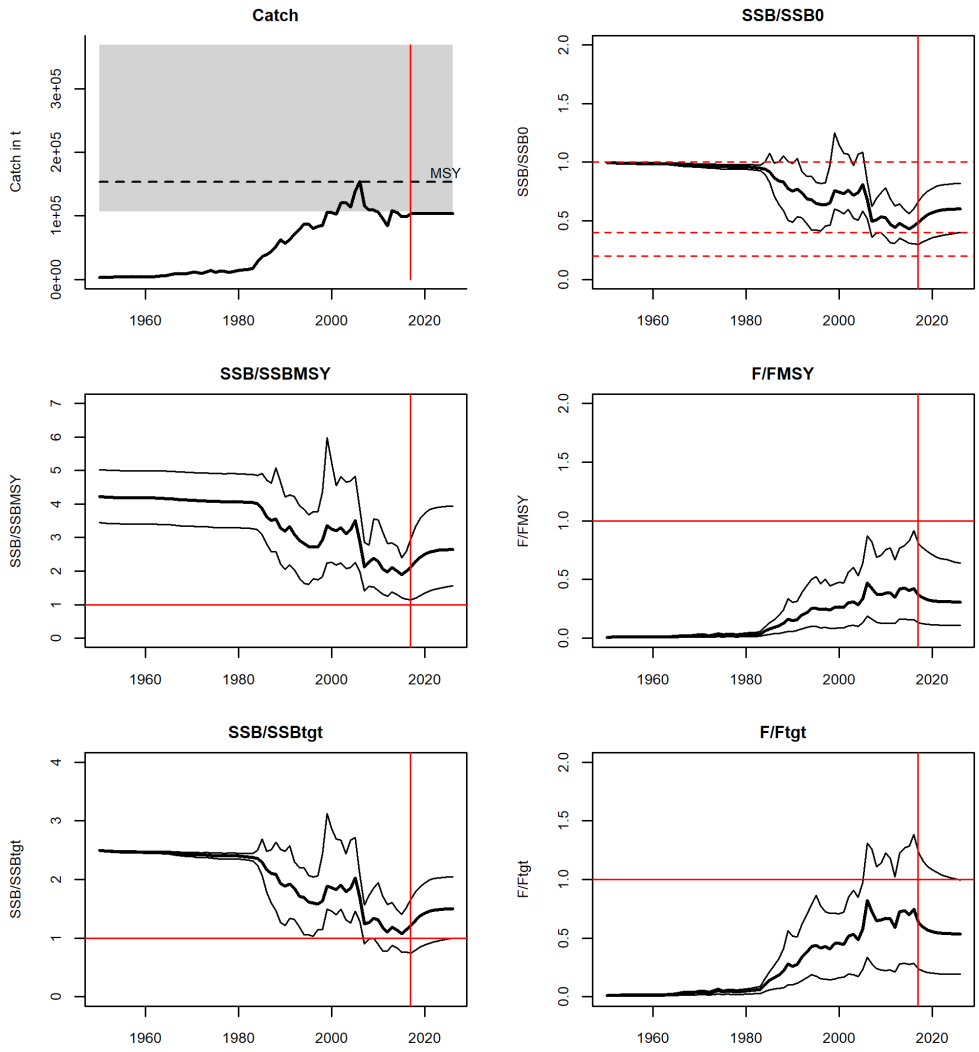

Figure 29: Stock status summary for the Indian Ocean Skipjack for assessment grid-Q0. Thick black lines represent the median of the results, thin lines represent 5th and 95th percentiles. In the catch plot, dotted lines represent mean MSY, the shaded area represents 5th and 95th percentiles. The red vertical line indicate the start of projection years. Catch, MSY, and biomass are calculated as seasonal average for the year.

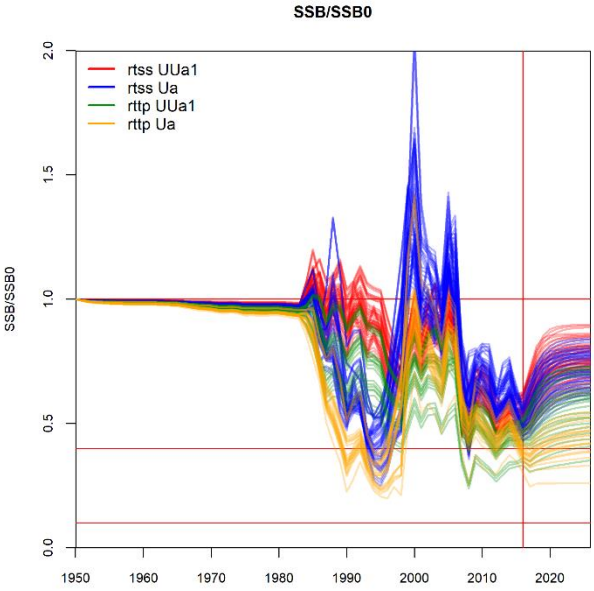

Figure 30: Time series of estimated deletion for all the models from assessment grid-IO, as grouped by tag and CPUE options. The red vertical line indicate the start of projection years. Horizontal lines indicate 100%, 40%, and 10% depletion levels.

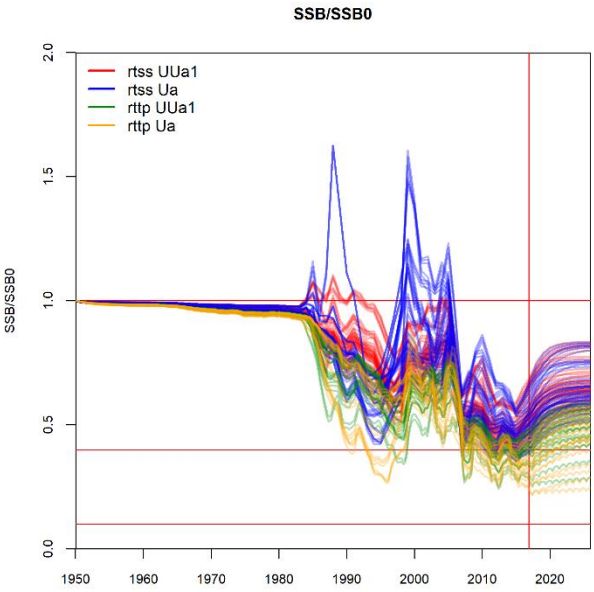

Figure 31: Time series of estimated deletion for all the models from assessment grid-Q0, as grouped by tag and CPUE options. The red vertical line indicate the start of projection years. Horizontal lines indicate 100%, 40%, and 10% depletion levels.

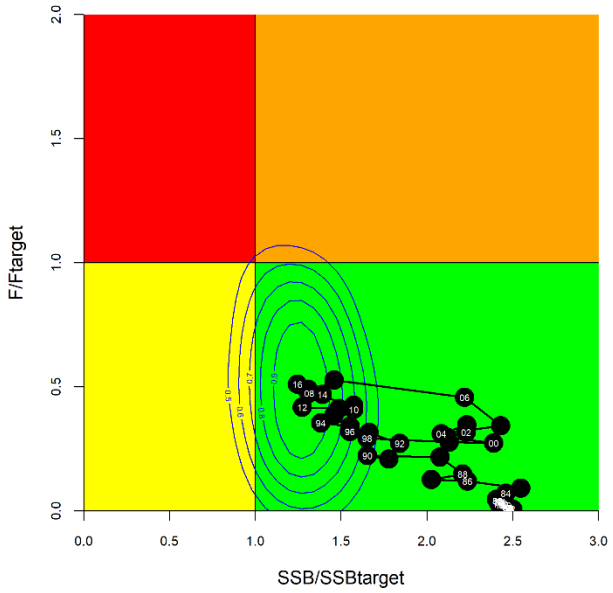

Figure 32: Kobe plot for SKJ showing the time series of spawning biomass and fishing mortality (F) in relation to target spawning stock size ($SSB_{40\%}$) and fishing mortality ($F_{\%40SSB}$) for assessment grid-IO (defined in Table 6). Black circles represent the annual medians of the aggregate distributions across all models. Contours represent the smoothed probability distribution for 2016 (isopleths are probability relative to the maximum).

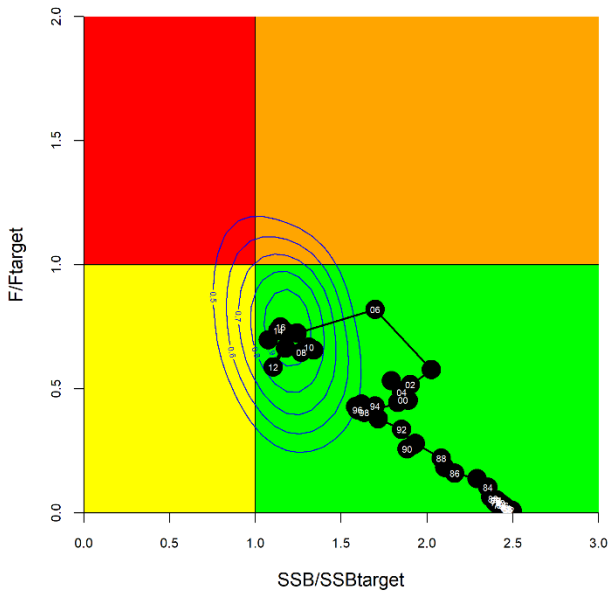

Figure 33: Kobe plot for SKJ showing the time series of spawning biomass and fishing mortality (F) in relation to target spawning stock size ($SSB_{40\%}$) and fishing mortality ($F_{\%40SSB}$) for assessment grid-Q0 (defined in Table 6). Black circles represent the annual medians of the aggregate distributions across all models. Contours represent the smoothed probability distribution for 2016 (isopleths are probability relative to the maximum).

.

Table 8: Stock status summary table for each of the assessment grid.

Management Quantity	Grid-IO
Curren catch	446 723
Mean catch over last 5 years	407 450
Current Data Period	1950–2016
MSY (t)	893 250 (430 710–1 622 320)
SSB0	2 468 450 (1 286 230–4 843 510
$SSB_{current}$	1261100 (461002–2764280)
$F_{40\%SSB}$	0.58 (0.47–0.79)
$F_{current}$ / $F_{40\%SSB}$	0.60 (0.24–1.21)
$SSB_{Current}$ / $SSB_{\%40}$	1.24 (0.90–1.52)
$SSB_{Current}$ / SSB0	0.49 (0.36–0.61)

Management Quantity	Grid-Q0
Current catch	111 680 (quarterly average)
Mean catch over last 5 years	101 862 (quarterly average)
Current Data Period	1950–2016
MSY (t) (quarter)	184 050 (106 620 – 369 250)
SSB0	1 971 340 (1 242 120 –3 972 500)
$SSB_{current}$	967 580 (373 350–2 437 530)
$F_{40\%SSB}$ (quarter)	0.13 (0.09–0.22)
$F_{Current}/F_{40\%SSB}$	0.83 (0.30–1.53)
$SSB_{Current}$ / $SSB_{\%40}$	1.17 (0.75–1.58)
$SSB_{Current}$ / SSB0	0.47 (0.30–0.63)

Table 9: Kobe 2 Strategy Matrix for Indian Ocean SKJ assessment grid-IO and grid-Q0. Probability (expressed as a percentage of the distribution of models) of exceeding the MSY-based spawning biomass and fishing mortality reference points.

grid-IO	Constant Catch Level (relative to 2015)				
	60%	80%	100%	120%	140%
SSB_{2019} <$SSB_{\%40}$	0.00	0.03	0.08	0.15	0.20
F_{2019} >$F_{40\%SSB}$	0.00	0.01	0.07	0.15	0.22
SSB_{2026} <$SSB_{\%40}$	0.00	0.03	0.08	0.15	0.22
F2026 >$F_{40\%SSB}$	0.00	0.01	0.07	0.16	0.22

grid-Q0	Constant Catch Level (relative to 2015)				
	60%	80%	100%	120%	140%
SSB_{2019} <$SSB_{\%40}$	0.00	0.03	0.11	0.22	0.42
F_{2019} >$F_{40\%SSB}$	0.00	0.00	0.07	0.24	0.46
SSB_{2026} <$SSB_{\%40}$	0.00	0.03	0.11	0.22	0.50
F2026 >$F_{40\%SSB}$	0.00	0.00	0.07	0.25	0.51

6. DISCUSSION

Skipjack is recognised as a difficulty species to assess and presents a number of problems in the development of a stock population model: the population dynamics are very rapid, spawning may be continuous, the length frequency is generally uninformative about year-class strength, relative abundance indices derived from pole and line and purse seine fisheries are generally considered to be less reliable than those derived from longline fisheries, there is a successful tagging program but the areas where skipjack have been tagged are quite limited and the reporting rate for some of the major fisheries are poorly quantified. As with earlier assessments, the models presented here, while fairly representing some of the data (e.g., the biomass indices), also show some signs of poor fit. The assessment tested various combinations of assumptions to explore the sensitivity and describe the uncertainty in the stock status. It is unlikely the estimates of historical stock size are very accurate. Current stock status as estimated here should thus be treated with caution.

Stock status was estimated for 144 models running a permutation of the assumptions and parameters including growth, natural mortality, steepness, CPUE and tagging data modelling options. Estimates from the majority of models suggested the Indian Ocean Skipjack stock as a whole is currently not overfished, and not subject to overfishing: $SSB_{current}/SSB_{\%40}$ is estimated to be 1.24 with a 90% quantile range 0.90–1.52, and $F_{current}/F_{\%40SSB}$ is estimated to be 0.60 with a 90% quantile range 0.24–1.21. The current stock size is estimated to be 49% of the unfished level. The 10-year projections for these models suggest the risk of the spawning biomass falling below the target (SSBMSY) is less than 10% by 2026 if the catch remains at the current level.

A sensitivity using alternative temporal structure (Calendar season as model year) running on the same permutation of parameters produced similar but slightly more pessimistic results: $SSB_{current}/SSB_{\%40}$ is estimated to be 1.17 (0.75 –1.58), and $F_{current}/F_{\%40SSB}$ is 0.83 (0.30–1.53). The sensitivity also suggested that the stock is not overfished, and is not subject to overfishing.

In most cases, the models estimated a highly productive stock, with high natural mortality, and moderate depletion. The models often suggested that a sizeable proportion of the spawning stock is essentially invulnerable to the fishery due to limited selectivity of the youngest spawners, and high recruitment compensation with declining spawning biomass. In some cases, the sustainable yield is estimated to increase with increasing effort, such that it may not be possible to seriously overfish the stock. The robustness of this conclusion clearly needs further consideration. There is also some question about the contribution of very large fish to the spawning biomass. Longliners report few skipjack, but they tend to catch some substantially larger fish than the other gears (Kolody et al. 2011)

The assessment included the standardised Maldives Pole and line CPUE, in combination with the EU Purse seine CPUE from associated schools. The Maldives PL CPUE is derived from the relatively small area of the Maldives EEZ and may not be a good index for the broader population. The French fleets operate over a broader area, and encompass a broader time period, but in general, FAD fishing might be expected to cause a hyper-stable relationship between CPUE and abundance (it may be partially overcome by improved standardisation methodology that takes into considerations a wide range of covariates that might affect the catch efficiency). The two time series were reasonably consistent over the period of overlap (except the increase in 2005-2006 in the PL CPUE was not observed in the PS indices). We probably have less confidence in the early part of PS indices as not all the covariates relating to vessel characterises are available for the standardisations.

The WPTT16 proposed the development of an alternative approach to deriving an index of abundance for skipjack tuna based on purse seine species composition, which avoids the problem of increasing fishing power that afflicts purse seine CPUE (Maunder and Hoyle 2007). Work to extend the Maldives series to pre-mechanization period in 1970 using MCMC is also underway. The longer time series can provide valuable information to verify the relative abundance in the period during the industrialisation of the fishery beginning in the 1980s, and serve to discriminate the degree to which short term

population fluctuations are due to fishery depletion or recruitment variability. However, the difficulty of this work arises from the lack of good covariates measuring fishing power and issues with past data collection (Paul Medley, pers. comm.). Abundance indices from other fisheries seem unlikely at this stage. Previous assessments have used CPUE from PS sets on free schools, the PSFS CPUE is not considered to be representative of SKJ stock biomass because of the highly peculiar occurrence of SKJ in the free school fishery (Alain Fonteneau, pers. comm.) and free schools of skipjack have dramatically decreased over time (Gaertner et al. 2017). Longline CPUE is not indicative of SKJ abundance in general, given the the erratic patterns in reported catch, effort and CPUE.

The CSMY (calendar season as model year) configuration was attempted in the assessment. This model structure is thought to be suitable for tropical tuna species where growth is fast and spawning is continuously (Langley 2016a, b, McKechnie et al. 2016). To fully assess the performance of each model structure requires a good understanding of the SS3 code. Analysis undertaken in the assessment so far did not reveal any major defect of either option. The SSYS model appear to be adequate in modelling most of the population processes at a finer temporal resolution, noting that the season definitions do not have to adhere to the standard four season definition. The SSYS approximates the continuous recruitment by apportioning recruits by season, although using an S-R relationship would make more biological sense. However, the data currently do not appear to contain strong seasonal signals to validate those estimates.

Being able to assign finer age classes is perhaps what distinguishes the CSMY from the SSYS models. But it appears that that for the SSYS model, when a tag release group is defined for specified season, area, and age, it is distributed among seasonal cohorts according to their distribution in the population at that season /age (biological morphs of different birthdates, Rick Methot pers. comm.) This means that SS3 internally partitions tagged fish according to the model's perceived distribution of seasonal cohorts (quarterly age classes), presuming that other data provides such information. On the other hand, the assignment of seasonal age classes for CSMY models is an external process. As the assignment is usually based on length, the usefulness might be limited if there is considerable uncertainty on the size at age.

Multi-area models account for differential depletion between regions, and heterogeneity in tag mixing can be dealt with by introducing appropriate spatial structures. Fonteneau (2014) suggested that the 2 area model by Sharma et al. (2012) is well fitted with the geographical scale of the observed skipjack movements, but this partition may not be ideal. Our limited investigation showed that the regional biomass distributions are not well estimated by the current spatial model. The reasons are not clear, but may be becausethe spatial coverage of tagging is limited, catchabilities are not comparable among different fishery sectors, and the tagging data is not informative of the skipjack exchange rate at the spatial boundary considered. The four-area stratification proposed by Fonteneau (2014) is worth pursuing but obviously more data are required to support its implementation.

7. ACKNOWLEDGMENTS

We are grateful to the many people that contributed to the collection of this data historically, analysts involved in the CPUE standardization, and to Rick Methot, Ian Taylor and other developers for providing the SS3 software, to Rishi Sharma, Dale Kolody, and Adam Langley for useful discussions on the alternative temporal structure of the model.

8. REFERENCES

Adam, M.S. 2010. Declining catches of skipjack in the Indian Ocean – observations from the Maldives. IOTC-2010-WPTT-09.

Bentley, N., Adam, S.M. 2016. Management strategy evaluation for the Indian Ocean skipjack tuna Fishery. IOTC-2016-WPM07-15 Rev_1.

Chassot E, Assan C, Esparon J,, Tirant A, Delgado d, Molina A, Dewals P, Augustin E, Bodin N. 2016. Length-weight relationships for tropical tunas caught with purse seine in the Indian Ocean: Update and lessons learned. IOTC-2016-WPDCS12-INF05.

Chassot E., L. Floch, P. Dewals, V. Fonteneauc, R. Pianet. 2010. Statistics of the main purse seine fleets fishing in the Indian Ocean, 1981-2009. IOTC-2010- WPTT-13.

Dammannagoda, S.T., Hurwood, D.A., Mather, P.B. 2011. Genetic analysis reveals two stocks of skipjack tuna (Katsuwonas pelamis) in the northwestern Indian Ocean. Can. J. Fish. Aquat. Sci. 68: 210-223.

Delgado de Molina, A., Areso, J.J. and Ariz, J. 2010. Statistics of the purse seine Spanish fleet in the Indian Ocean (1984-2009). IOTC-2010- WPTT-19.

Dorizo, J., C. Assan and A. Fonteneau. 2008. Analysis of tuna catches and CPUEs by Purse Seiners fishing in the Western Indian Ocean over the period January to July 2008. IOTC 2008-WPTT-20.

Eveson, J.P. 2011. Preliminary application of the Brownie-Petersen method to skipjack tag-recapture data. IOTC-2011-WPTT-13-31Rev_1

Eveson, J.P., J. Million. 2008. Growth of tropical tunas using the Laslett, Polacheck and Eveson (LEP) method. IOTC-2008-WPTT-09.

Eveson, J.P., Million, J., Sardenne, F. , Le Croizier, G. 2012. Updated Grwoth estimates for Skipjack, Yellowin And Bigeye Tuna in the Indian Ocean using the most recent Tag-Recapture and Otolith data. IOTC-2011-WPTT-14-23Rev_1

Eveson J P, Million J, Sardenne F & Le Croizier G (2015) Estimating growth of tropical tunas in the Indian Ocean using tag-recapture data and otolith-based age estimates. Fisheries Research: Indian Ocean Tuna Tagging Programme special issue

Fontenea. 2014. On the movements and stock structure of skipjack (Katsuwonus pelamis) in the Indian ocean. IOTC–2014–WPTT16–36.

Francis, R. I. C. C. (1992). Use of risk analysis to assess fishery management strategies: A case study using orange roughy (Hoplostethus atlanticus) on the Chatham Rise, New Zealand. Canadian Journal of Fisheries and Aquatic Science, 49:922-930.

Gaertner D, Katara I, Billet N, Fonteneau A, Lopez J, Murua H, Daniel P. 2017. Workshop for the development of Skipjack indices of abundance for the EU tropical tuna purse seine fishery operating in the Indian Ocean. 17-21 July 2017. AZTI, Spain.

Gaertner, D. and J.P. Hallier. 2009. An updated analysis of tag-shedding by tropical tunas in the Indian Ocean. IOTC-2009-WPTT-34.

Grande, M., H. Murua, I. Zudaire, and M. Korta. 2010. Spawning activity and batch fecundity of skipjack, Katsuwonus pelamis, in the Western Indian Ocean. IOTC-2010- WPTT-47.

Hallier, J.P. and J.Million. 2009. The contribution of the regional tuna tagging project – Indian Ocean to IOTC stock assessment. IOTC-2010-WPTT-24.

Hillary, R., J. Million and A. Anganuzzi. 2008. Exploratory modelling of Indian Ocean tuna growth incorporating both mark-recapture data and otolith data. IOTC-2008-WPTDA-03.

Hoyle, S., P. Kleiber, N. Davies, A. Langley, and J. Hampton. 2011. Stock assessment of skipjack tuna in the western and central Pacific Ocean. WCPFC-SC7-2011/SA-WP-04.

ICCAT 2009. Report of the 2008 ICCAT yellowfin and skipjack stock assessments meeting (Florianópolis, Brazil – July 21 to 29, 2008). Collect. Vol. Sci. Pap. ICCAT, 64(3): 669-927 (2009).

IOTC (2016) . RESOLUTION 16/02. ON HARVEST CONTROL RULES FOR SKIPJACK TUNA IN THE IOTC AREA OF COMPETENCE. IOTC RESOLUTION 16/02

IOTC–TCMP01 2017. Report of the 1st IOTC Technical Committee on Management Procedures. Yogyakarta, Indonesia 20 May 2017. IOTC–2017–TCMP01–R[E]: 23 pp.

ISSF (2011). Report of the 2011 ISSF stock assessment workshop. Technical Report ISSF Technical Report 2011-02, Rome, Italy, March 14-17, 2011.

Itano, D. (2000). The reproductive biology of yellowfin tuna (Thunnus albacares) in Hawaiian waters and the western tropical Pacific Ocean: Project summary. JIMAR Contribution 00-328 SOEST 00-01.

ICCAT 2009. Report of the 2008 ICCAT yellowfin and skipjack stock assessments meeting (Florianópolis, Brazil – July 21 to 29, 2008). Collect. Vol. Sci. Pap. ICCAT, 64(3): 669-927 (2009).

Jauharee, A.R. and M.S. Adam. 2009. Small Scale Tuna Tagging Project – Maldives 2007 Project Final Report - October 2009. Marine Research Centre, Malé 20-025, Republic of Maldives. Unpublished report, 17p.

Kayama,S., Tanabe, T., Ogura, M., Okamoto, H. and Y. Watanabe. 2004. Daily age of skipjack tuna, Katsuwonus pelamis (Linnaeus), in the eastern Indian Ocean. IOTC-2004-WPTT-03.

Khan, M. 2017. Status Gillnet fisheries and data reconstruction of Tropical Tuna in Pakistan. IOTC-IOTC-2017 -WPTT19-xx.

Kolody, D., Herrera, M., Million, J. 2011. Indian Ocean Skipjack Tuna Stock Assessment 1950-2009 (Stock Synthesis). IOTC-2011-WPTT13-31_Rev1.

Langley, A. (2016a). Stock assessment of bigeye tuna in the Indian Ocean for 2016 — model development and evaluation. IOTC-2016-WPTT18-20

Langley, A. (2016b). An update of the 2015 Indian Ocean Yellowfin Tuna stock assessment for 2016. IOTC-2016-WPTT18-27

Laslett, G. M., Eveson, J.P., Polacheck, T. 2002. A flexible maximum likelihood approach for fitting growth curves to tag-recapture data. Can. J. Fish. Aquat. Sci. 59: 976-986.

McKechnie, S. Hampton, J., Pilling, G. M., Davies N. 2016. Stock assessment of skipjack tuna in the western and central Paci_c Ocean. WCPFC-SC12-2016/SA-WP-04.

Mohamed, S. 2007. A bioeconomic analysis of Maldivian skipjack tuna fishery. M.Sc. thesis, University of Tromso. 39 pp.

Marsac, F., Fonteneau, A., Lucas, J., Báez, J., Floch, L. Data-derived fishery and stocks status indicators for skipjack tuna in the Indian Ocean Floch. IOTC-2017-WPTT19-09.

Maunder, M.N. 2009. Updated indicators of stock status for skipjack tuna in the eastern Pacific Ocean. IATTC 2009 SAR-11-SKJ.

Maunder, M.N. and S.J. Harley. 2003. Status of skipjack tuna in the eastern Pacific Ocean in 2003 and outlook for 2004. IATTC 2003 SAR5_SKJ_ENG.

Methot Jr, R.D., Wetzel, C.R. (2013) Stock synthesis: A biological and statistical framework for fish stock assessment and fishery management. Fisheries Research, 142(0): 86-99.

Methot Jr, R.D. 2014. User Manual for Stock Synthesis. Model Version 3.24s. Available from https://vlab.ncep.noaa.gov/group/stock-synthesis

Nishikawa, Y., Honma, M., Ueyanagi, S., Kikawa, S. 1985. Average distribution of larvae of oceanic species of scombrid fishes, 1956–1981. Far Seas Fisheries Research Laboratory, Shimizu. S Series 12. WPTT-04-06.

Nokome, B., Adam, S.M. 2015. An operating model for the Indian Ocean skipjack tuna fishery. OTC-2015-WPTT17-35

Rice, J., Harley, S., Davies, N., and Hampton, J. (2014). Stock assessment of skipjack tuna in the Western and Central Pacific Ocean. WCPFC-SC10-2014/SA-WP-05.

Sharma, R., Herrera, M., Million, J. 2012. Indian Ocean Skipjack Tuna Stock Assessment 1950-2011 (Stock Synthesis). IOTC–2012–WPTT14–29 Rev–1.

Sharma, R., Herrera, M., Million, J. 2014. Indian Ocean Skipjack Tuna Stock Assessment 1950-2013 (Stock Synthesis). IOTC–2014–WPTT16–43 Rev_3.

Worm, B. & Tittensor, D. P. 2011. Range contraction in large pelagic predators. Proc. Natl Acad. Sci. USA 108: doi:10.1073/pnas.1102353108.

Wujdi, A., Setyadji, Bram., Nugroho, S. C. 2017. Preliminary stock structure study of skipjack tuna (katsuwonus pelamis) from south java using otolith shape analysis. IOTC-2017-WPTT19-xx.

APPENDIX A: SELECTED EXPLORATORY MODEL OUTPUTS

Ua U1 U3

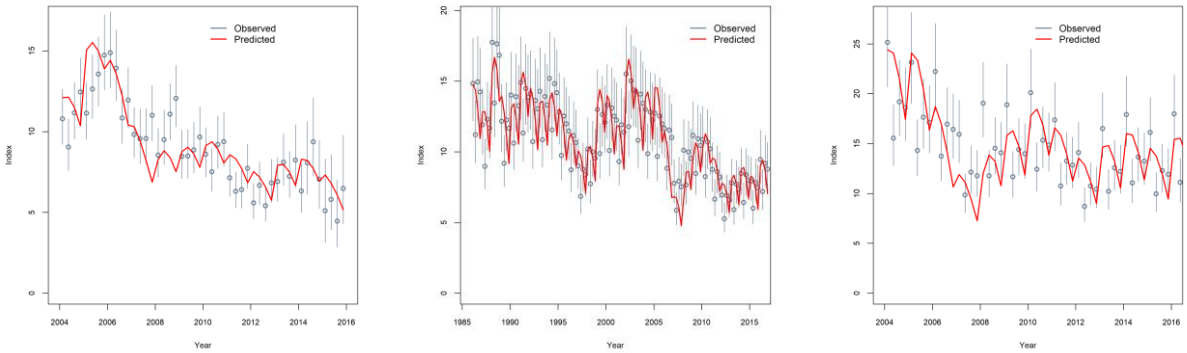

Figure A1: Fits to Maldives PS CPUE from model Ua (left), the EU long PS series from model U1 (middle), and EU short PS series from model U3 (right)

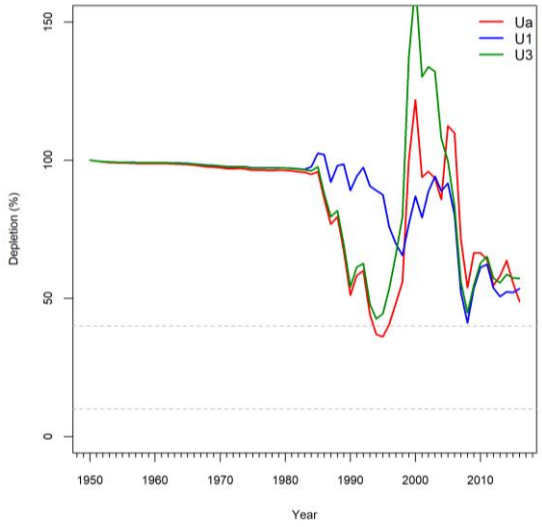

Figure A2: Comparisons of estimated stock depletion between Ua (PL CPUE), U1 (PS long CPUE), and U3 (PS short CPUE).

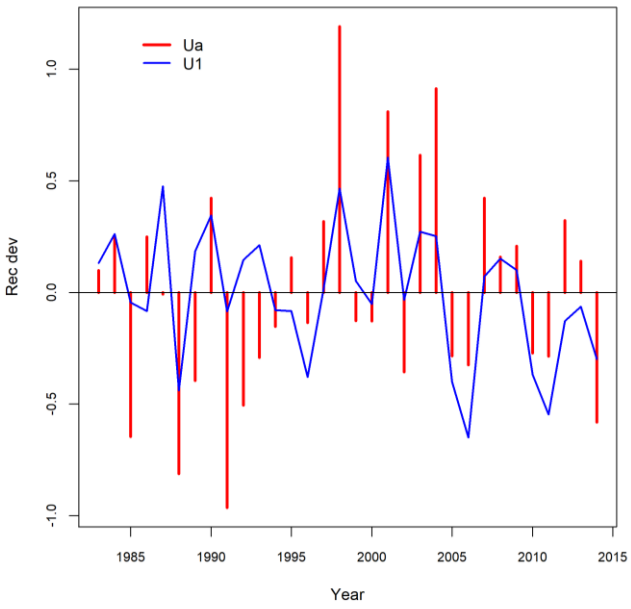

Figure A3: Comparisons of recruitment deviations between Ua (PL CPUE) and U1 (PS long CPUE).

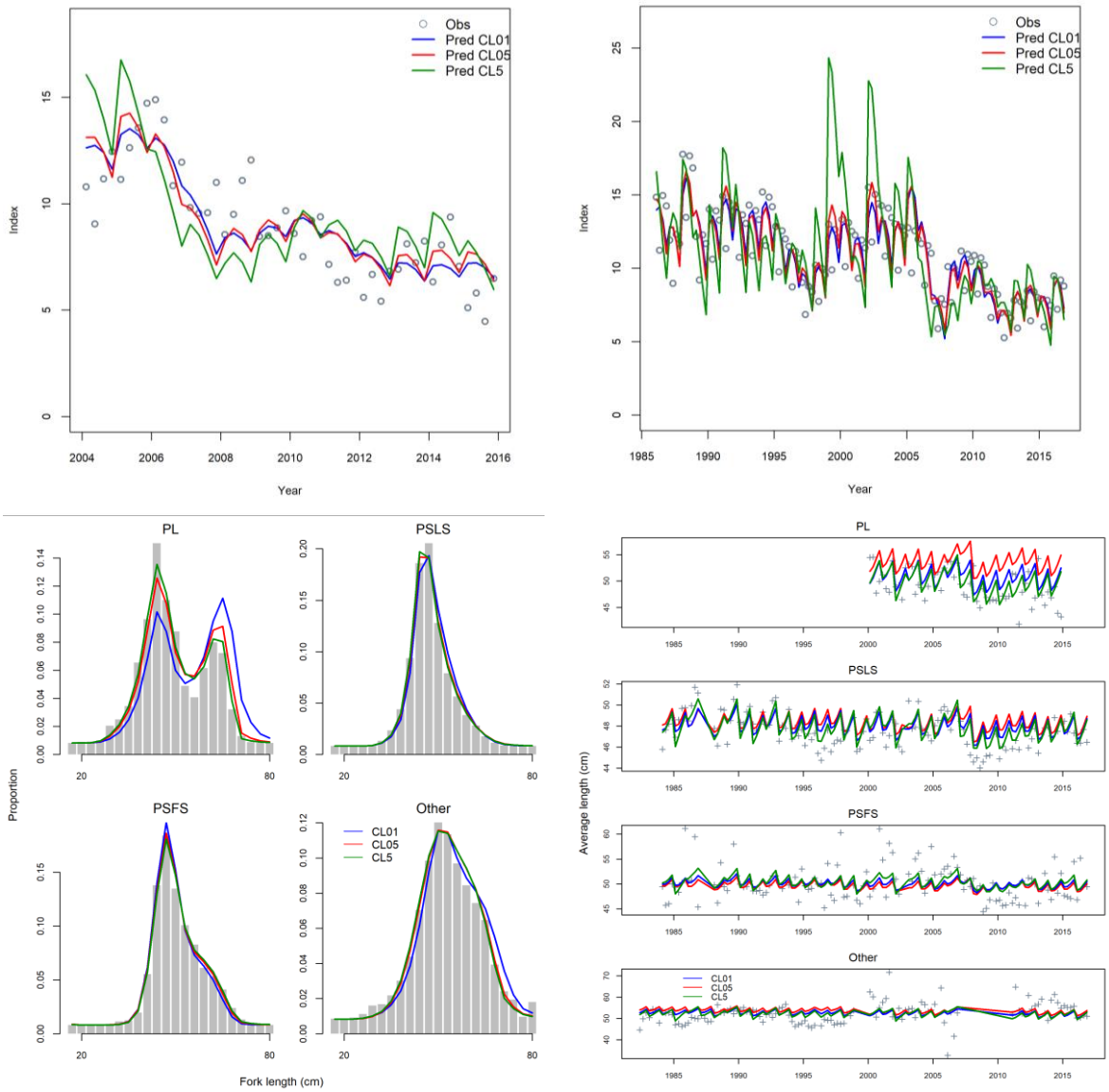

Figure A4: Comparisons of fits to the PL CPUE (top-left), EU PS long CPUE (top-right), aggregated LF by fisheries, and mean LF by season between models of different catch-at-size sample size options: CL01, CL05 (reference model IO), and CL5.

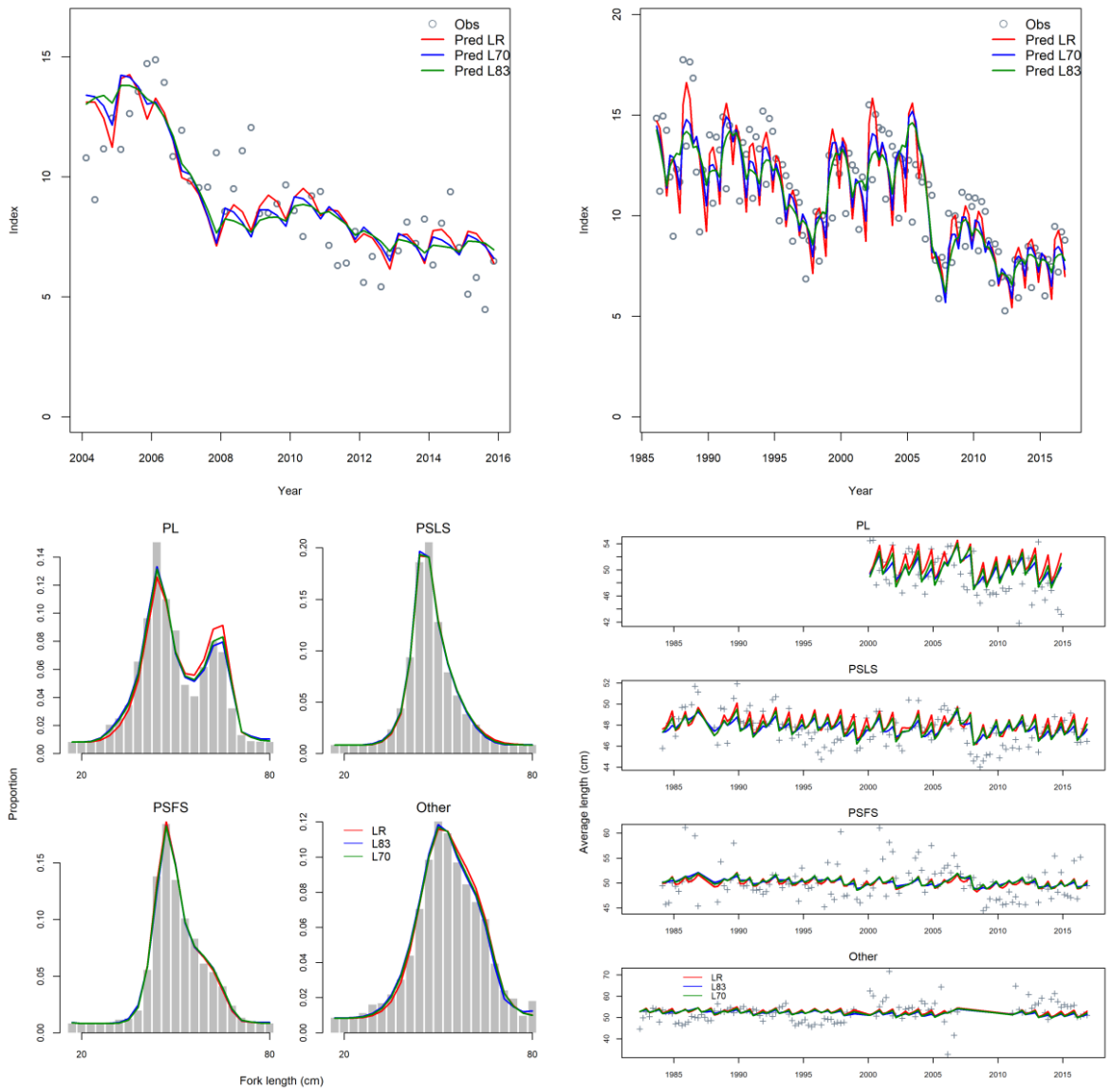

Figure A5: Comparisons of fits to the PL CPUE (top-left), EU PS long CPUE (top-right), aggregated LF by fisheries, and mean LF by season between models of different growth options: LR (reference model IO), L83, and L70.

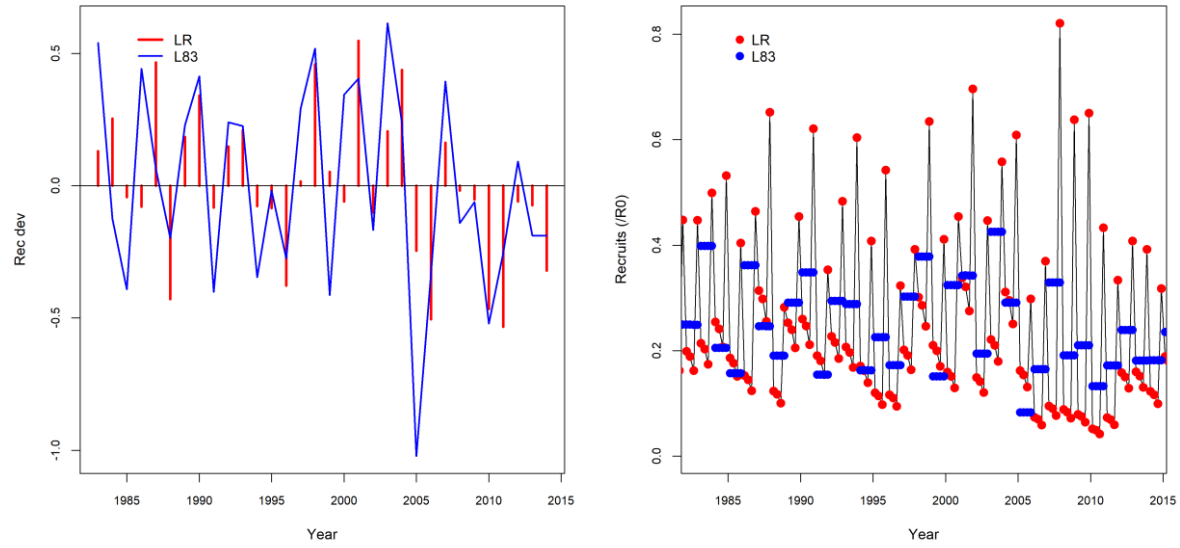

Figure A6: Comparison of estimated annual recruitment deviations (left) and recruits by season (right) between models with different growth options: LR and L83.

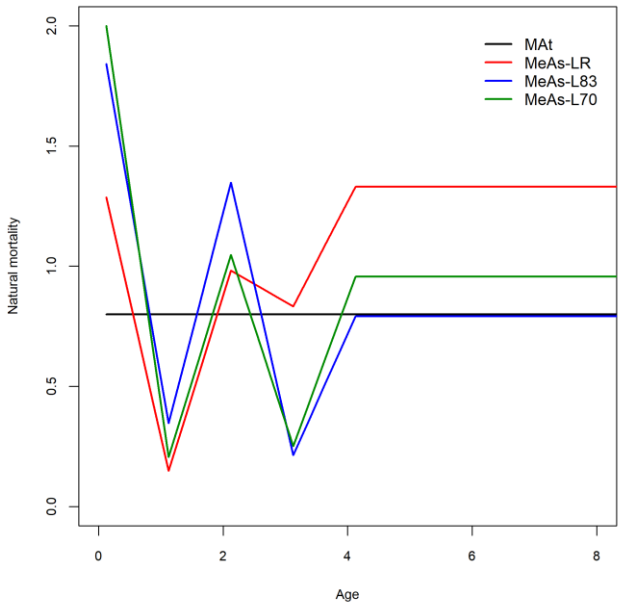

Figure A7: estimated SKJ natural mortality from models with different growth options (MeAs-LR, MeAs-L83, and MeAs-L70). The constant values (0.8) from ICCAT assessment used for the reference model IO is also shown (MAt).

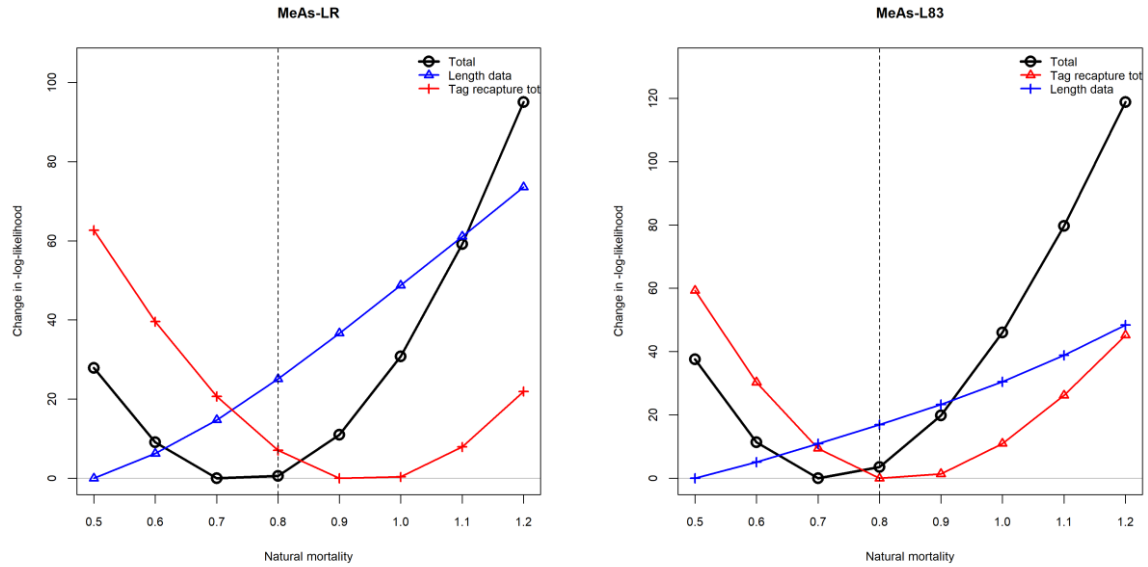

Figure A8: Likelihood profile on natural mortality for models with different growth options: MeAs-LR (left), and MeAs-L83 (right). Dashed line is the constant value (0.8) used in the reference model.

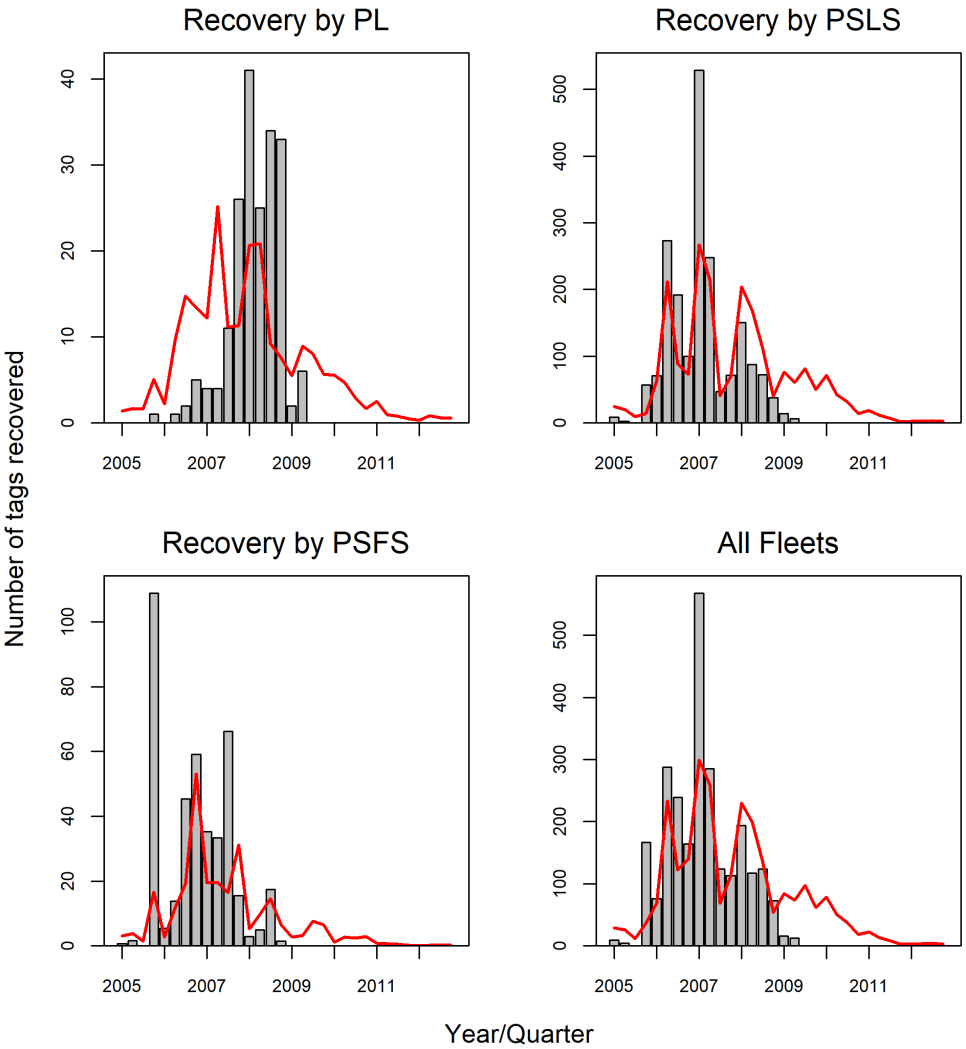

Figure A9：Predicted and observed tag recaptures by recapture year/quarter and fleets aggregated across tag groups for model t4 (tag mixing period t = 4 quarters). Note that only observed recaptures after the mixing period are included

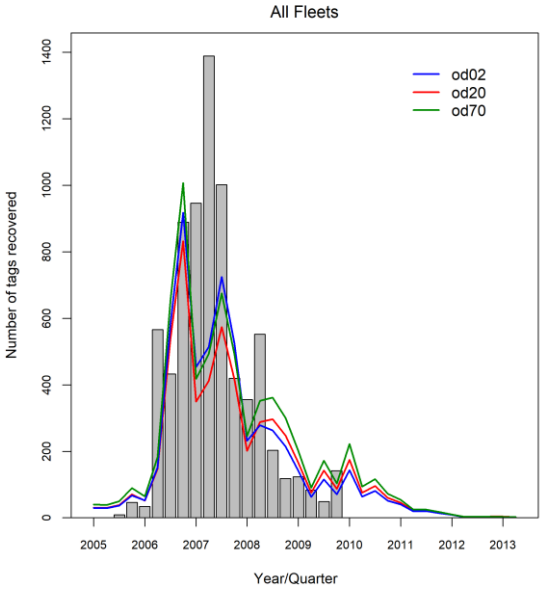

Figure A10：Predicted and observed tag recaptures by recapture year/quarter aggregated across tag groups for models using different recovery overdispersion parameters. Note that only observed recaptures after the mixing period are included.

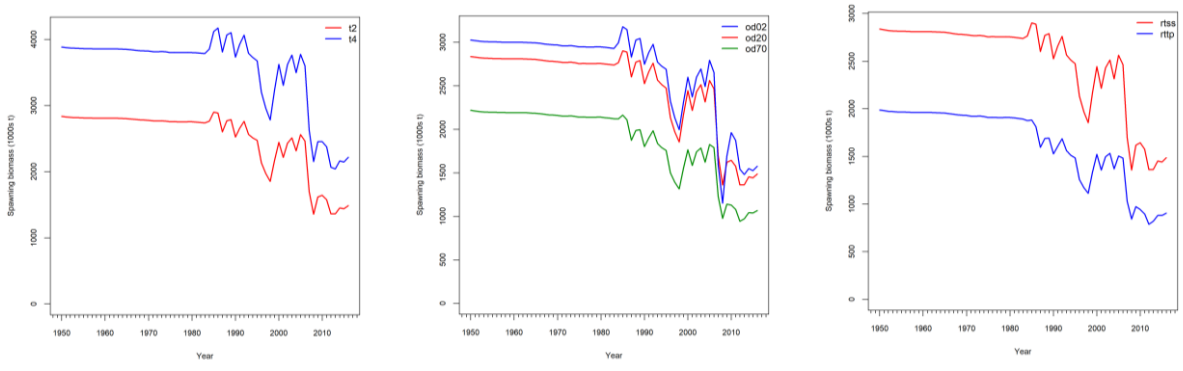

Figure A11: Comparisons of estimated spawning biomass between models with different tag mixing period (left), tag recovery overdispersion parameter (middle), and tag program option (right).

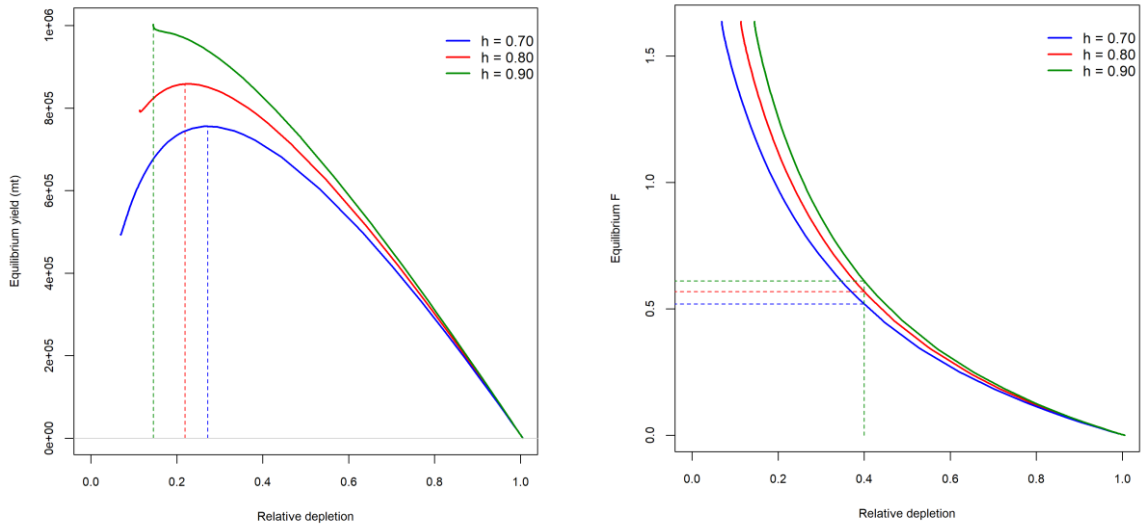

Figure A12: Equilibrium yield curves (left) and F curves (right), and for exploratory models with different steepness h70, h80 (IO model) and h90. The dashed lines in the left panel illustrating the depletion levels at SSBMSY, the dashed line in the right panel illustrate F corresponding to 40% unfished spawning biomass.

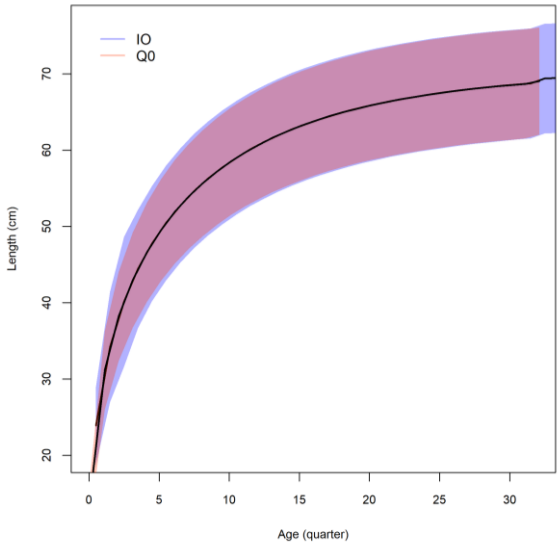

Figure A13: A comparison of quarterly growth (Richard growth) between model IO and Q0.

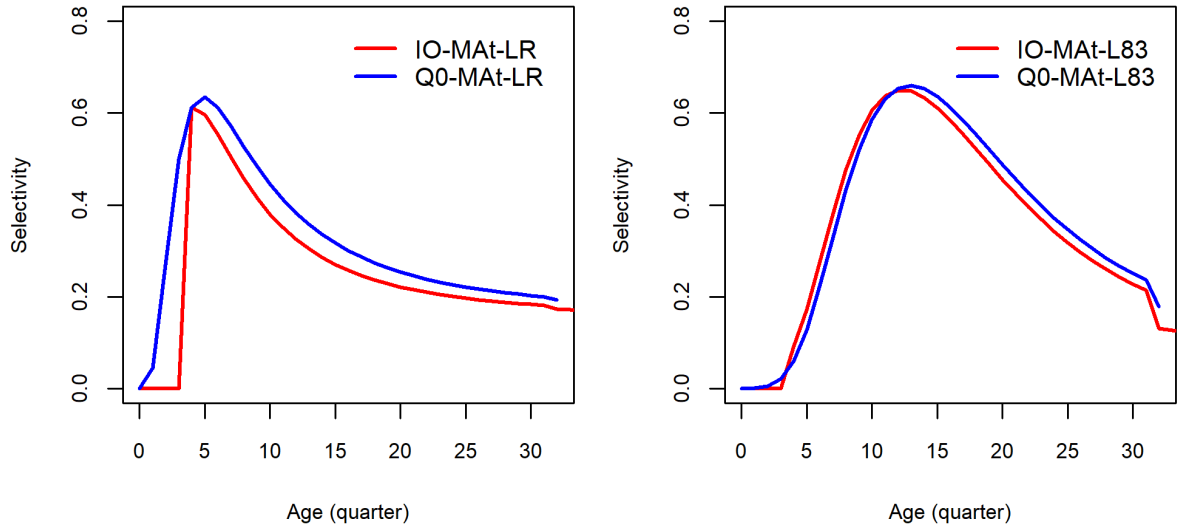

Figure A14 A comparison of selectivity at age (quarterly age) between models IO and Q0 (left, growth LR), and between models IO-L83 and Q0-L83 (right, growth L83).

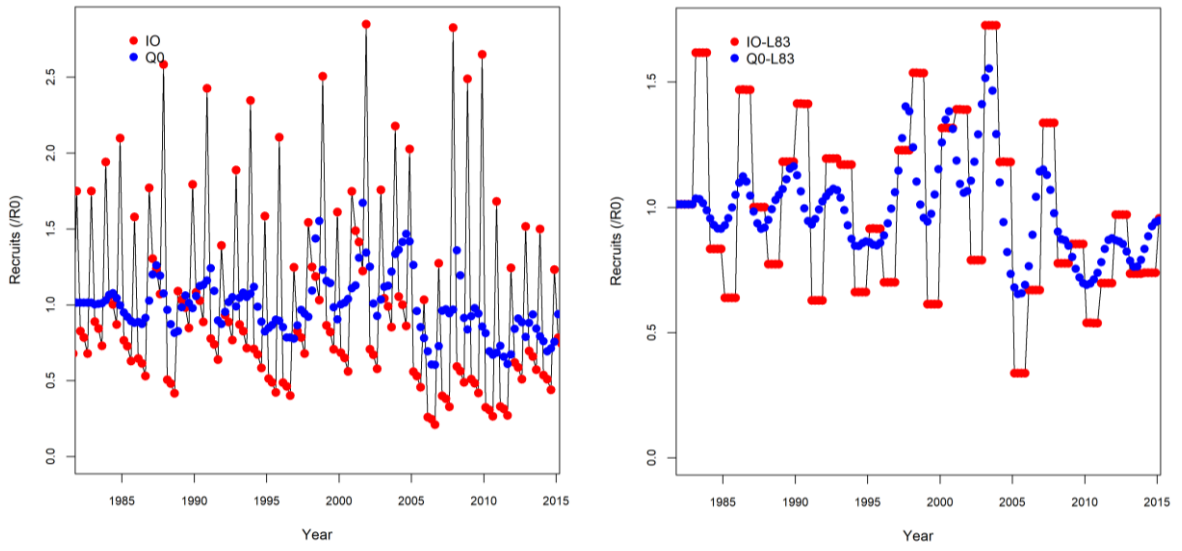

Figure A15: A comparison of seasonal recruitment pattern between models IO and Q0 (left, LR growth), and between models IO-L83 and Q0-L83 (right, L83 growth).

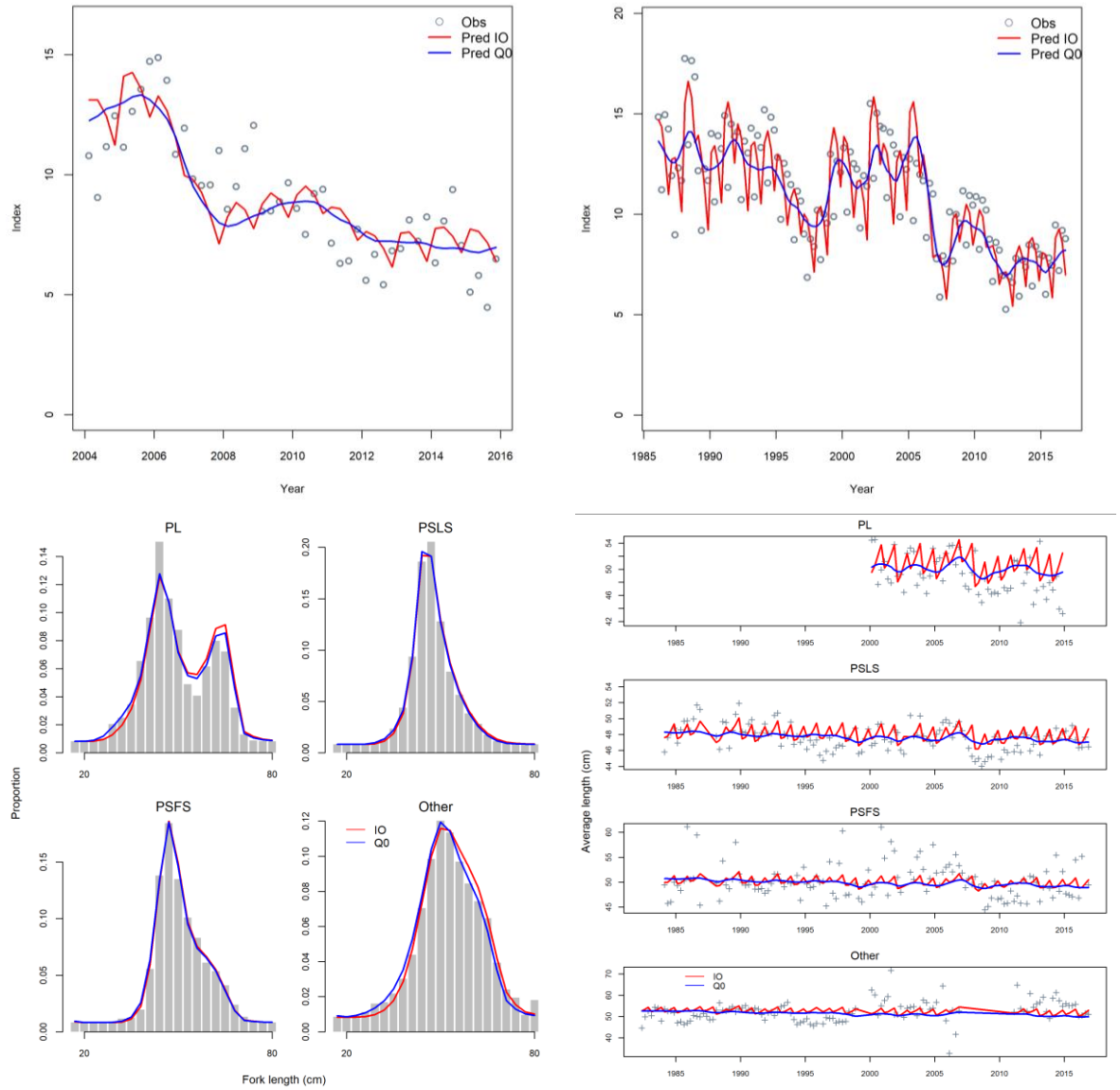

Figure A16: Comparison of fits to the PL CPUE (top-left), PS long CPUE (top-right), aggregated LF by fisheries (bottom left, and mean quarterly (bottom right) LF over time between model IO and Q0.

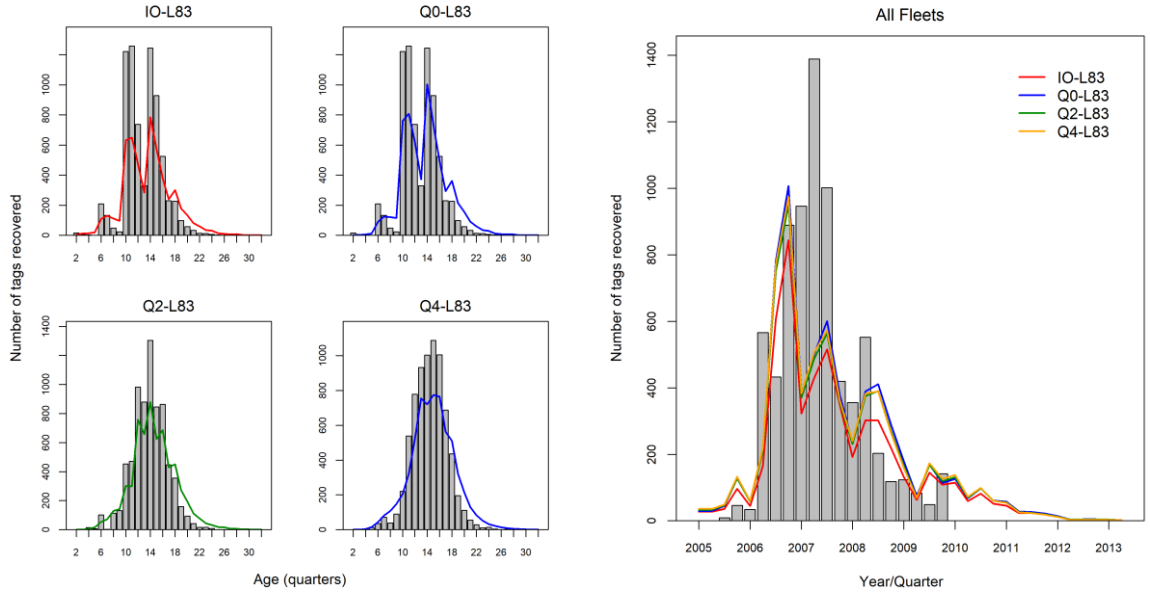

Figure A17: Predicted and observed tag recaptures by quarterly age at recovery (left), and by recovery year/quarter (right), aggregated across tag groups for models IO-L83, Q0-L83, Q2-L83, and Q4-L83 (growth L83). For IO-L83, quarterly recovery age is calculated as the annual age (in quarters) at release plus time-at-liberty. Note that only observed recaptures after the mixing period are included.

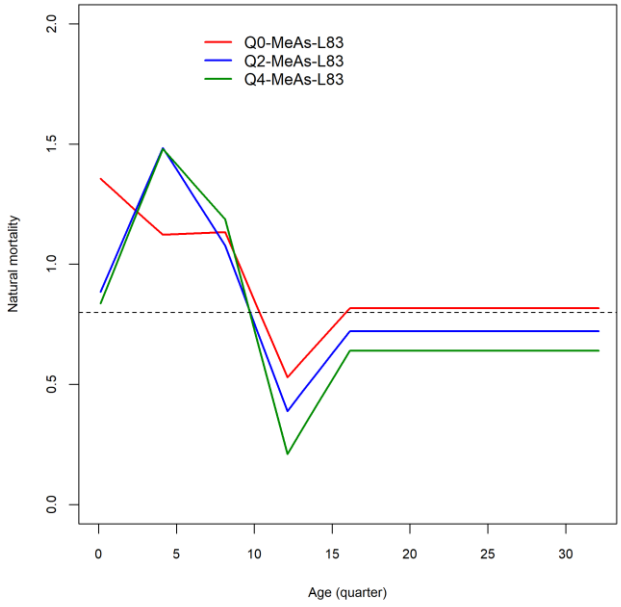

Figure A18: A comparison of M estimates between models, Q0-MeAs-L83, Q2-MeAs-L83, Q4-MeAs-L83 (L83 growth).

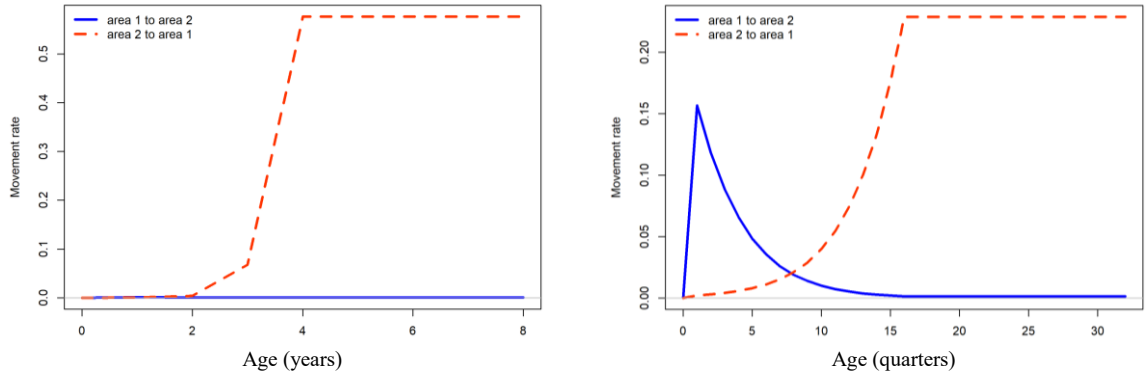

Figure A19: estimated movement rate of SKJ between the eastern (area 1) and western Indian Ocean from model IO2 (left) and IO2Q0 (right). Both models used the rtss tag progam option.

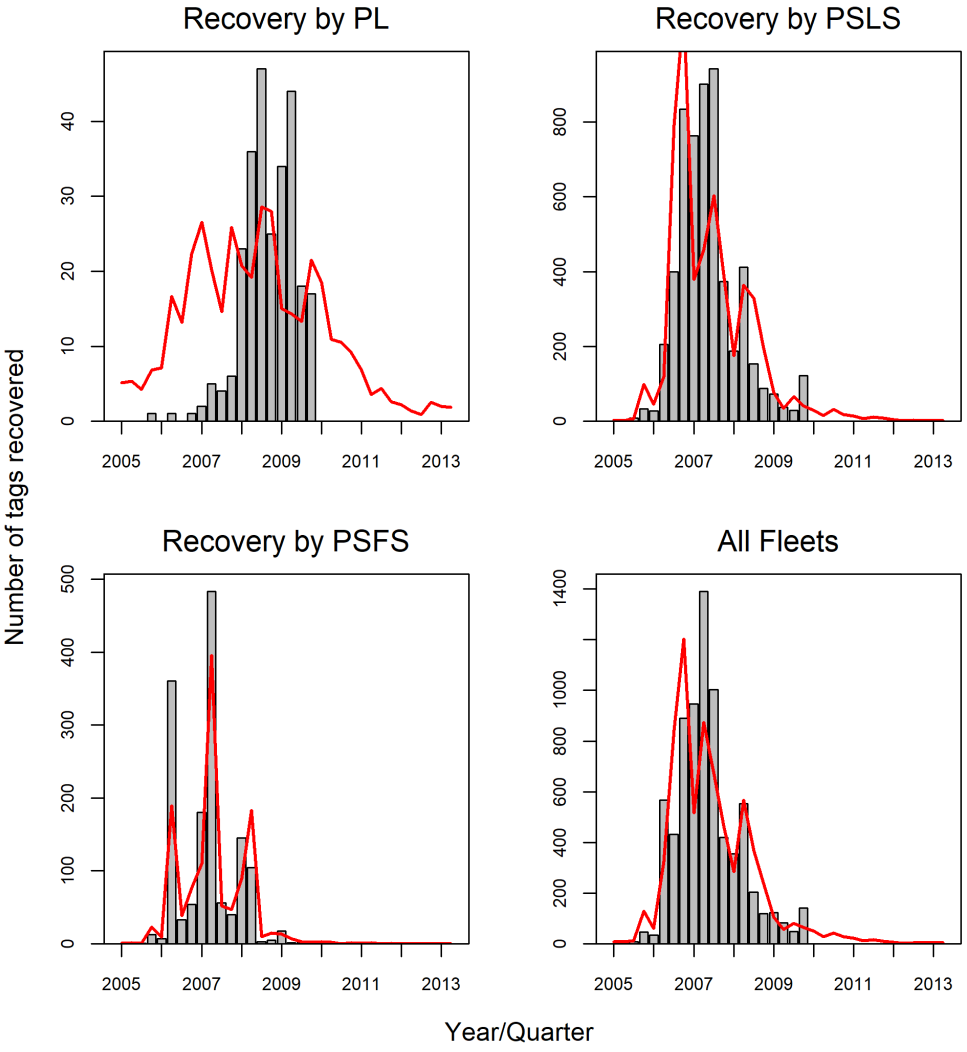

Figure A20: Predicted and observed tag recaptures by recovery year/quarter, aggregated across tag groups for model IO2-RTSS. Note that only observed recaptures after the mixing period are included.

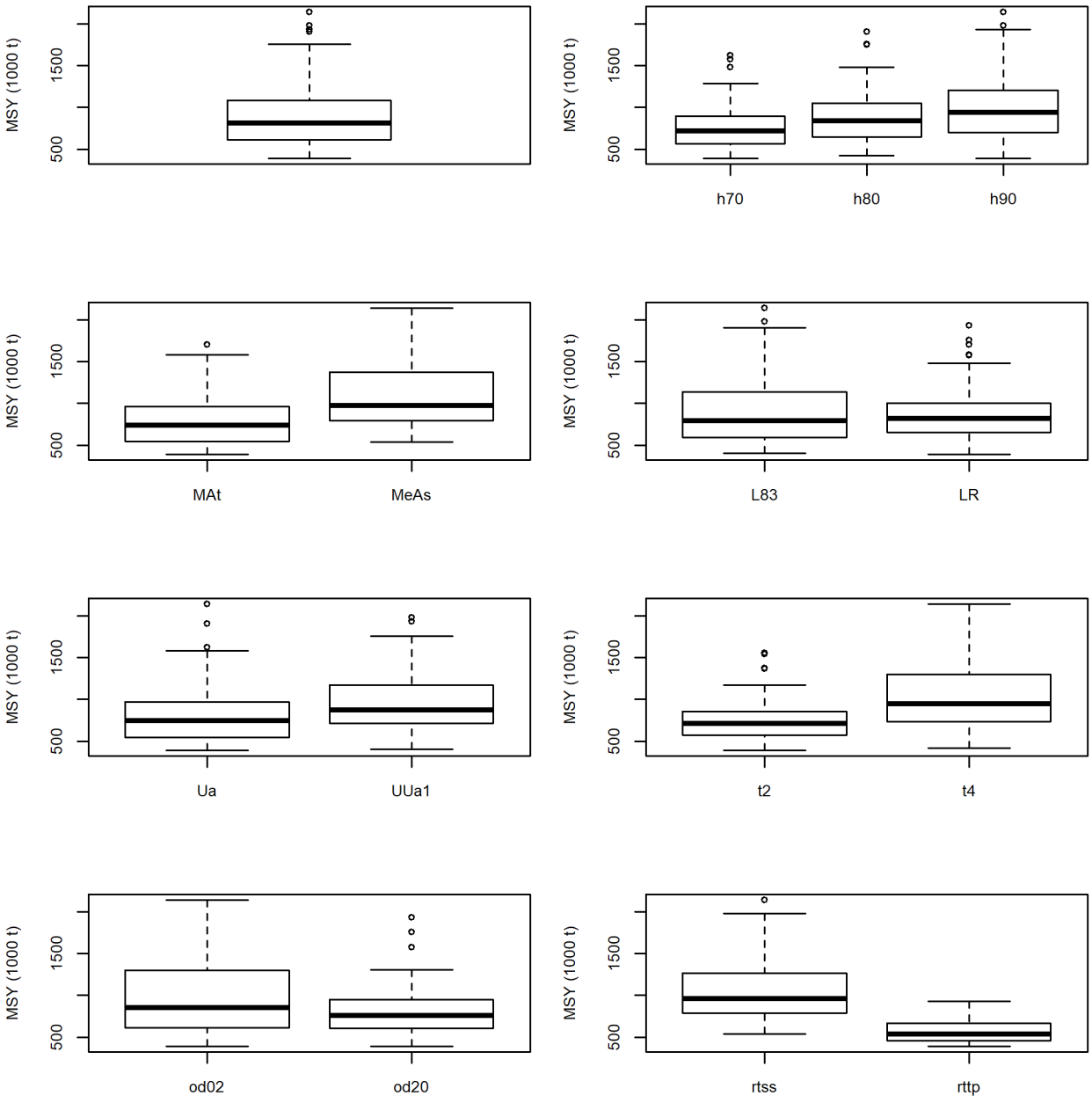

Figure A21: Key management quantities estimates: MSY for the 1422 models included in grid-IO, partitioned by assessment options.

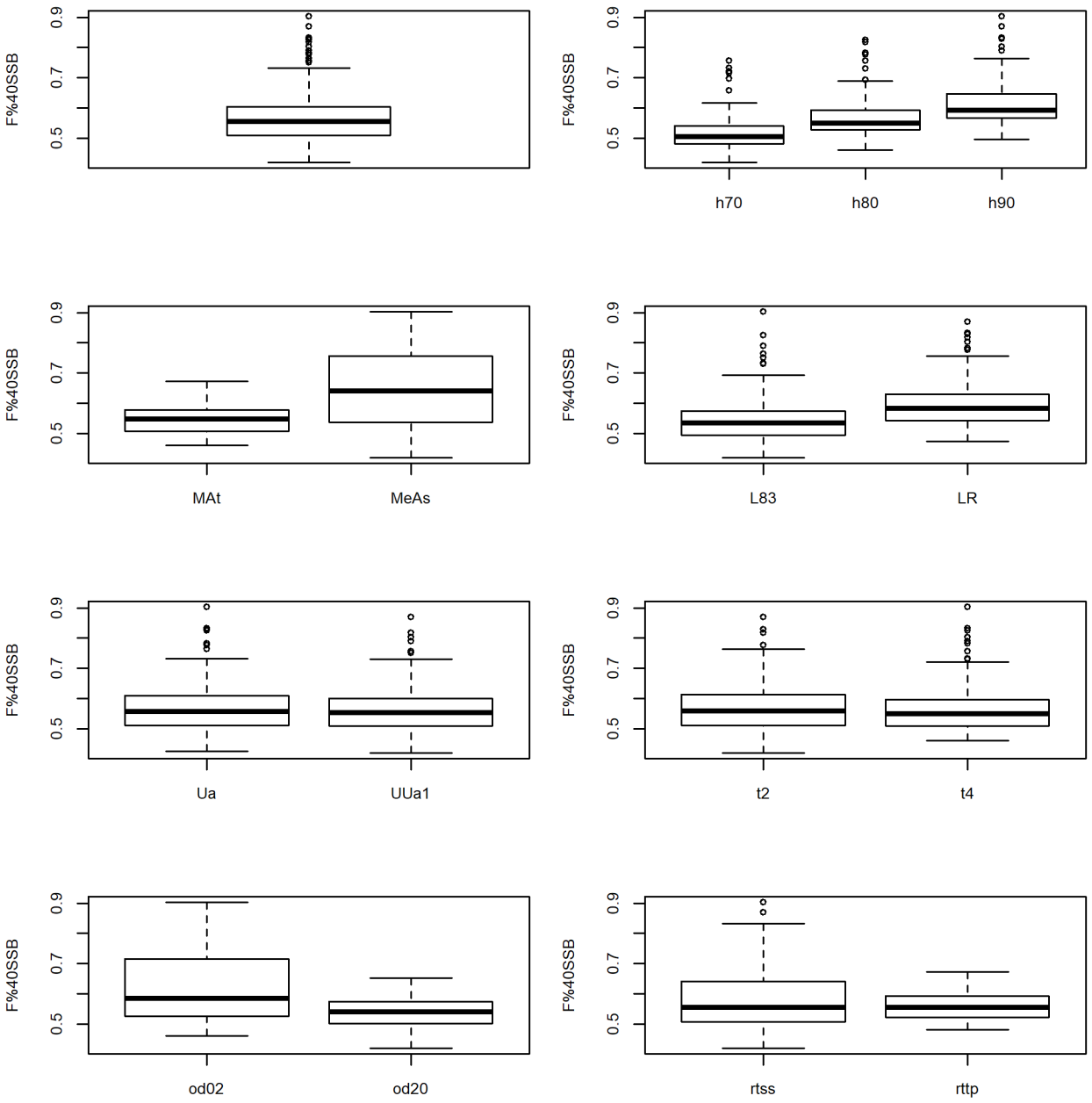

Figure A22: Key management quantities estimates: $F_{\%40SSB}$ for the 142 models included in grid-IO, partitioned by assessment options.

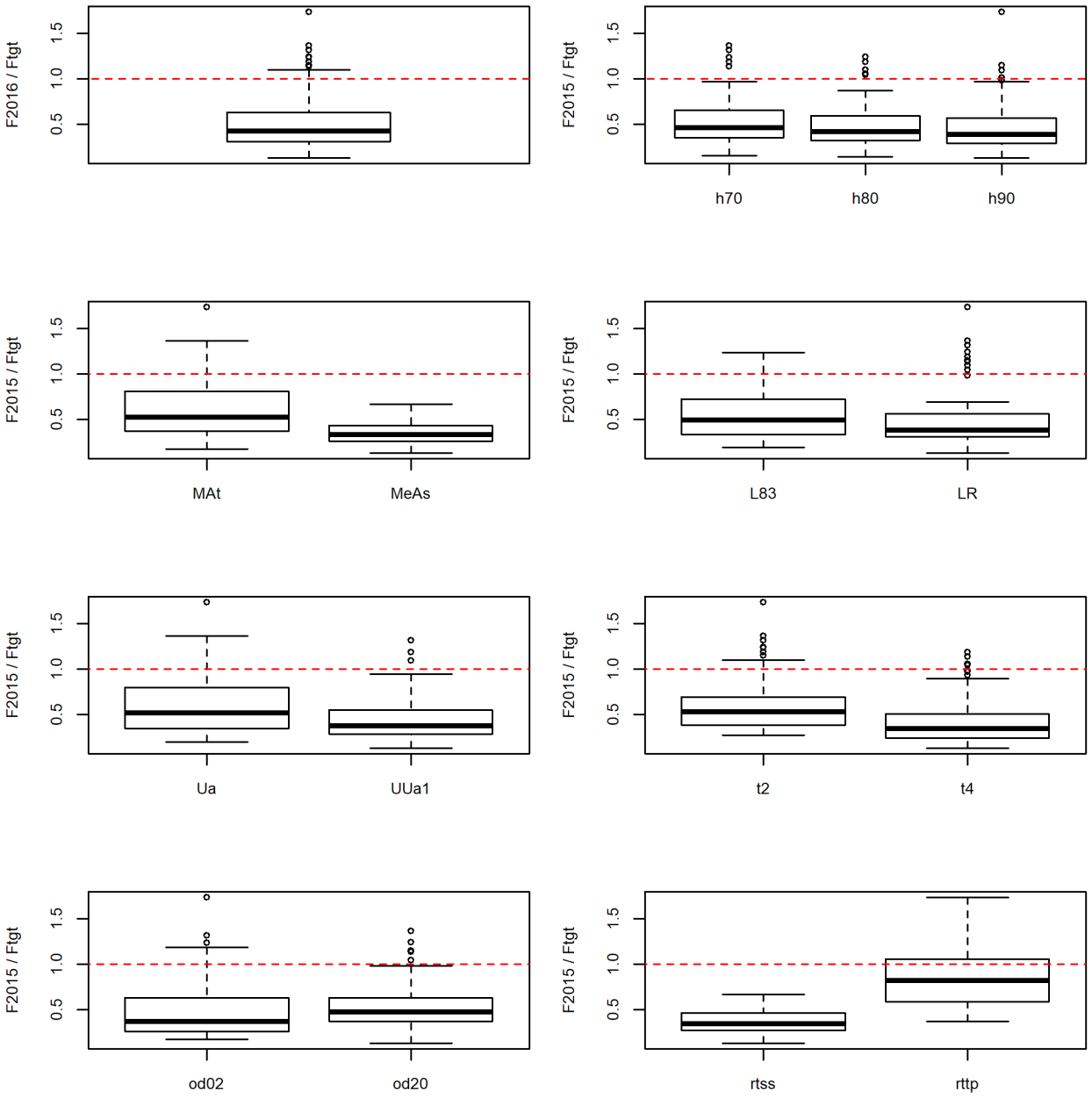

Figure A24: Key management quantities estimates: F_{2016} / $F_{\%40SSB}$ for the 142 models included in grid-IO, partitioned by assessment options.

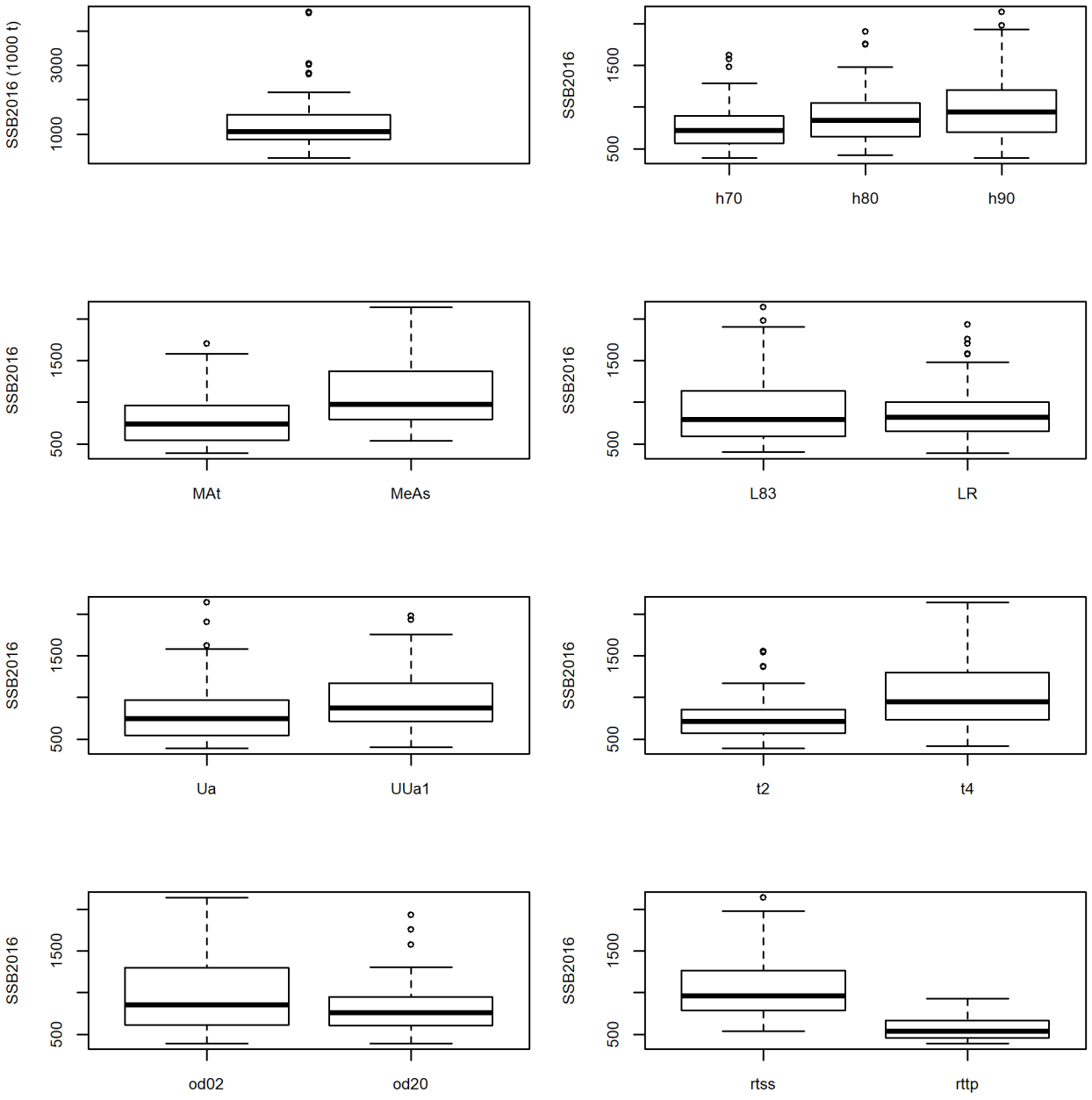

Figure A23: Key management quantities estimates: SSB2016 for the 142 models included in grid-IO, partitioned by assessment options.

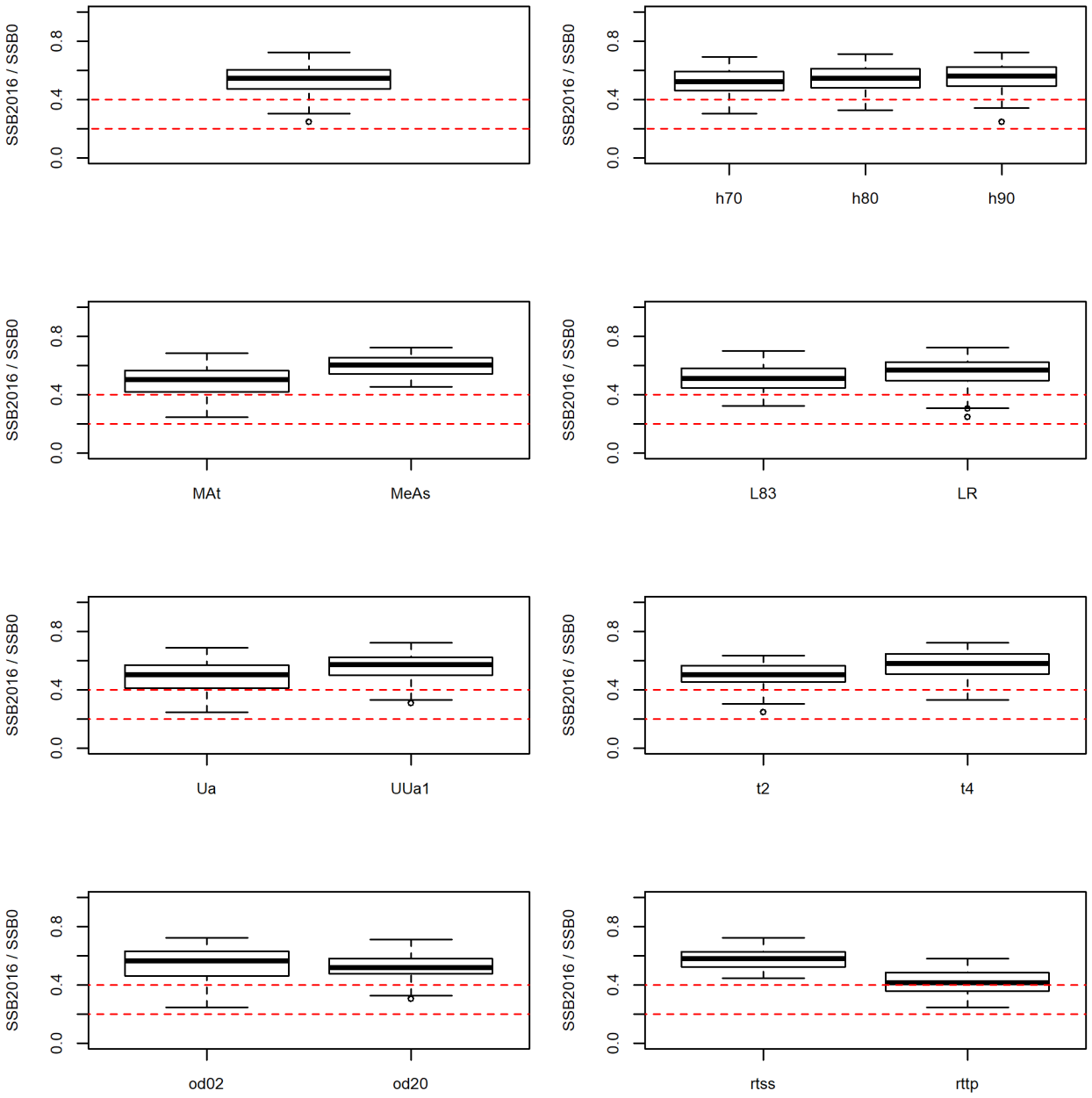

Figure A25: Key management quantities estimates: SSB2016 / SSB0 for the 142 models included in grid-IO, partitioned by assessment options.

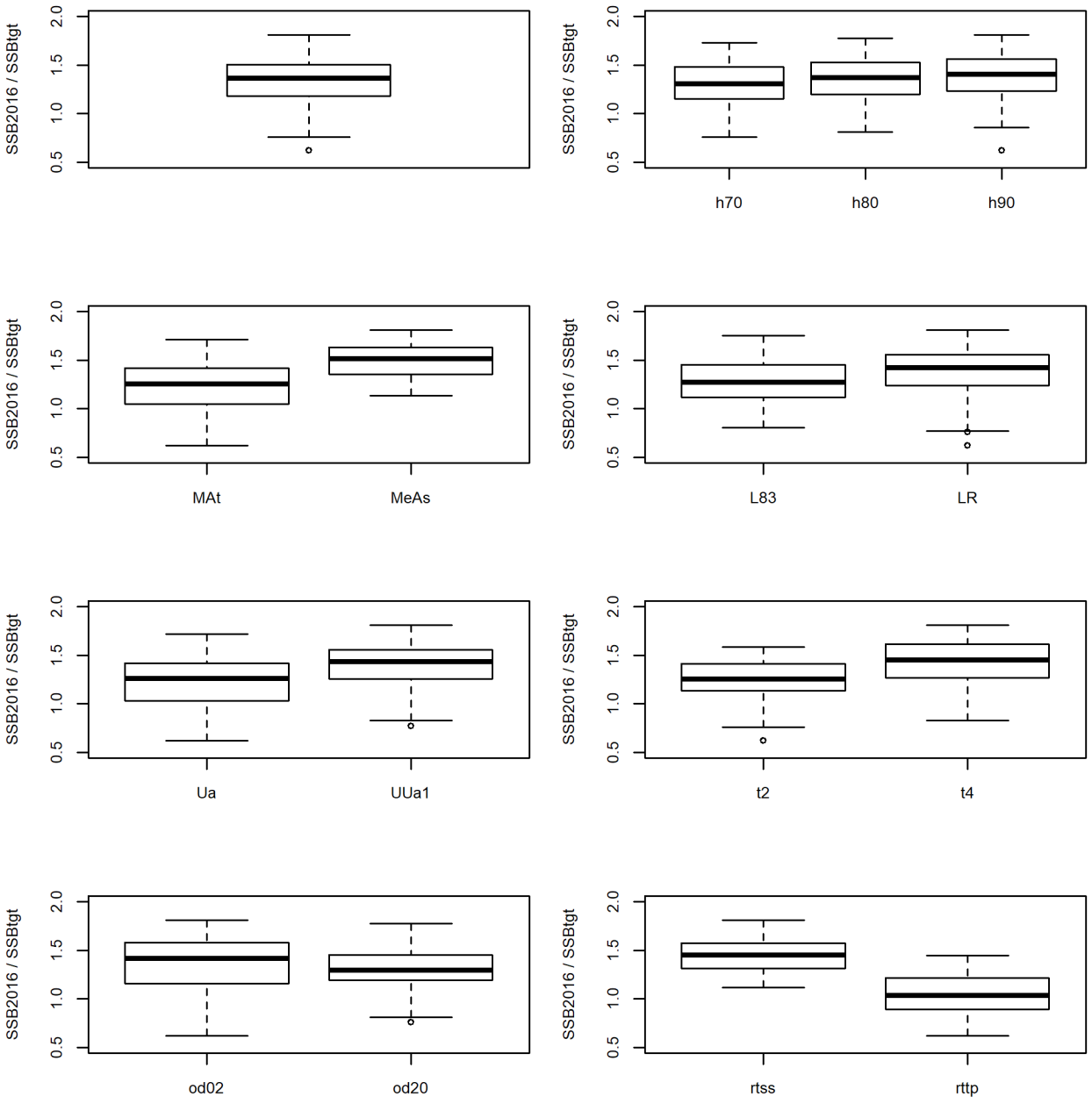

Figure A26: Key management quantities estimates: $SSB_{2016}/SSB_{\%40}$ for the 142 models included in grid-IO, partitioned by assessment options.

APPENDIX B: SS3 CONTROL.SS FILE TEMPLATE

Each model assumption from Table 5 is created by the automated removal of flagged comment markers (only for the single area, SS internal year season model). The section defining tag loss parameters and tag overdispersion parameters are omitted.

```
1 #_N_Growth_Patterns
1 #_N_Morphs_Within_GrowthPattern
# 1 #_Morph_between/within_stdev_ratio (no read if N_morphs=1)
# 1 #vector_Morphdist_(-1_in_first_val_gives_normal_approx)
# 1 #   number of recruitment designs
4 #  number of recruitment designs
0 # recruitment interaction requested
#GP seas pop
 1 1 1
 1 2 1
 1 3 1
 1 4 1
# 1 2 1
# 1 3 1
# 1 4 1
# 0 # N_movement_definitions goes here if pop > 1
# 1.0 # first age that moves (real age at begin of season, not integer)
# 1 1 1 2 4 10 # example move definition for seas=1, morph=1, source=1 dest=2, age1=4, age2=10
2 #_Nblock_Designs
5 5 # N_Blocks_per design
1960 1988 1989 1993 1994 1998 1999 2003 2004 2009
1960 1976 1977 1984 1985 1992 1993 2000 2001 2009
0.5 #_fracfemale
1 #_natM_type:_0=1Parm;
1=N_breakpoints;_2=Lorenzen;_3=agespecific;_4=agespec_withseasinterpolate
#5 #_N_breakpoints
#.75  1.25  1.75 2.25 3.75  # age(real) at M breakpoints

# xxx MAt 5 #_N_breakpoints
# xxx MAt 0 1 2 3 4 # age(real) at M breakpoints
# xxx M07 5 #_N_breakpoints
# xxx M07 0 1 2 3 4 # age(real) at M breakpoints
# xxx M09 5 #_N_breakpoints
# xxx M09 0 1 2 3 4 # age(real) at M breakpoints
# xxx MeA1 4 #_N_breakpoints
# xxx MeA1 1 2 3 4 # age(real) at M breakpoints
# xxx MeAs 5 #_N_breakpoints
# xxx MeAs 0 1 2 3 4 # age(real) at M breakpoints
# xxx MB 6 #_N_breakpoints
# xxx MB 1.99 2 2.99 3 3.99 4 # age(real) at M breakpoints

# xxx L83 1 # GrowthModel: 1=vonBert with L1&L2; 2=Richards with L1&L2; 3=not implemented; 4=not implemented
# xxx L70 1 # GrowthModel: 1=vonBert with L1&L2; 2=Richards with L1&L2; 3=not implemented; 4=not implemented
# xxx LR 2 # GrowthModel: 1=vonBert with L1&L2; 2=Richards with L1&L2; 3=not implemented; 4=not implemented
```

```
0 #_Growth_Age_for_L1 #mid-season used for calculations
999 #_Growth_Age_for_L2 (999 to use as Linf)
0.1 #_SD_add_to_LAA (set to 0.1 for SS2 V1.x compatibility)
#Should see if alternate t0 0 is better to admit growth effects of younger ages inflating CV
0 #_CV_Growth_Pattern:  0 CV=f(LAA); 1 CV=F(A); 2 SD=F(LAA); 3 SD=F(A)
1 #_maturity_option:  1=length logistic; 2=age logistic; 3=read age-maturity matrix by
growth_pattern
#_placeholder for empirical age-maturity by growth pattern
1 #_First_Mature_Age
1 #_fecundity option:(1)eggs=Wt*(a+b*Wt);(2)eggs=a*L^b;(3)eggs=a*Wt^b
0 ### Hermaphroditism season ###
3 #_parameter_offset_approach (1=none, 2= M, G, CV_G as offset from female-GP1, 3=like SS2
V1.x)
1 #_env/block/dev_adjust_method (1=standard; 2=with logistic trans to keep within base parm
bounds)
#_growth_parms
#_LO HI INIT PRIOR PR_type SD PHASE env-var use_dev dev_minyr dev_maxyr dev_stddev
Block Block_Fxn

# ICCAT flat M
# xxx MAt 0.075 2 0.8 0.8 0 1 -5 0 0 0 0 0.5 0 0 # NatM_p_1_Fem_GP:1_
# xxx MAt -3 3 -0.0 -0.0  0 1 -7 0 0 0 0 0.5 0 0 # NatM_p_2_Fem_GP:1_
# xxx MAt -3 3 -0.0 -0.0  0 1 -7 0 0 0 0 0.5 0 0 # NatM_p_2_Fem_GP:1_
# xxx MAt -3 3 -0.  -0.   0 1 -6 0 0 0 0 0.5 0 0 # NatM_p_2_Fem_GP:1_
# xxx MAt -3 3 -0.  -0.   0 1 -6 0 0 0 0 0.5 0 0 # NatM_p_2_Fem_GP:1_

# flat M 0.7
# xxx M07 0.075 2 0.7 0.7 0 1 -5 0 0 0 0 0.5 0 0 # NatM_p_1_Fem_GP:1_
# xxx M07 -3 3 -0.0 -0.0  0 1 -7 0 0 0 0 0.5 0 0 # NatM_p_2_Fem_GP:1_
# xxx M07 -3 3 -0.0 -0.0  0 1 -7 0 0 0 0 0.5 0 0 # NatM_p_2_Fem_GP:1_
# xxx M07 -3 3 -0.  -0.   0 1 -6 0 0 0 0 0.5 0 0 # NatM_p_2_Fem_GP:1_
# xxx M07 -3 3 -0.  -0.   0 1 -6 0 0 0 0 0.5 0 0 # NatM_p_2_Fem_GP:1_

# flat M 0.9
# xxx M09 0.075 2 0.9 0.9 0 1 -5 0 0 0 0 0.5 0 0 # NatM_p_1_Fem_GP:1_
# xxx M09 -3 3 -0.0 -0.0  0 1 -7 0 0 0 0 0.5 0 0 # NatM_p_2_Fem_GP:1_
# xxx M09 -3 3 -0.0 -0.0  0 1 -7 0 0 0 0 0.5 0 0 # NatM_p_2_Fem_GP:1_
# xxx M09 -3 3 -0.  -0.   0 1 -6 0 0 0 0 0.5 0 0 # NatM_p_2_Fem_GP:1_
# xxx M09 -3 3 -0.  -0.   0 1 -6 0 0 0 0 0.5 0 0 # NatM_p_2_Fem_GP:1_


# ICCAT flat M initial
# RTTP only
# xxx MeA1 0.075 2 0.8  0.8  0 1 5 0 0 0 0 0.5 0 0 # NatM_p_1_Fem_GP:1_
# xxx MeA1 -5    3 -0. -0.   0 1 7 0 0 0 0 0.5 0 0 # NatM_p_2_Fem_GP:1_
# xxx MeA1 -5    3 -0. -0.   0 1 7 0 0 0 0 0.5 0 0 # NatM_p_2_Fem_GP:1_
# xxx MeA1 -5    3 -0. -0.   0 1 6 0 0 0 0 0.5 0 0 # NatM_p_2_Fem_GP:1_
# small-scale
# xxx MeAs 0.075 2 0.8  0.8  0 1 5 0 0 0 0 0.5 0 0 # NatM_p_1_Fem_GP:1_
# xxx MeAs -5    3 -0. -0.   0 1 7 0 0 0 0 0.5 0 0 # NatM_p_2_Fem_GP:1_
# xxx MeAs -5    3 -0. -0.   0 1 7 0 0 0 0 0.5 0 0 # NatM_p_2_Fem_GP:1_
# xxx MeAs -5    3 -0. -0.   0 1 6 0 0 0 0 0.5 0 0 # NatM_p_2_Fem_GP:1_
# xxx MeAs -5    3 -0. -0.   0 1 6 0 0 0 0 0.5 0 0 # NatM_p_2_Fem_GP:1_
```

```
# Brownie (but not BP) L83 alt fixed
# Linf=83, Brownie: a(1:4)=   0.68      0.50      0.13      0.82
# xxx MB  0.075 2 0.68  0.68  0 1 -5 0 0 0 0 0.5 0 0 # NatM_p_1_Fem_GP:1_
# xxx MB  -5    3 -0.2926 -0.2926   0 1 -7 0 0 0 0 0.5 0 0 # NatM_p_2_Fem_GP:1_
# xxx MB  -5    3 -0. -0.   0 1 -7 0 0 0 0 0.5 0 0 # NatM_p_2_Fem_GP:1_
# xxx MB  -5    3 -1.347 -1.347   0 1 -6 0 0 0 0 0.5 0 0 # NatM_p_2_Fem_GP:1_
# xxx MB  -5    3 -0. -0.   0 1 -6 0 0 0 0 0.5 0 0 # NatM_p_2_Fem_GP:1_
# xxx MB  -5    3 1.8417 1.8417   0 1 -6 0 0 0 0 0.5 0 0 # NatM_p_2_Fem_GP:1_

# xxx L83  -30 30   20  20 0 100 -5 0 0 0 0 0.5 0 0 # L_at_Amin_Fem_GP_1
# xxx L83  50 100  83   83 0 100 -5 0 0 0 0 0.5 0 0 # L_at_Amax_Fem_GP_1
# xxx L83  -3 3  0.22 0.22 0 100 -1 0 0 0 0 0.5 0 0 # VonBert_K_Fem_GP_1
# xxx L70  -30 30   20  20 0 100 -5 0 0 0 0 0.5 0 0 # L_at_Amin_Fem_GP_1
# xxx L70  50 100  70.2   70.2 0 100 -5 0 0 0 0 0.5 0 0 # L_at_Amax_Fem_GP_1
# xxx L70  -3 3  0.373 0.373 0 100 -1 0 0 0 0 0.5 0 0 # VonBert_K_Fem_GP_1
# xxx LR  -30     30      5.89629 20      0       100     -5      0       0       0       0       0.5     0       0       #
L_at_Amin_Fem_GP_1
# xxx LR  50      100     70.3509 70.2    0       100     -5      0       0       0       0       0.5     0       0       #
L_at_Amax_Fem_GP_1
# xxx LR  -3      3       0.34809 0.373   0       100     -1      0       0       0       0       0.5     0       0       #
VonBert_K_Fem_GP_1
# xxx LR  0       5       2.9096  1       -1      1       -5      0       0       0       0       0       0       0       #
Richards_Fem_GP_1


# start with CV20%, decrease to 10% at older ages
   0.01 60 0.2 0.2 0 100 -5 0 0 0 0 0.5 0 0 # CV_young_Fem_GP_1_ #try alternates to account for
growth
   -3 3 -0.69 -0.69 0 100 -5 0 0 0 0 0.5 0 0  # CV_old_Fem_GP_1_ #try alternates to account for
growth

-3 3 4.97e-006 4.97e-006 0 100 -1 0 0 0 0 0.5 0 0  # Wtlen1_Fem #IOTC value 5.32e-006 5.32e-006
 2 4 3.39292 3.39292  0 100 -1 0 0 0 0 0.5 0 0     # Wtlen2_Fem #IOTC value 3.34958 3.34958

 1 150 38 38 0 100 -1 0 0 0 0 0.5 0 0 # Mat50_Fem
## xxx MAtm58 1 150 58 58 0 100 -1 0 0 0 0 0.5 0 0 # Mat50_Fem
## xxx MAtm38 1 150 38 38 0 100 -1 0 0 0 0 0.5 0 0 # Mat50_Fem
## xxx MeA1m58 1 150 58 58 0 100 -1 0 0 0 0 0.5 0 0 # Mat50_Fem
## xxx MeA1m38 1 150 38 38 0 100 -1 0 0 0 0 0.5 0 0 # Mat50_Fem
## xxx MeA.1m58 1 150 58 58 0 100 -1 0 0 0 0 0.5 0 0 # Mat50_Fem
## xxx MeA.1m38 1 150 38 38 0 100 -1 0 0 0 0 0.5 0 0 # Mat50_Fem
## xxx MBm58 1 150 58 58 0 100 -1 0 0 0 0 0.5 0 0 # Mat50_Fem
## xxx MBm38 1 150 38 38 0 100 -1 0 0 0 0 0.5 0 0 # Mat50_Fem


# xxx check maturity slope sensible...
 -8 1 -1.25 -1.25 0 100 -1 0 0 0 0 0.5 0 0 # Mat_slope_Fem
 0 2 1 1 0 100 -1 0 0 0 0 0.5 0 0 # Eggs1_Fem
 -1 1 0 0 0 100 -1 0 0 0 0 0.5 0 0 # Eggs2_Fem
 -4 4 0 0 -1 99 -3 0 0 0 0 0.5 0 0 # RecrDist_GP_1_
 -4 4 0 0 -1 99 -3 0 0 0 0 0.5 0 0 # RecrDist_Area_1_
 -4 4 0 0 -1 99 -3 0 0 0 0 0.5 0 0 # RecrDist_Seas_1_
 -4 4 0 0 0 0.1 5 0 1 1983 2015 0.3 0 0 # RecrDist_Seas_2_
 -4 4 0 0 0 0.1 5 0 1 1983 2015 0.3 0 0 # RecrDist_Seas_3_
 -4 4 0 0 0 0.1 5 0 1 1983 2015 0.3 0 0 # RecrDist_Seas_4_
```

```
 1 1 1 1 -1 99 -3 0 0 0 0 0.5 0 0 # CohortGrowDev
# 0  #custom_MG-env_setup (0/1)
# -2 2 0 0 -1 99 -2 #_placeholder for no MG-environ parameters
# 0  #custom_MG-block_setup (0/1)
# -2 2 0 0 -1 99 -2 #_placeholder for no MG-block parameters
#_seasonal_effects_on_biology_parms
 0 0 0 0 0 0 0 0 0 0 #_femwtlen1,femwtlen2,mat1,mat2,fec1,fec2,Malewtlen1,malewtlen2,L1,K
# -2 2 0 0 -1 99 -2 #_placeholder for no seasonal MG parameters
# -2 2 0 0 -1 99 -2 #_placeholder for no MG dev parameters
5 # placeholder for #_MGparm_Dev_Phase
#_Spawner-Recruitment
6 #_SR_function: 1=null; 2=Ricker; 3=std_B-H; 4=SCAA; 5=Hockey; 6=B-H_flattop;
7=Survival_3Parm
#_LO HI INIT PRIOR PR_type SD PHASE
 0 35 20 20 0 10 1 # SR_R0 ##
# xxx h70 0.201 0.99 0.70 0.70 0 10 -2 # SR_steepness
# xxx h80 0.201 0.99 0.80 0.80 0 10 -2 # SR_steepness
# xxx h90 0.201 0.99 0.90 0.90 0 10 -2 # SR_steepness
  0 10 0.6 0.6 0 10 6 # SR_sigmaR
 -5 5 0 0 0 1 -3 # SR_envlink
 -5 5 0 0 0 1 -4 # SR_R1_offset ## changed from -4 (fixed) to 1 (estimated) ##
 0 0.5 0 0 -1 99 -2 # SR_autocorr
0 #_SR_env_link
0 #_SR_env_target_0=none;1=devs;_2=R0;_3=steepness
# xxx r0   0 #do_recdev:  0=none; 1=devvector; 2=simple deviations
# xxx rqs  1 #do_recdev:  0=none; 1=devvector; 2=simple deviations
1983 # first year of main recr_devs; early devs can preceed this era
2014 # last year of main recr_devs; forecast devs start in following year
4 #_recdev phase
1 #0 # (0/1) to read 11 advanced options
0 #_recdev_early_start (0=none; neg value makes relative to recdev_start)
-4 #_recdev_early_phase
-10 #_forecast_recruitment phase (incl. late recr) (0 value resets to maxphase+1)
1 #_lambda for prior_fore_recr occurring before endyr+1
1960 #_last_early_yr_nobias_adj_in_MPD
1983 #_first_yr_fullbias_adj_in_MPD
2014 #_last_yr_fullbias_adj_in_MPD
2015 #_first_recent_yr_nobias_adj_in_MPD
1 #_max_bias_adj_in_MPD
0 # period of cycle in recruitment
-15 #min rec_dev
15 #max rec_dev
0 #_read_recdevs
#_end of advanced SR options
#Fishing Mortality info
0.15 # F ballpark for tuning early phases
2000 # F ballpark year(neg value to disable)
3 # F_Method:  1=Pope; 2=instan. F; 3=hybrid (hybrid is recommended)
7 # max F or harvest rate, depends on F_Method ## We can changed from 0.99 to 4 if F_method is
hyblid(3) ##
# no additional F input needed for Fmethod 1
# read overall start F value; overall phase; N detailed inputs to read for Fmethod 2
5 # read N iterations for tuning for Fmethod 3 (recommend 3 to 7)
# Fleet Year Seas F_value se phase (for detailed setup of F_Method=2)
#_initial_F_parms
```

```
#_LO HI INIT PRIOR PR_type SD PHASE ## changed the following maximum values from 0.9 to
3.99 ##

 0 3.99 0.0 0.0   0 100  -1 # InitF_1_LL (longline)
 0 3.99 0.0 0.0   0 100  -1 # InitF_2_PSFS
 0 3.99 0.0 0.0   0 100  -1 # InitF_3_PSLS
 0 3.99 0.0 0.0   0 100  -1 # InitF_4_Other

#_Q_setup
 # A=do power, B=env-var, C=extra SD, D=devtype(<0=mirror, 0/1=none, 2=cons, 3=rand,
4=randwalk); E=0=num/1=bio, F=err_type
 #_A  B  C  D  E  F ## change the following values of error-type from 0 to 30 for the future ##
 0 0 0 0
 0 0 0 0
 0 0 0 0
 0 0 0 0
 0 0 0 0
 0 0 0 0
 0 0 0 0
 # 0 #_0=read one parm for each fleet with random q; 1=read a parm for each year of index
#_Q_parms(if_any)
# # Double normal size selectivity option
# # Start Size Sel Block
# #_size_selex_types
# #_Pattern Discard Male Special


#_size_selex_types
#_Pattern Discard Male Special
# piecewise size selex


# cubic spline size selex
 27 0 0 7 # 1
 27 0 0 5 # 2
 27 0 0 5 # 3
 27 0 0 5 # 4
 5 0 0 1 # CPUE mirror 1
 5 0 0 2 # CPUE mirror 3
 5 0 0 2 # CPUE mirror 3
#_age_selex_types = none
10 0 0 0 # f1
10 0 0 0 # f2
10 0 0 0 # f3
10 0 0 0 # f4
10 0 0 0 # cpue1
10 0 0 0 # cpue LSLS
10 0 0 0 # cpue FSLS
#_LO HI INIT PRIOR PR_type SD PHASE env-var use_dev dev_minyr dev_maxyr dev_stddev
Block Block_Fxn
## 1. LL (longline)
#
# fishery 1 #max age 15
# LO HI INIT PRIOR PR_type SD PHASE
#len bounds
```

```
# LO HI INIT PRIOR PR_type SD PHASE env-var use_dev dev_minyr dev_maxyr dev_stddev
Block Block_Fxn
 0 0 0 0 -1 0 -99 0 0 0 0 0.5 0 0 # SizeSpline_Code_PL_1
 -0.001 1 0.247221 0 1 0.001 3 0 0 0 0 0.5 0 0 # SizeSpline_GradLo_PL_1
 -1 0.001 -0.658209 0 1 0.001 3 0 0 0 0 0.5 0 0 # SizeSpline_GradHi_PL_1
 1 1 22.6447 0 -1 0 -99 0 1 2004 2008 0.05 0 0 # SizeSpline_Knot_1_PL_1
 1 1 37.5977 0 -1 0 -99 0 1 2004 2008 0.05 0 0 # SizeSpline_Knot_2_PL_1
 1 1 42.0377 0 -1 0 -99 0 1 2004 2008 0.05 0 0 # SizeSpline_Knot_3_PL_1
 1 1 45.702 0 -1 0 -99 0 1 2004 2008 0.05 0 0 # SizeSpline_Knot_4_PL_1
 1 1 51.7386 0 -1 0 -99 0 1 2004 2008 0.05 0 0 # SizeSpline_Knot_5_PL_1
 1 1 59.9904 0 -1 0 -99 0 1 2004 2008 0.05 0 0 # SizeSpline_Knot_6_PL_1
 1 1 71.3145 0 -1 0 -99 0 1 2004 2008 0.05 0 0 # SizeSpline_Knot_7_PL_1
 -9 7 -4.42509 0 1 0.001 2 0 1 2004 2008 0.05 0 0 # SizeSpline_Val_1_PL_1
 -9 7 -2.2233 0 1 0.001 2 0 1 2004 2008 0.05 0 0 # SizeSpline_Val_2_PL_1
 -9 7 -1.56912 0 1 0.001 2 0 1 2004 2008 0.05 0 0 # SizeSpline_Val_3_PL_1
 -9 7 -1 0 -1 0 -99 0 1 2004 2008 0.05 0 0 # SizeSpline_Val_4_PL_1
 -9 7 -1.26099 0 1 0.001 2 0 1 2004 2008 0.05 0 0 # SizeSpline_Val_5_PL_1
 -9 7 -0.55179 0 1 0.001 2 0 1 2004 2008 0.05 0 0 # SizeSpline_Val_6_PL_1
 -9 7 -0.579285 0 1 0.001 2 0 1 2004 2008 0.05 0 0 # SizeSpline_Val_7_PL_1
 0 0 0 0 -1 0 -99 0 0 0 0 0.5 0 0 # SizeSpline_Code_PSLS_2
 -0.001 1 0.622317 0 1 0.001 3 0 0 0 0 0.5 0 0 # SizeSpline_GradLo_PSLS_2
 -1 0.001 -0.110388 0 1 0.001 3 0 0 0 0 0.5 0 0 # SizeSpline_GradHi_PSLS_2
 1 1 23.125 0 -1 0 -99 0 1 2004 2008 0.05 0 0 # SizeSpline_Knot_1_PSLS_2
 1 1 41.9035 0 -1 0 -99 0 1 2004 2008 0.05 0 0 # SizeSpline_Knot_2_PSLS_2
 1 1 45.6322 0 -1 0 -99 0 1 2004 2008 0.05 0 0 # SizeSpline_Knot_3_PSLS_2
 1 1 50.2975 0 -1 0 -99 0 1 2004 2008 0.05 0 0 # SizeSpline_Knot_4_PSLS_2
 1 1 70.9228 0 -1 0 -99 0 1 2004 2008 0.05 0 0 # SizeSpline_Knot_5_PSLS_2
 -9 7 -8.9974 0 1 0.001 -2 0 1 2004 2008 0.05 0 0 # SizeSpline_Val_1_PSLS_2
 -9 7 -2.05844 0 1 0.001 2 0 1 2004 2008 0.05 0 0 # SizeSpline_Val_2_PSLS_2
 -9 7 -1 0 -1 0 -99 0 1 2004 2008 0.05 0 0 # SizeSpline_Val_3_PSLS_2
 -9 7 -0.954789 0 1 0.001 2 0 1 2004 2008 0.05 0 0 # SizeSpline_Val_4_PSLS_2
 -9 7 -2.24451 0 1 0.001 2 0 1 2004 2008 0.05 0 0 # SizeSpline_Val_5_PSLS_2
 0 0 0 0 -1 0 -99 0 0 0 0 0.5 0 0 # SizeSpline_Code_PSFS_3
 -0.001 1 0.0149309 0 1 0.001 3 0 0 0 0 0.5 0 0 # SizeSpline_GradLo_PSFS_3
 -1 0.001 -0.245826 0 1 0.001 3 0 0 0 0 0.5 0 0 # SizeSpline_GradHi_PSFS_3
 1 1 23.1313 0 -1 0 -99 0 1 2004 2008 0.05 0 0 # SizeSpline_Knot_1_PSFS_3
 1 1 44.1442 0 -1 0 -99 0 1 2004 2008 0.05 0 0 # SizeSpline_Knot_2_PSFS_3
 1 1 48.4634 0 -1 0 -99 0 1 2004 2008 0.05 0 0 # SizeSpline_Knot_3_PSFS_3
 1 1 54.7779 0 -1 0 -99 0 1 2004 2008 0.05 0 0 # SizeSpline_Knot_4_PSFS_3
 1 1 71.2972 0 -1 0 -99 0 1 2004 2008 0.05 0 0 # SizeSpline_Knot_5_PSFS_3
 -9 7 -8.99994 0 1 0.001 -2 0 1 2004 2008 0.05 0 0 # SizeSpline_Val_1_PSFS_3
 -9 7 -2.04755 0 1 0.001 2 0 1 2004 2008 0.05 0 0 # SizeSpline_Val_2_PSFS_3
 -9 7 -1 0 -1 0 -99 0 1 2004 2008 0.05 0 0 # SizeSpline_Val_3_PSFS_3
 -9 7 -1.02858 0 1 0.001 2 0 1 2004 2008 0.05 0 0 # SizeSpline_Val_4_PSFS_3
 -9 7 -1.20735 0 1 0.001 2 0 1 2004 2008 0.05 0 0 # SizeSpline_Val_5_PSFS_3
 0 0 0 0 -1 0 -99 0 0 0 0 0.5 0 0 # SizeSpline_Code_Other_4
 -0.001 1 0.0655165 0 1 0.001 3 0 0 0 0 0.5 0 0 # SizeSpline_GradLo_Other_4
 -1 0.001 -0.202624 0 1 0.001 3 0 0 0 0 0.5 0 0 # SizeSpline_GradHi_Other_4
 1 1 22.5552 0 -1 0 -99 0 1 2004 2008 0.05 0 0 # SizeSpline_Knot_1_Other_4
 1 1 44.2844 0 -1 0 -99 0 1 2004 2008 0.05 0 0 # SizeSpline_Knot_2_Other_4
 1 1 51.4468 0 -1 0 -99 0 1 2004 2008 0.05 0 0 # SizeSpline_Knot_3_Other_4
 1 1 58.8149 0 -1 0 -99 0 1 2004 2008 0.05 0 0 # SizeSpline_Knot_4_Other_4
 1 1 72.4351 0 -1 0 -99 0 1 2004 2008 0.05 0 0 # SizeSpline_Knot_5_Other_4
 -9 7 -4.41096 0 1 0.001 2 0 1 2004 2008 0.05 0 0 # SizeSpline_Val_1_Other_4
 -9 7 -1.92167 0 1 0.001 2 0 1 2004 2008 0.05 0 0 # SizeSpline_Val_2_Other_4
```

```
 -9 7 -1 0 -1 0 -99 0 1 2004 2008 0.05 0 0 # SizeSpline_Val_3_Other_4
 -9 7 -0.364211 0 1 0.001 2 0 1 2004 2008 0.05 0 0 # SizeSpline_Val_4_Other_4
 -9 7 0.286711 0 1 0.001 2 0 1 2004 2008 0.05 0 0 # SizeSpline_Val_5_Other_4
 1 1 1 1 1 99 -3 0 0 0 0 0.5 0 0 # SizeSel_5P_1_PL_CPUE
 22 22 22 22 1 99 -3 0 0 0 0 0.5 0 0 # SizeSel_5P_2_PL_CPUE
 3 3 3 3 3 99 -3 0 0 0 0 0.5 0 0 # SizeSel_5P_1_LSFS_CPUE
 22 22 22 22 1 99 -3 0 0 0 0 0.5 0 0 # SizeSel_5P_2_LSFS_CPUE
 3 3 3 3 3 99 -3 0 0 0 0 0.5 0 0 # SizeSel_5P_1_PSFS_CPUE
 22 22 22 22 1 99 -3 0 0 0 0 0.5 0 0 # SizeSel_5P_2_PSFS_CPUE

# xxx sa 4 # selparm_Dev_Phase
# xxx sa 1 # selparm_adjust_method 1=direct, 2=logistic transform

# xxx ss -4 # selparm_Dev_Phase
# xxx ss 1 # selparm_adjust_method 1=direct, 2=logistic transform



1 # TG_custom:  0=no read; 1=read
#tag loss parameter - for each tag grp
# -10 10 9 9 1 0.001 -4 0 0 0 0 0 0 0 # TG_loss_init_1_
# chronic tag loss - for each tag group
# -10 10 9 9 1 0.001 -4 0 0 0 0 0 0 0 # TG_loss_chronic_1_
# Overdispersion  for the negative binomial for each tag group
# 1 10 200 200 1 0.001 -4 0 0 0 0 0 0 0 # TG_overdispersion_1_
#tag loss parameter - for each tag grp
# -10 10 9 9 1 0.001 -4 0 0 0 0 0 0 0 # TG_loss_init_1_
#set to negligible value


# Initial tag reporting rate for each fleet, tansformation = rep rate = exp(p)/(1+exp(p)) (apparently if
so upper bound 0 = 100%, -1 = about 50%)
# check transformation; if correct, suggests that if RR=100% p= -0.6935
# This suggests that BET assessment (p=0) was probably wrong!
# But should have failed with INF error; what is going on here?  must be 1/(1+exp(-p))...
# this would still mean BET 2010 was wrong

#PS recoveries already inflated by RR (PSLS and PSFS), estimate PL, force zero for others
#_LO HI INIT PRIOR PR_type SD PHASE env-var use_dev dev_minyr dev_maxyr dev_stddev
Block Block_Fxn
-20     20      0       0       1       99      1       0       0       0       0       0       0
        0       #       TG_report_fleet:_1_
-20     20      10      10      1       0.2     -4      0       0       0       0       0       0
        0       #       TG_report_fleet:_2_
-20     20      10      10      1       0.2     -4      0       0       0       0       0       0
        0       #       TG_report_fleet:_2_
-20     20      -10.    -10.    1       2.      -4      0       0       0       0       0       0
        0       #       TG_report_fleet:_1_
# LO HI INIT PRIOR PR_type SD PHASE
# Exponential decay rate in reporting rate for each fleet (default=0, negative value to get decay)
 -4 0 0 0 0 2 -4 0 0 0 0 0 0 0 # TG_rpt_decay_fleet:_1_
 -4 0 0 0 0 2 -4 0 0 0 0 0 0 0 # TG_rpt_decay_fleet:_2_
 -4 0 0 0 0 2 -4 0 0 0 0 0 0 0 # TG_rpt_decay_fleet:_1_
 -4 0 0 0 0 2 -4 0 0 0 0 0 0 0 # TG_rpt_decay_fleet:_2_
```

```
1 #_Variance_adjustments_to_input_values
#_1 2 3
  0 0 0 0 0 0 0 #_add_to_survey_CV
  0 0 0 0 0 0 0 #_add_to_discard_CV
  0 0 0 0 0 0 0 #_add_to_bodywt_CV
# xxx CL1   1.0 1.0 1.0 1.0 1 1 1 #_mult_by_lencomp_N
# xxx CL5   0.5 0.5 0.5 0.5 1 1 1 #_mult_by_lencomp_N
# xxx CL2   0.2 0.2 0.2 0.2 1 1 1 #_mult_by_lencomp_N
# xxx CL05   0.05 0.05 0.05 0.05 1 1 1 #_mult_by_lencomp_N
# xxx CL01   0.01 0.01 0.01 0.01 1 1 1 #_mult_by_lencomp_N
  1 1 1 1 1 1 1 #_mult_by_agecomp_N
  1 1 1 1 1 1 1 #_mult_by_size-at-age_N
# 30 #_DF_for_discard_like
# 30 #_DF_for_meanbodywt_like
4 #_maxlambdaphase
1 #_sd_offset
12 # number of changes to make to default Lambdas (default value is 1.0)
# Like_comp codes:  1=survey; 2=disc; 3=mnwt; 4=length; 5=age; 6=SizeFreq; 7=sizeage; 8=catch;
# 9=init_equ_catch; 10=recrdev; 11=parm_prior; 12=parm_dev; 13=CrashPen; 14=Morphcomp;
15=Tag-comp; 16=Tag-negbin
#like_comp fleet/survey  phase  value  sizefreq_method

#CPUE
#keep or drop PSFS coupled with PL series
# xxx Ua 1 5 1 1.  1
# xxx Ua 1 6 1 0.  1
# xxx Ua 1 7 1 0.  1
# xxx U1 1 5 1 0.  1
# xxx U1 1 6 1 1.  1
# xxx U1 1 7 1 0.  1
# xxx U3 1 5 1 0.  1
# xxx U3 1 6 1 0.  1
# xxx U3 1 7 1 1.  1
# xxx UUa1 1 5 1 1.  1
# xxx UUa1 1 6 1 1.  1
# xxx UUa1 1 7 1 0.  1

#size
  4 1 1 1. 1
  4 2 1 1. 1
  4 3 1 1. 1
  4 4 1 1. 1
# tags...not clear on assignment definitions
# 15 tag-comp does not seem to do anything?
#
 15 2 2 1.  1
 15 3 2 1.  1
#seems to do something
 16 1 2 1.  1
 16 2 2 1.  1
 16 3 2 1.  1
# lambdas (for info only; columns are phases)
#  0 #_CPUE/survey:_1
#  0 #_CPUE/survey:_2
#  1 #_CPUE/survey:_3
```

```
#  1 #_lencomp:_1
#  1 #_lencomp:_2
#  0 #_lencomp:_3
#  1 #_init_equ_catch
#  1 #_recruitments
#  1 #_parameter-priors
#  0 #_parameter-dev-vectors
#  100 #_crashPenLambda
0 # (0/1) read specs for extra stddev reporting
 # 0 1 -1 5 1 5 1 -1 5 # placeholder for selex type, len/age, year, N selex bins, Growth pattern, N growth ages, NatAge_area(-1 for all), NatAge_yr, N Natages
 # -1 1 1 1 1 # placeholder for vector of selex bins to be reported
 # -1 1 1 1 1 # placeholder for vector of growth ages to be reported
 # -1 1 1 1 1 # placeholder for vector of NatAges ages to be reported
999
```

APPENDIX C: SENSITIVITY USING EU.SPAIN AND EU.FRANCE SIZE DATA

There were some concerns on the use of raised size frequencies from the EU PS fleets (Figures C1-C3). A sensitivity was untaken to use the unraised size frequency data from Spanish and French fleets (provided to the Secretariat prior to the WPTT meeting). These data are also different to the PS size data used in the assessment, as they are 1) for Spanish and French PS fleets only, and 2) covering the 1990 to 2016 timeframe.

The raw size frequency for the associated schools (PSLS) are very similar between the Spanish and French fleets (Figure C1-left). There are some appreciable differences for the free schools (PSFS) (Figure C1-right), where the Spanish fleet appeared to have caught larger skipjack in some years (i.e. 2011 and 2014). Accordingly, the unraised LF (EU.France and EU.Spain combined) is very close to the raised LF for the PSLS (Figure C2-left), and there are marked differences for the PSFS in some years (Figure C2-right).

The fits to the unraised PSFS is not impressive, in particular for years where the size frequency exhibited a few modes, as a result of combining fleets with different length distribution (Figure C1). The overall biomass estimates are similar to the reference model, with the difference mostly explained by the small difference in estimated recruitment deviations (Figure C4).

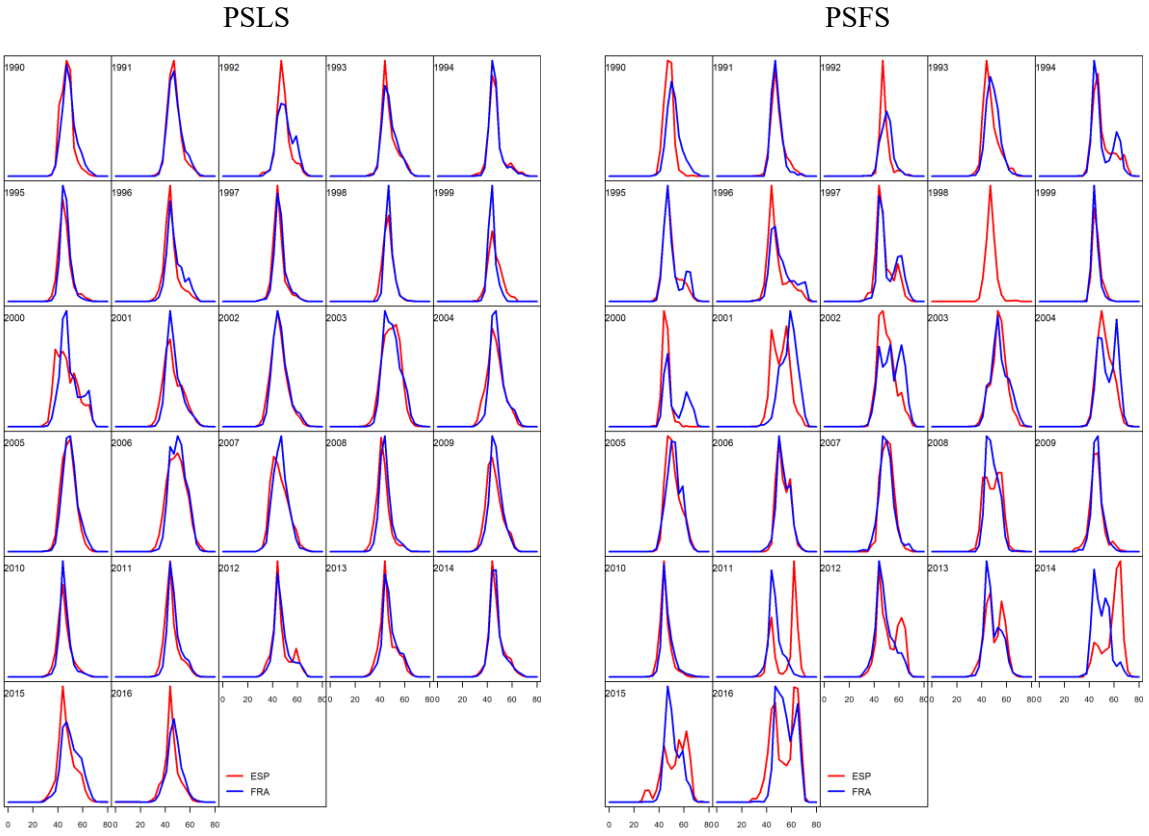

Figure C1: Compare the raw size frequencies between EU.Spain and EU.France PS fleets

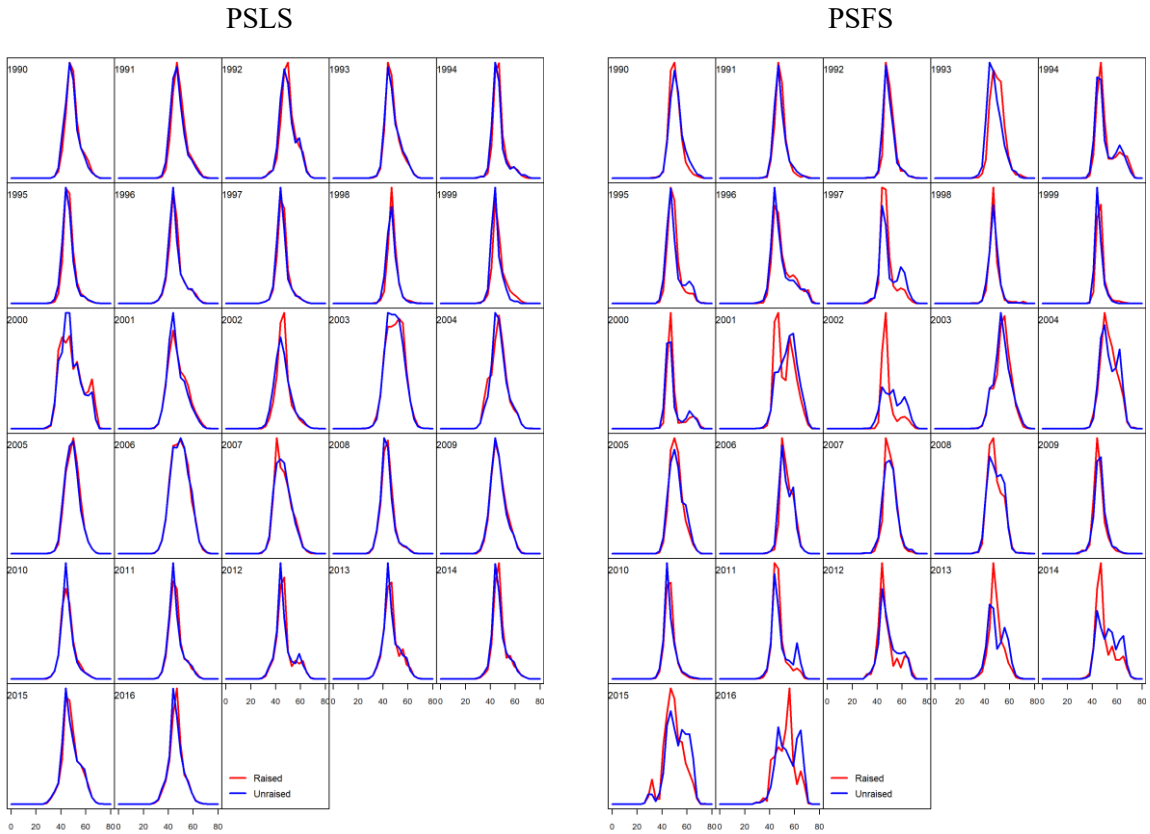

Figure C2: Compare the unraised (raw) and raised (reported) size frequencies from EU PS fleets for 1990-2016. The unraised size frequencies are from EU.Spain and EU.France.

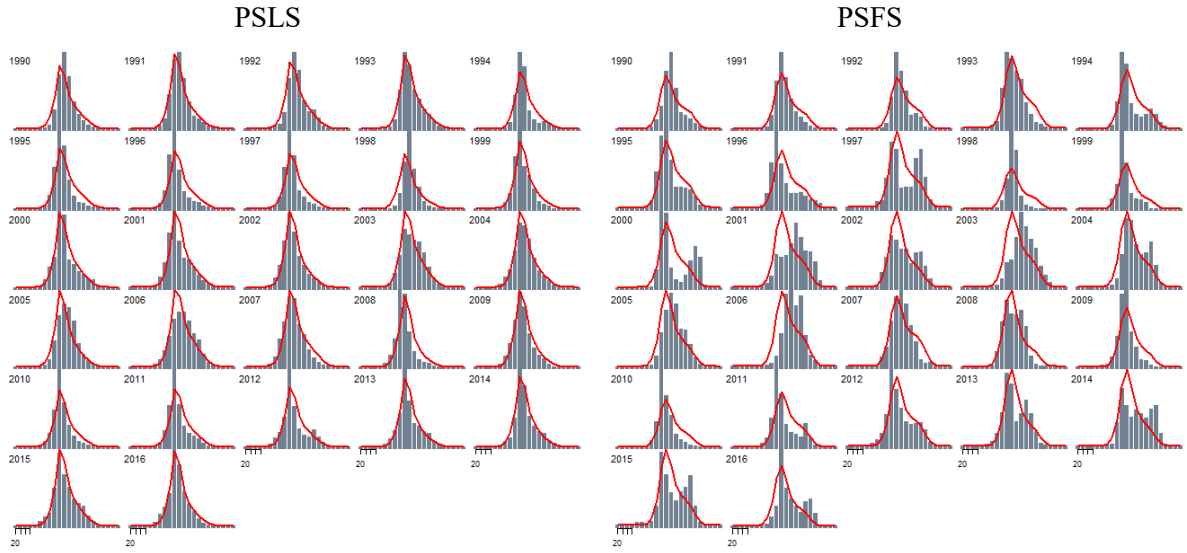

Figure C3: Annual aggregated fits to the unraised PSLS and PLFS length frequency from the EU PS fleet. The unraised size frequencies are from EU.Spain and EU.France.

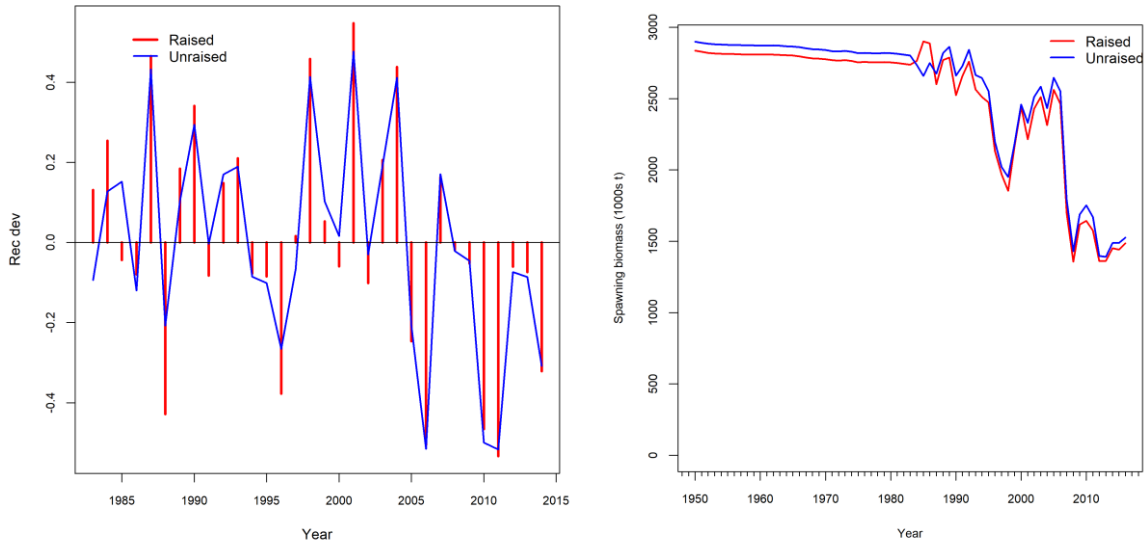

Figure C4: Compare annual recruitment deviations (left) and biomass estimates (right) between the sensitivity model using the unraised (raw) EU PS size and the reference model (IO) using the raised (reported) EU PS size frequencies. The unraised size frequencies are from EU.Spain and EU.France only.